NEURAL AND MOLECULAR MECHANISMS OF PATHOGEN AVOIDANCE IN *CAENORHABDITIS ELEGANS*

By

Adam R. Filipowicz

A DISSERTATION

Presented to the Neuroscience Graduate Program
and the Oregon Health & Science University
School of Medicine
in partial fulfillment of
the requirements for the degree of

Doctor of Philosophy

June 2022

TABLE OF CONTENTS

LIST OF FIGURES

ACKNOWLEDGEMENTS

This dissertation is being presented by one individual as part of the fulfillment of requirements for a doctorate, but it by no means represents an individual achievement. Like every endeavor, it is built off of the support and kindness of collectives of people working together, and so it would be impossible to name all of the people who have contributed to this work. However, I will do my best to name and thank a few.

First off, I would like to thank my mentor, Alejandro Aballay. Alejandro, thank you for always providing the scientific, professional, and personal support I needed over these last five years. You were always encouraging, especially at my lowest points, scientifically and otherwise. It was a joy to share exciting results with you and I always looked forward to our weekly meetings, knowing that I would walk away from them reinvigorated to keep pushing forward.

I would also like to thank the entire Aballay lab, past and present, for making the lab feel so welcoming and a great place to come to work each day. Yu Sang, Jessica, Casey, and Benson, thank you for always being there for help with lab protocols, answering questions, and your support. Supender, you taught me all of the basics of *C. elegans* research from pouring plates to picking worms, and were an invaluable resource in my rotation and beyond. Jogender, thank you for all of the insightful conversations we had during your time in the lab. Jonathan, you were the ideal office-mate and soccer buddy. I'll miss getting to work with all of you.

Thank you to my dissertation advisory committee members, Drs. Kelly Monk, Paul Barnes, Anusha Mishra, Larry Sherman, and Aakanksha Singhvi. I couldn't have asked for a better committee. You all are wonderful scientists and even nicer people. Thank you for the great questions and comments during our meetings together. Thank you also to Dr. Mary Logan for agreeing to be an outside reviewer of the dissertation.

Thank you to Dr. Danielle A. Garsin for providing the *E. faecalis* and *E. faecium* strains and to Dr. Fred Ausubel for providing the *P. aeruginosa* strains. They were crucial in completing this dissertation. The broader *C. elegans* research community is an amazing group of researchers and many others in the community were also very helpful in providing resources whenever asked, and in giving feedback during conferences and meetings.

To the friends I've made in Portland, I certainly couldn't have gotten through this without your support. The pandemic cut short much of the time we would've had together, but I will always remember and cherish the memories we made. To the past and present graduate researchers at OHSU and members of our union, Graduate Researchers United, thank you and solidarity, comrades.

My mom and dad, Cheryl and Ron Filipowicz, deserve much of the credit for raising me to be the person I am today. I am so lucky to have them as my parents. Their love and support are allowing me to become the first PhD in our family. Mom and dad, you two don't have to read the rest of this dissertation. Just read this part and know how much I love you.

Finally, I would like to thank my partner, Emma Bridges. We met right before the COVID-19 pandemic, and thank goodness we did. Emma, you mean the world to me. This research and writing couldn't have been done without you by my side, supporting me every step of the way. I love you so much and can't wait to start the next phase of our life together.

ABSTRACT

Upon exposure to harmful microorganisms, hosts engage in protective molecular and behavioral immune responses, both of which are ultimately regulated by the nervous system. As discussed in Chapter 1 of this dissertation, the use of *Caenorhabditis elegans* bacterial infection models have allowed for many insights into the mechanisms of these immune responses, including some of the chemosensory neurons involved in the reduction of pathogen exposure via altering of behavior, or pathogen avoidance. However, key questions remain unanswered: how does intestinal infection lead to pathogen avoidance? What does the neural circuitry between chemosensory neurons that sense pathogenic bacterial cues and the motor neurons responsible for avoidance-associated locomotion look like? This dissertation attempts to answer these questions by using the genetic and computational tools available in *C. elegans* to probe the molecular pathways and neural circuits underlying pathogen avoidance.

The research presented here is divided into two parts. In Chapter 2, ingestion of the bacteria *Enterococcus faecalis* is shown to lead to a fast pathogen avoidance behavior that results in aversive learning. Multiple sensory neuronal pathways are involved in the regulation of avoidance of *E. faecalis*: the G-protein coupled receptor (GPCR) NPR-1-dependent oxygen-sensing pathway opposes this avoidance behavior, while an ASE neuron-dependent pathway and an AWB and AWC neuron-dependent pathway are directly required for avoidance. Additionally, colonization of the anterior part of the intestine by *E. faecalis* leads to AWB and AWC mediated olfactory aversive learning. Importantly, two transient receptor potential melastatin (TRPM) channels, GON-2 and GTL-2, mediate this newly described rapid pathogen avoidance.

Chapter 3 begins by describing the finding that backward locomotion is a key component of learned pathogen avoidance, as animals pre-exposed to *Pseudomonas*

aeruginosa or *E. faecalis* show reflexive aversion to drops of the bacterial pathogens. This requires ASI, AWB, and AWC neurons for avoidance of *P. aeruginosa*, and ASE, AWB, and AWC neurons for avoidance of *E. faecalis*. This response also requires intestinal distention and, for *E. faecalis*, expression of the TRPM channels described above. The use of whole-brain simulation and functional assays reveals a sensorimotor circuit governing learned reflexive aversion. This four-layer neural circuit composed of olfactory neurons, interneurons, and motor neurons controls the backward locomotion crucial for learned reflexive aversion to pathogenic bacteria, learned avoidance, and a repulsive odor.

Together, these results suggest a mechanism by which TRPM channels may sense the intestinal distention caused by bacterial colonization to elicit pathogen avoidance and aversive learning by detecting changes in host physiology. The discovery of a complete sensorimotor circuit for this aversion demonstrates the utility of using the *C. elegans* connectome and computational modeling in uncovering new neuronal regulators of behavior, and furthers our understanding of pathogen avoidance mechanisms. Pathogen avoidance is a key line of defense against pathogen attack for nearly all animals; therefore, mechanistic insight into pathogen avoidance is crucial in furthering our understanding of human health and disease.

CHAPTER 1: INTRODUCTION[1]

Overview

Pathogen avoidance

The majority of research on animal responses to pathogens has historically focused on how immune systems counter infections. Engaging these systems is energetically costly to animals (1); therefore, they have evolved an alternate response: avoidance of infection altogether. This pathogen avoidance response has seen relatively little attention from researchers until recent times. The strategies animals develop to avoid infection range from the relatively simple learned association between pathogen cues and infection, which will be the subject of this dissertation, to complex human sociopolitical policies that attempt to limit pandemics, such as the response to SARS-CoV-2. This range in strategies demonstrates the many levels that pathogen avoidance operates at: molecular, cellular, physiological, behavioral, and societal (2). Like all animal processes, these levels are not hierarchical or deterministic but rather interdependent—molecular mechanisms, for instance, influence and are influenced by an animal behaving in its social environment. Take, for example, the case of COVID-19. Molecular evolution of a coronavirus capable of infecting and killing humans at high levels resulted in societal and individual behavioral responses meant to contain the spread of the virus. Bourgeois concerns over property, profit, and capital, along with other factors such as the politicization of mask wearing and vaccination, curtailed these efforts, leading to continued sickness, death, and evolution of the virus to this day.

[1] This chapter is largely based on A. Filipowicz, A. Aballay, and V. Singh, Cellular and Organismal Responses to Infections in *Caenorhabditis elegans*. *Encyclopedia of Cell Biology*, 2nd Edition (Forthcoming).

Understanding the cellular and molecular mechanisms of pathogen avoidance, therefore, is just one, albeit important, step in uncovering the puzzle of pathogen avoidance. Research into these mechanisms has been done in a variety of organisms, with simpler ones lending themselves well to detailed molecular manipulations. While the rest of this dissertation will focus on the pathogen avoidance responses in one such simple organism—the free-living transparent nematode *Caenorhabditis elegans*, a staple model organism for molecular neurobiological research ever since Sydney Brenner proposed using it to study neural development nearly 60 years ago—some of the insights from other organisms deserve a brief mention.

Detection of pathogens and infected conspecifics seems to depend on chemical cues across a broad spectrum of species, ranging from the fruit fly *Drosophila melanogaster* to the dung beetle *Scarabaeus lamarcki* to laboratory mouse strains to bonobos (2). For the fruit fly and the dung beetle, phenol produced by pathogenic bacteria found on feces acts as an avoidance signal (3). The vomeronasal system in mice, meanwhile, detects pheromones from infected conspecifics and induces an aversive behavioral response (4). In contrast to these olfactory induced responses, bonobos seem to use a variety of sensory modalities to shape their pathogen avoidance strategies, responding to visual, tactile, gustatory, and olfactory cues (5).

The research presented in this dissertation lends further evidence to the widespread role of olfaction in pathogen avoidance, although it also suggests that even in an organism as simple as *C. elegans* multisensory learned pathogen avoidance responses are possible. Before getting to that research, it is important to look at why researchers use *C. elegans* to study responses to pathogens in the first place.

C. elegans as a model system to study responses to pathogens

C. elegans is a microscopic nematode with only 959 somatic cells in the adult hermaphrodite. It is a powerful experimental organism with a number of traits that facilitate genetic and genomic analysis, including its hermaphroditic lifestyle, short two-to-three-week lifespan,and small genome, which offers an ideal compromise between complexity and tractability. Unlike bacteria, yeast, or other single-celled organisms, *C. elegans* has muscles, nerves, reproductive organs, and digestive system, in spite of its small, one-millimeter-long body. It responds to touch, taste, and odor molecules resulting in various robust behaviors thanks to its small, yet complex, nervous system composed of 300 neurons (or 302 if the CAN cells are included). These neurons are referred to by a two or three letter name that is somewhat arbitrary, but usually gives some indication of their class, location, function, or morphology (*e.g.*, AWB, NSM, and VA). Neurons classes that are radially symmetrical are usually have an "L" (left), "R" (right), "D" (dorsal), and/or "V" (ventral) appended to their class name to indicate their position within the class, while for some classes the case name is followed by a number to indicate the neuron number within the class. For example, the AWBL/R neurons are the Amphid Wing B Left/Right neurons, the NSML/R neurons are the NeuroSecretory Motor Left/Right neurons, and VA1 is the 1st Ventral A-type motor neuron. Most neurons can be divided into three types: sensory, inter, and motor neurons. Connections generally flowing from sensory to inter to motor, though there is also significant connectivity within the same neuron type. The location within adult *C. elegans* of some of the neurons important to this dissertation are depicted in **Figure 1**.

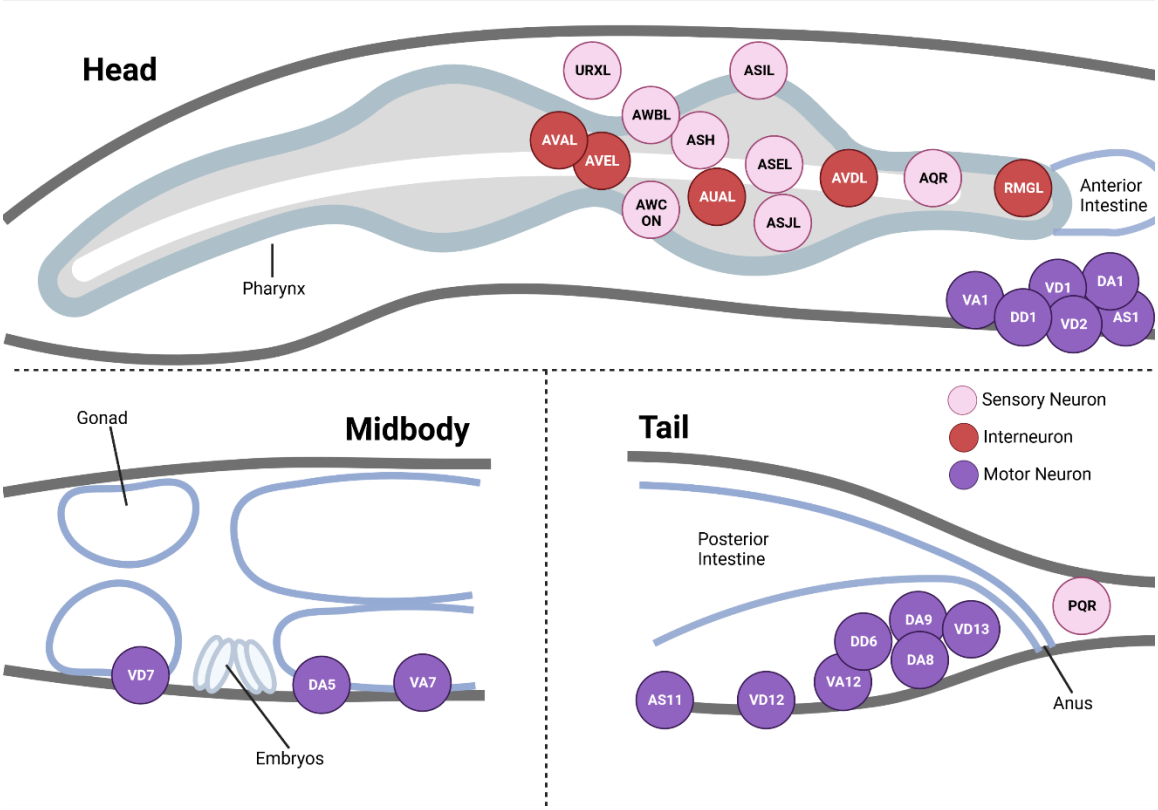

Fig. 1. Illustration of important *C. elegans* neurons. Approximate neuron locations within the body of *C. elegans* are depicted. The pharynx, anterior intestine, gonads, embryos, posterior intestine, and anus are also depicted to give landmarks for where neurons are located. Sensory neurons are colored pink, interneurons red, and motor neurons purple. Radially symmetrical neuron classes are represented by their left (L) neuron, or for the AWC neuron class the ON neuron (during development, one AWC neuron becomes an ON response cell, while the other becomes an OFF response cell; this process is stochastic, meaning either the AWCL or AWCR neuron can become the ON cell, with the other becoming the OFF cell).

In nature, *C. elegans* is found in decaying organic matter rich in microorganisms, which can serve as a food source but can also be pathogenic. To date, more than 40 microbes have been shown to be pathogenic to *C. elegans*, including bacteria, fungi,and viruses. The major routes of infection are through the intestine and the epidermis. Because the nematode lacks adaptive immunity and professional phagocytes involved in

the clearance of infecting microbes, the cells in direct contact with different microbes, intestinal and epidermal epithelial cells, provide the primary defense against pathogens. Despite lacking adaptive immunity, *C. elegans* can mount protective responses to pathogen infection by avoiding certain pathogens or by triggering evolutionarily conserved mechanisms that control microbicidal pathways and pathogen avoidance behaviors. Avoidance responses vary from naïve reflexive aversion towards microbial toxins to trans-generationally stable learned avoidance behaviors. Activation of different cellular signaling pathways can lead to the production of immune effectors such as lectins, lysozymes, lipases, and antimicrobial peptides, which act directly to fight off the invading pathogens. The defensive response that results in activated signaling pathways and induced immune effectors is pathogen-specific, indicating that the nematode can distinguish different infecting microbes. The nervous system controls not only pathogen avoidance behaviors but also the activation of microbicidal mechanisms. All of these characteristics make *C. elegans* an excellent model organism for the study of both innate and behavioral immune responses to pathogenic microbes.

C. elegans interactions with microbes

Before describing the protective responses that *C. elegans* mounts to combat pathogen infection, a brief overview of the variety of *C. elegans* interactions with microbes is warranted. In its natural environment, *C. elegans* encounters numerous microbes, especially in microbe-rich environments such as rotting fruits. These microbes can serve as a food source, form a core microbiota, or be pathogenic (**Fig. 2A**). Many studies indicate that the gut microbiota consists of many genera, including *Enterobacteria*, *Pseudomonas, Stenotrophomonas, Ochrobactrum*, and *Sphingomonas* (6).

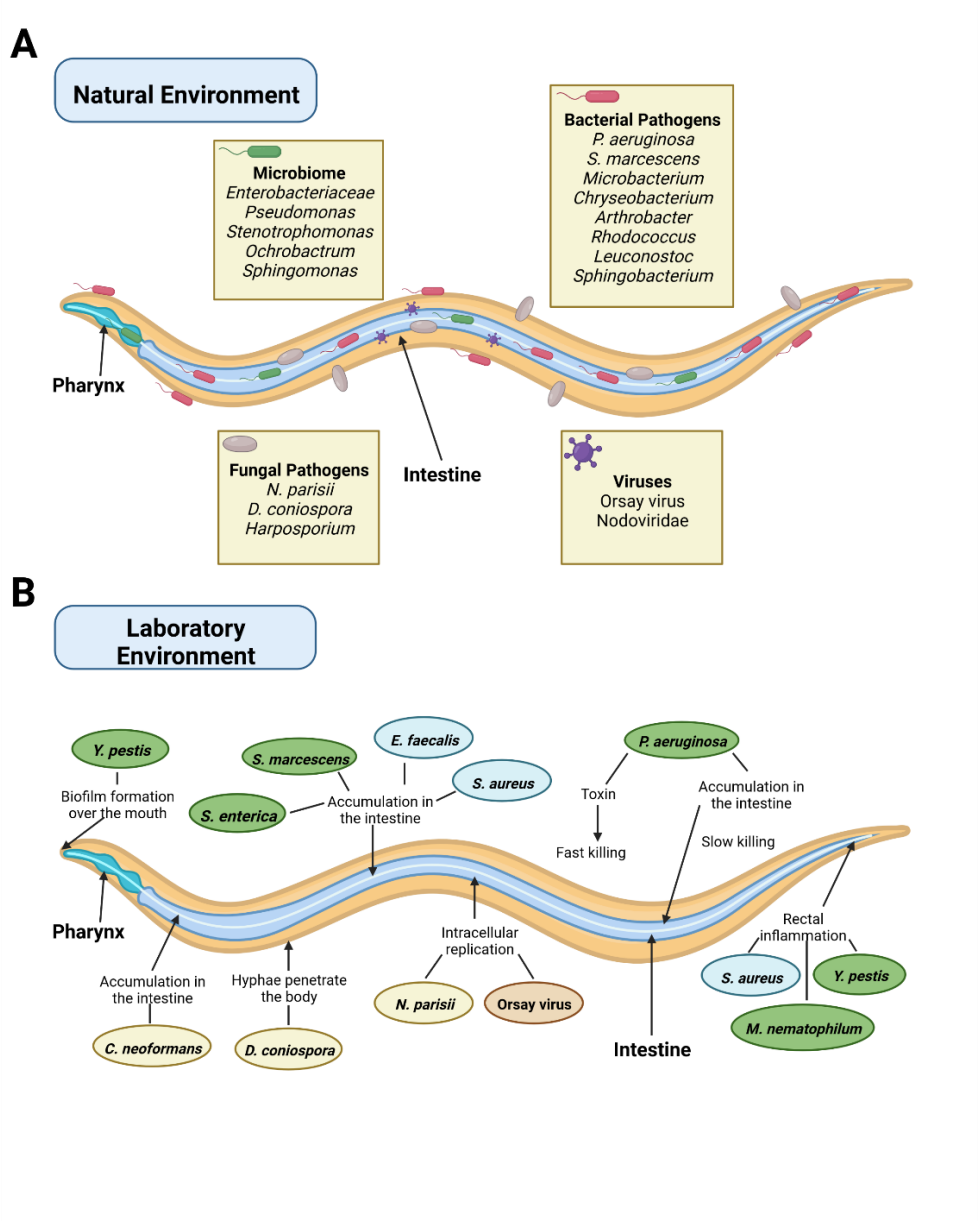

Fig. 2. *Caenorhabditis elegans* encounters various microbes in nature and in the laboratory. (A) In nature, *C. elegans* interacting microbes include its microbiome, bacterial and fungal pathogens, and viruses. Each of these interact with different tissues of the nematode. (B) In the laboratory, pathogens also colonize different tissues of the nematode. Gram negative bacteria, green; Gram positive bacteria, blue; fungi, yellow; viruses, orange.

A handful of natural intracellular parasites have been found in wild *C. elegans*. The most common species, *Nematocida parisii*, a microsporidian parasite related to

fungi, infects the animal's intestinal cells (7, 8). Other natural intracellular pathogens include Orsay virus and other viruses of the nodoviridae family (9, 10). Two prominent natural extracellular fungal pathogens are *Drechmeria* and *Harposporium*. *D. coniospora* enters through the cuticle and penetrates all body tissues (11, 12). *Harposporium* spores, on the other hand, enter through the gut, with the intestinal epithelium being the first tissue attacked (13). Natural extracellular bacterial pathogens include some of the pathogens used in the laboratory, such as *Pseudomonas aeruginosa* and *Serratia marcescens* (see below). Other suspected pathogens, based on their effect on brood size, include members of *Microbacterium, Chryseobacterium, Arthrobacter, Rhodococcus, Leuconostoc*, and *Sphingobacterium genera* (6). *Microbacterium nematophilum* and *Leucobacter musarum* induce rectal swelling while a related pathogen, *Leucobacter celer*, coats the whole surface of the animal (6).

In laboratory settings, the *C. elegans* Bristol strain N2 is used as the reference "wild-type" strain, and is fed the Gram-negative bacterium *Escherichia coli* (OP50) grown on agar in petri dishes. The majority of bacterial and fungal pathogens used in the lab are also grown on agar petri dishes and remain extracellular in worms (**Fig. 2B**). These include pathogens that are also found in the *C. elegans* natural environment such as *P. aeruginosa*, *S. marcescens, M. nematophilum*, and *D. coniospora*. *P. aeruginosa* can kill *C. elegans* using toxins in a matter of hours by a process termed 'fast killing' (14). It can also kill nematodes in 2–4 days by an infection-like process termed 'slow-killing,' a process requiring bacterial replication in the intestinal lumen of the host (15). Laboratory-introduced pathogens include *Yersinia pestis, Enterococcus faecalis*, and *Staphylococcus aureus*. *Y. pestis* strains capable of forming biofilm cover the mouth of *C. elegans* and prevent feeding, reminiscent of *Y. pestis* infection of plague carrier fleas (16). The Gram-positive bacteria *E. faecalis* and *S. aureus* colonize

the intestine (17, 18). An interesting aspect of *S. aureus* infection is that it causes extensive loss of intestinal microvilli of the host and rectal inflammation (18).

Two fungal pathogens used in the laboratory are *Cryptococcus neoformans* and *Candida albicans*. The yeast form of the human opportunistic pathogen *C. neoformans* accumulates in the nematode intestine and causes a lethal infection (19). *C. albicans*, a fungus that causes nosocomial infections in humans, is pathogenic to *C. elegans* in both its hyphal and yeast forms.

Immune Effectors

Although this dissertation focuses on pathogen avoidance in *C. elegans*, it is worth taking some time to describe the immune effectors and signaling pathways in the nematode. There is extensive interaction between the innate and behavioral immune systems as well as overlap in the neuronal regulation of the innate and behavioral immune responses. Additionally, the studies described in this dissertation will make use of some of these immune effectors and signaling pathways, namely *clec-60, ilys-3, pmk-1, fshr-1,* and *bar-1*. This section focuses on the immune effectors involved in responses to pathogens, while the next focuses on the immune-related signaling pathways.

Upon infection, several immune effectors are produced in *C. elegans* that confer the nematode protective immunity against microbial pathogens. These effectors either directly inhibit the growth of invading pathogens, conferring resistance, or counteract infection-induced damage to host cells, conferring tolerance. The following subsections describe the variety of effectors used by *C. elegans* for pathogen defense.

Antibacterial factors (ABFs)

ABF-1 to ABF-6 in *C. elegans* are small cationic peptides similar to human cysteine-rich host defense peptides (defensins). ABF-2 has antimicrobial activity against Gram-negative bacteria, Gram-positive bacteria, and yeast (20). ABF-1 and ABF-2 are expressed in the pharynx of *C. elegans*, which is one of the most anterior parts of the alimentary canal and the first organ in direct contact with pathogens. Expression of antibacterial factors requires TOL-1, and cell death receptor CED-1 (21).

Caenacins

Caenacins are putative antimicrobial peptides structurally related to neuropeptide-like proteins. Some of these genes are upregulated in the epidermis following infection with the fungal pathogen D. *coniospora*. Upregulation of caenacins in the epidermis requires neural-produced TGFβ homolog DBL-1 (22). In addition, overexpression of caenacins enhances *C. elegans* immunity against D. *coniospora*.

Caenopores

Caenopores are a family of proteins containing a saposin domain in *C. elegans*, similar to protozoan amoebapores, mammalian NK-lysin, and granulysin. *C. elegans* has a group of 28 *spp* genes that encode 33 different caenopores (23). Antibacterial, membrane-permeabilizing, and pore-forming activities have been demonstrated for SPP-1, SPP-3, SPP-5, and SPP-12 (23–26). SPP-1 protects *C. elegans* against *S. enterica* and *P. aeruginosa*. Down-regulation of SPP-1 by *P. aeruginosa* is under the control of the FOXO transcription factor DAF-16.

C-type lectins

C-type lectins are a group of proteins that contain one or more C-type lectin-like domains (CTLD) and that recognize complex carbohydrates on cells and tissues (27, 28). 278 genes encoding CTLD proteins are present in the *C. elegans* genome (29).

More than 60 CTLD proteins are induced during pathogen infection. Distinct expression profiles of CTLD genes during different infections indicate that these proteins might contribute to pathogen specificity of *C. elegans* immune responses. For instance, RNAi knockdown of *clec-17*, *clec-60* and *clec-86* caused enhanced susceptibility to *M. nematophilum* (30). Also, knockdown of *clec-65* or *clec-70* resulted in enhanced susceptibility to *Escherichia coli* LF82 or *S. aureus*, respectively (18, 31). Simultaneous overexpression of *clec-60* and *clec-61*, or *clec-70* and *clec-71* led to increased resistance to *S. aureus* but decreased resistance to *P. aeruginosa* (18). C-type lectins often bind carbohydrates in a calcium-dependent manner. However, a study revealed that CLEC-39 and CLEC-49 directly recognize live *S. marcescens* in a calcium-independent manner, suggesting a nonclassical recognition of *S. marcescens* by both CTLD proteins (32).

CUB domain proteins

More than 50 genes in the *C. elegans* genome encode proteins containing a CUB (C1r/C1s, Uegf, and Bmp1) domain, which is a structural motif of about 100 residues (33). RNAi inhibition of three of the CUB genes (F08G5.6, F20G2.5, *dct-17*) enhances *C. elegans* susceptibility to *P. aeruginosa* and RNAi inhibition of two other CUB genes (C17H12.8 and C32H11.12) enhances *C. elegans* susceptibility to *Y. pestis* infection. Interestingly, CUB genes that are usually upregulated in response to bacterial infections are down-regulated in response to fungi such as *C. albicans* and *D. coniospora* (34).

Infection response genes (IRGs)

Three IRGs, *irg-1, irg-2* and *irg-3*, are upregulated in the *C. elegans* intestine during infection with *P. aeruginosa* and encode small molecular proteins that may act as immune effectors (35). The inhibition of protein translation machinery of the host either via *P. aeruginosa* ToxA or via cycloheximide treatment leads to their

upregulation in a bZIP family transcription factor ZIP-2 dependent manner (35, 36). Loss of ZIP-2 function leads to enhanced susceptibility of worms to *P. aeruginosa*. The upregulation of IRGs during *P. aeruginosa* infection is also regulated by neuronal signaling originating from AWB odor sensory neurons (37).

Lysozymes

Lysozymes are glycosyl hydrolase enzymes that degrade bacterial cell walls and that are present in both plants and animals. The *C. elegans* genome has 10 protist type lysozyme encoding genes (*lys-1 to lys-10*) and 5 invertebrate type lysozyme encoding genes (*ilys-1* to *ilys-5*) (38). Many lysozyme genes are expressed in the intestine and upregulated in response to microbial infections (39). RNAi inhibition of *lys-1* causes enhanced susceptibility to *S. aureus*, while overexpression of *lys-4* and *lys-5* increases resistance to *S. aureus* (40, 41). Overexpression of *lys-4* enhances resistance to *S. marcescens* (41). *lys-7* mutants are also more susceptible to *C. neoformans* infection but resistant to *S. typhimurium* infection (42).

Neuropeptide-like proteins

Neuropeptides are bioactive peptides that play a role in synaptic signaling. *C. elegans* has 32 genes encoding neuropeptide-like proteins (NLPs) (43). Some of the NLPs encoding genes are upregulated during microbial infection. NLP-31 has antimicrobial activity *in vitro* and NLP-29 is expressed in the intestine and hypodermis (44). Up-regulation of *nlp-29* cluster (6 genes) in the hypodermis during *D. coniospora* infection requires signaling molecules such as TIR-1, PMK-1/p38 MAPK, and DCAR-1/GPCR.

Immune-Related Signaling Pathways

Detection of pathogen attack leads to activation of cellular signaling pathways that induce expression of defensive genes to limit microbial growth, destroy invading microbes, detoxify xeno/endobiotics, and repair damage. These pathways include innate immune and stress response pathways activated in various tissues during infection with bacterial or fungal pathogens (**Fig. 3 and 4**). Numerous studies have demonstrated the complexity and specificity of these responses: different signaling pathways regulate expression of distinct but overlapping sets of effector genes, individual pathogens induce genes controlled by multiple pathways, and the set of genes regulated by each pathway is also pathogen-specific.

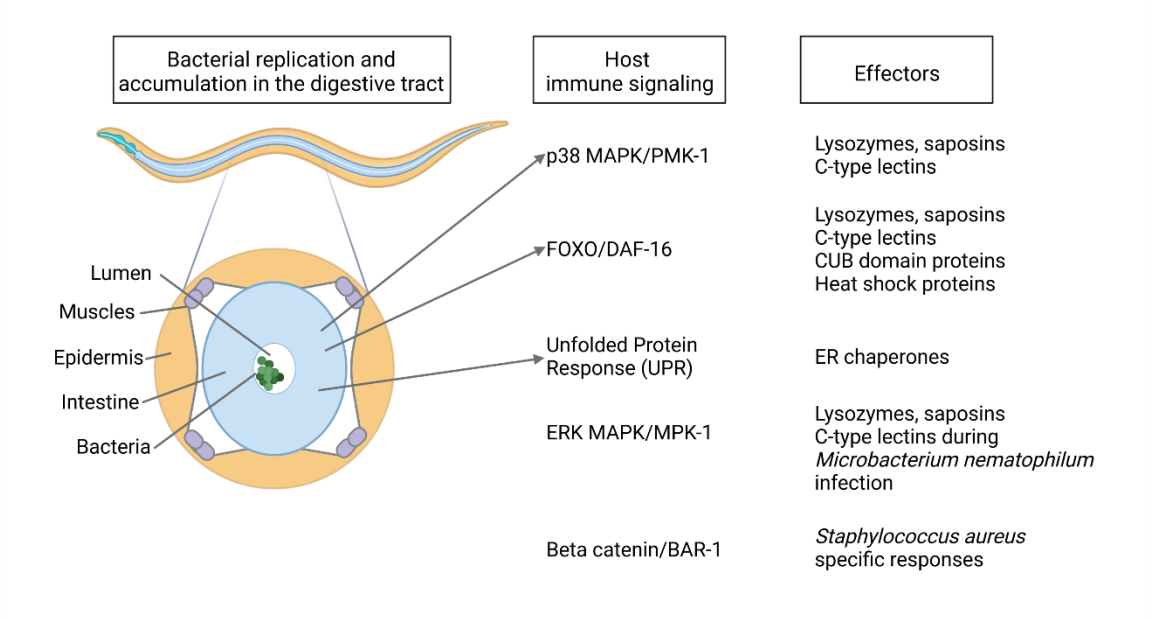

Fig. 3. Cellular responses to bacterial infection in *C. elegans*. Replication and accumulation of Gram-negative bacteria in the intestine leads to activation of many signaling pathways. Some of the better-studied pathways include p38 MAPK, insulin signaling involving FOXO transcription factor Daf-16 as well as UPR in the intestinal cells. These produce effector molecules including antimicrobial molecules, chaperones etc. The site of activation of beta catenin or the ERK MAPK pathway is not known.

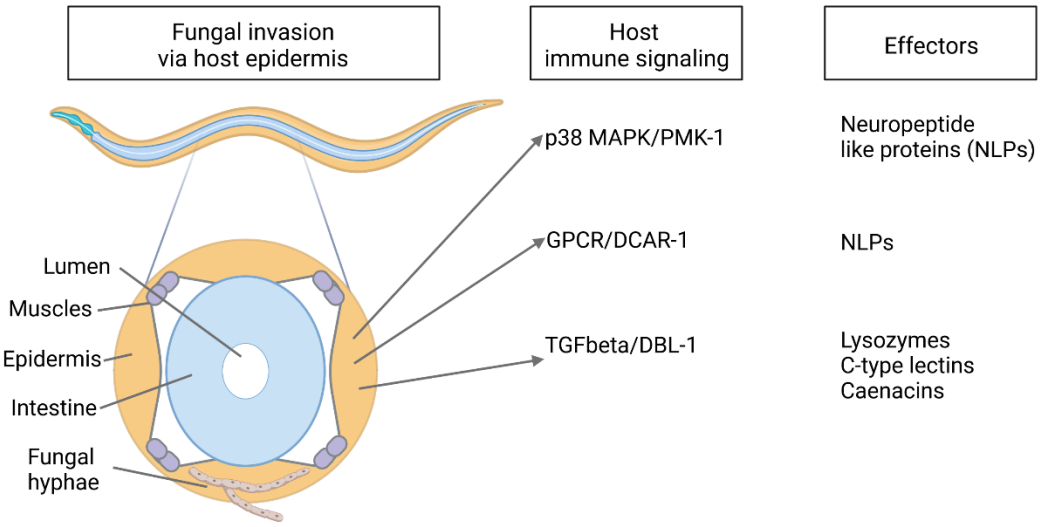

Fig. 4. Cellular responses to fungal infection in *C. elegans*. Invasion of the epidermis by the hyphal form of fungus *Drechmeria coniospora* leads to induction of defenses in that tissue. The p38 MAPK pathway regulates antimicrobial peptides such as NLP genes in the epidermis while the TGFβ pathway regulates anti-fungal products such as caenacins, C-type lectins and lysozymes. DCAR-1, a G protein-coupled receptor (GPCR) in the epidermis, regulates NLP gene expression partly through the PMK-1 pathway.

The p38 MAPK pathway and related pathways

The conserved p38 MAPK pathway plays a major role in the antimicrobial response of *C. elegans*. Forward and reverse genetic studies have demonstrated that the p38 MAPK pathway culminating in PMK-1 is required for immunity against a variety of pathogens and xenobiotics, including Gram-negative and positive bacteria, fungi, pore-forming toxins (PFTs), and many types of stress such as oxidative stress and heavy metal stress (45, 46). This pathway includes the TIR domain protein TIR-1, neuronal symmetry family member 1 (*nsy-1*), SAPK/ERK kinase 1 (*sek-1*), and p38 MAPK family member 1 (*pmk-1*) (47, 48). The signal is transduced in the form of protein phosphorylation, where NSY-1 phosphorylates SEK-1, which in turn phosphorylates PMK-1. TIR-1 and

two protein kinases, PKCδ and PKD, act upstream of NSY-1 (49–51). It has also been demonstrated that *C. elegans* ATF-7, a transcription factor orthologous to mammalian ATF2, functions downstream of PMK-1 as a repressor of PMK-1-regulated genes, and undergoes a switch to an activator upon phosphorylation by PMK-1 (52).

Activation of the p38 MAPK pathway induces the expression of a set of secreted immune response genes. Several microarray studies showed that genes upregulated by PMK-1 include those encoding proteins containing CUB-like domains, C-type lectins, antibacterial peptides, lysozymes, NLPs, and caenacins (53). Besides p38, two other MAPKs, extracellular signal-regulated kinase (ERK) and c-Jun N-terminal kinase (JNK), are also involved in the nematode's defense against infections. Upon infection with *M. nematophilum*, the ERK pathway is activated and mediates a protective response by inducing the production of C-type lectins, lysozymes, proteases, and other defense-related proteins (30, 54). The JNK pathway is a key regulator of the transcriptional and functional responses to bacterial PFTs (55).

The DAF-2/DAF-16 pathway

The DAF-2/DAF-16 pathway, which is well known for its regulation of the lifespan of *C. elegans*, also plays an important role in the immune response against bacterial infections. Activation of the DAF-2 receptor by an agonist ligand, such as the insulin-like peptide DAF-28, activates a phosphorylation cascade that results in the phosphorylation of the FOXO family transcription factor DAF-16. Phosphorylated DAF-16 is retained in the cytoplasm. In *daf-2* mutants or in the presence of an antagonist ligand such as INS-1, un-phosphorylated DAF-16 translocates into the nucleus, where it regulates the expression of a wide variety of genes (56). It has been suggested that the PMK-1 and DAF-16 pathways act in parallel to promote immunity. While PMK-1 controls both basal and infection-induced expression of pathogen response genes, DAF-

16 regulates a constitutively expressed response or a general stress response to microbes (53, 57). This is in agreement with the role of DAF-16 in regulating the expression of many genes involved in resistance to various forms of stress, including heat, oxidative stress, hypoxia, osmotic stress, heavy metal toxicity, ultraviolet radiation, proteotoxicity, and microbial infection (58). A number of antimicrobial effectors are regulated by DAF-16, including lysozymes LYS-7 and LYS-8, the saposins SPP-1, SPP-9 and SPP-12, DUF-23, and C-type lectins (57, 58). Most of these effectors appear to be secreted proteins that function to disrupt microbial cell membranes.

Lipid homeostasis pathways

A number of studies have demonstrated that lipid homeostasis is crucial for the nematode's immune response. Monounsaturated fatty acids such as the oleate C18:n1Δ9 enhance the immune response of *C. elegans* to *P. aeruginosa*; conversely, loss of fatty acid desaturase essential for producing MUFAs causes enhanced susceptibility to the pathogen. SBP-1, an ortholog of human sterol response element-binding protein, is a regulator of fatty acid desaturase and is essential for *C. elegans* survival during *P. aeruginosa* infection (59). Indeed, activation of lipid breakdown pathways is a conserved feature of *C. elegans* response to Gram-negative pathogens (*P. aeruginosa* and *S. enterica*), Gram-positive pathogens (*E. faecalis* and *S. aureus*), and pathogenic yeast (*C. neoformans*) (39). An acyl co-A synthetase, *acs-2*, is upregulated during infection and a mutation in *acs-2* causes enhanced susceptibility to *E. faecalis* infection. NHR-49, the nematode ortholog of human PPAR alpha, regulates fatty acid beta-oxidation enzymes, including *acs-2*, during *E. faecalis* infection (39). SKN-1 also suppresses lipid droplet loss during *P. aeruginosa* infection (60). HLH-30, the nematode ortholog of human TFEB, regulates survival of *C. elegans* during *S. aureus*

infection (61) and is also known to regulate initial steps of lipolysis during starvation (62).

The unfolded protein response pathway

In the endoplasmic reticulum (ER), proteostasis surveillance is mediated by the unfolded protein response (UPR). ER homeostasis is critical for ensuring proper folding and release of modified proteins to the Golgi. In response to pathogen infection, increased demands on the protein folding machinery cause stress in the ER, which activates UPR pathways to restore ER homeostasis. Activation of UPR in *C. elegans* is required for defense against a variety of pathogens, including *B. thuringiensis*, *S. enterica*, and *P. aeruginosa* (63–65). UPR is regulated by the p38, JNK, and MAPK pathways in response to PFTs (55, 63). Interestingly, the activation of UPR is also required by p38 MAP kinase/PMK-1 mediated defense against *P. aeruginosa* (65). Upon infection with *S. typhimurium*, the apoptotic receptor CED-1 activates the expression of *pqn/abu* genes in the noncanonical UPR pathway to promote immune response (64). In lights of studies indicating that there is strong developmental regulation of certain *abu/pqn* genes (66), further investigation will be required to fully address whether such genes are part of the UPR and whether their role in resistance to pathogen infection is related to cuticle and pharynx integrity rather than UPR. A study demonstrated that SKN-1, the *C. elegans* homolog of Nrf1/2/3 that functions in oxidative stress resistance and longevity, transcriptionally regulates core UPR transcription factors and downstream effectors in the ER-stress response, and the UPR plays a role in the activation of the antioxidant/detoxification response (67).

Response to intracellular pathogens

Canonical defense pathways operative during bacterial infection of the intestine, such as p38 MAPK and insulin/insulin-like growth factor signaling pathways, do not appear

to play roles in resistance to the intracellular pathogen *N. parisii* (68). Instead, ubiquitin-mediated pathways, the proteasome, and xenophagy components are involved in host response and defense against *N. parisii* infection (69). The ubiquitin-mediated response is also important for defense against the Orsay virus, another natural intracellular pathogen of *C. elegans* (69).

Studies using laboratory introduced viruses such as Flock House virus (FHV), vesicular stomatitis virus (VSV), and vaccinia virus (VV) have identified a prominent role for the RNA interference (RNAi) machinery in viral restriction, a conserved defense mechanism that was first characterized in plants (45). These studies confirmed that the RNAi pathway is important for the protection of worms from viral infection. In addition, the RNAi pathway has also been implicated in the defense against three viruses that are distantly related to nodaviruses, Orsay, Santeuil, and Le Blanc. These viruses cause morphological abnormalities in the nematode intestine (9). *C. elegans* mutants lacking RNAi factors (RDE-1, RDE-4, RNaseD MUT-7, or dicer-related helicase DRH-1) have an elevated viral infection load.

Neuronal Regulation of Immunity

The nervous and immune systems interact in multiple ways to control the immune response to pathogen attacks. The nervous system controls not only the activation of immune-related pathways (**Fig. 5**) but also the animal's aversive behaviors (**Fig. 6**). It plays a critical role in the control of microbicidal mechanisms, which if left unregulated, damage the host. Although the nervous system of *C. elegans* seems to mostly suppress immune system function, neuronal activators of innate immunity have also been uncovered. A number of GPCRs, predominantly in the nervous system, as well as specific neurotransmitters and their receptors, regulate innate immune responses to various pathogens. Neuropeptide-like proteins, NLPs and FMRF peptides, and their

receptors are also involved in immune regulation during infection. This section will briefly touch on these neuronal regulators of innate immunity, while the subsequent section will focus on neural control of aversive behaviors.

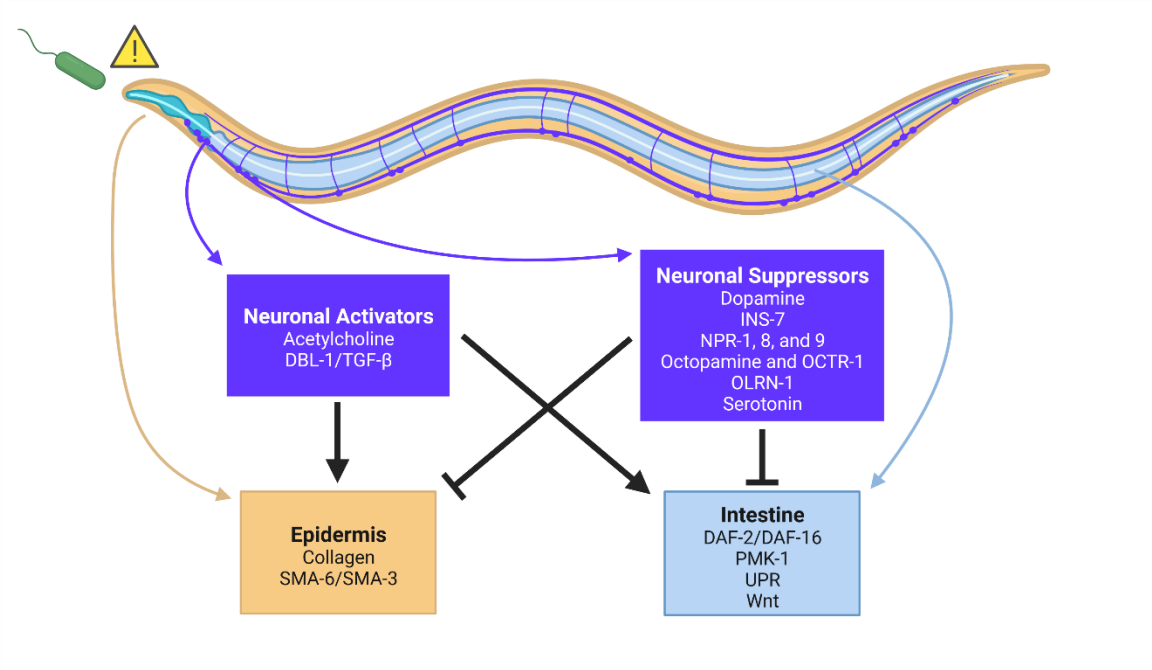

Fig. 5. The nervous system activates and suppresses immune signaling pathways upon encountering pathogens. Neuronal activation and suppression of innate immunity occur in both the epidermis and intestine. How the nervous system is activated by pathogens and how signals are sent from one tissue to the other remains poorly understood.

Acetylcholine

One immune activator is the neurotransmitter acetylcholine (ACh). *C. elegans* infection by *S. aureus* leads to ACh release from the nervous system and activation of muscarinic receptors in the intestinal epithelium (70). This receptor activation leads to induction of Wnt signaling, ultimately resulting in increased C-type lectin and lysozyme expression. Over half of the 302 neurons in *C. elegans* are cholinergic (71). Which of these cholinergic neurons are important for activation of defense pathways is an important

question for future research. Additionally, because the intestine of *C. elegans* is not directly innervated, how ACh reaches the muscarinic receptors in the intestinal epithelium remains to be elucidated.

TGFβ signaling (DBL-1)

The DBL-1 pathway in *C. elegans*, another activator of immunity, is homologous to the mammalian TGFβ cascade, and was first described as involved in resistance to infection by *P. aeruginosa* and *S. marcescens* (41, 72). DBL-1 is found in AVA interneurons (73), where it binds to the membrane-anchored heterodimeric DAF-4/SMA-6 receptor, leading to the phosphorylation and activation of the cytoplasmic signal transducer SMAD complex (SMA-2, –3 and –4); the transducer then translocates into the nucleus, where it activates gene expression. *dbl-1* mutants exhibit increased susceptibility to infection with *S. marcescens*. The DBL-1 pathway up-regulates the expression of many defense genes, including lectins and lysozymes, and is required for avoidance behaviors (41). Upon infection with fungus *D. coniospora*, *dbl-1* gene is also required for induction of *cnc-2* expression (22).

Dopamine

Dopamine is another neurotransmitter that regulates the immune response in *C. elegans*. Inhibition of neuronal dopamine signaling leads to increased survival of nematodes on *P. aeruginosa* and enhanced PMK-1/p38 MAPK signaling activity in the intestine (74). Thus, neuronally derived dopamine must normally suppress the PMK-1/p38 MAPK pathway. It was found that CEP neurons release dopamine that acts on the D1-like dopamine receptor DOP-4 in ASG neurons. ASG neurons go on to inhibit the PMK-1/p38 MAPK pathway. Similar to the situation with ACh, the mechanisms of CEP release of dopamine upon infection, and ASG communication to the intestine, are open questions.

Insulin-like peptide 7 (INS-7)

The *C. elegans* genome encodes a number of insulin-like peptides, many of which are expressed in the nervous system. One such peptide, INS-7, is expressed in response to *P. aeruginosa* infection (75). INS-7 activates the insulin-like receptor DAF-2. This leads to phosphorylation and retention in the cytoplasm of a transcription factor, DAF-16, as discussed above.

NPR-1

NPR-1, a GPCR related to mammalian neuropeptide Y receptors, was one of the first neuronal components to be implicated in the suppression of innate immunity in *C. elegans*. In addition to its role in pathogen avoidance (see next section), NPR-1 regulates the expression of genes controlled by the PMK-1/p38 MAPK signaling pathway in the intestine (76). Animals lacking NPR-1 exhibit enhanced susceptibility to infections by *P. aeruginosa, S. enterica, E. faecalis*, and *S. aureus* (76, 77). It was shown that NPR-1 activity in the oxygen-sensing AQR, PQR, and URX neurons is sufficient to reverse this phenotype. A more recent study found that NPR-1 functions downstream of the ASG neuronally expressed GABAergic transcription factor PITX1/UNC-30 to regulate immunity via ELT-2 and PMK-1, as well as longevity via MDL-1 and PQM-1 (78).

NPR-8

NPR-8, expressed in AWB, ASJ, and AWC neurons, negatively regulates the immune response by suppressing cuticular collagen expression (79). Unlike NPR-1, NPR-8 seems to play no role in avoidance or bacterial cue sensation. Animals lacking NPR-8 are resistant to the thinning and wrinkling of their cuticles during infection, an

interesting case of the nervous system dynamically controlling the outermost defense barrier of via collagen expression.

NPR-9

Another GPCR, the gastrin-releasing peptide receptor homolog, NPR-9, also inhibits the innate immune response. Loss of NPR-9 leads to enhanced expression of the immunity-related genes *pqm-1, dod-22, F08G5.6*, and *F55G11.7* upon *P. aeruginosa* infection (80). NPR-9 is expressed in the interneuron AIB and seems to antagonize the activity of this neuron. How this leads to suppression of the innate immune response remains unclear.

Octopamine and OCTR-1

Screens for enhanced resistance to *P. aeruginosa* infection revealed that loss of the catecholamine GPCR OCTR-1 leads to longer survival upon infection. OCTR-1 suppresses PMK-1/p38 MAPK signaling as well as canonical and non-canonical UPR in the ER (81, 82). In the nervous system, OCTR-1 activity in the ASH neuron suppresses the AIA interneuron, which is required for the release of NLP-20 (83). It is this neuropeptide that regulates the induction of UPR and innate immune genes controlled by PMK-1 signaling. Octopamine, the endogenous ligand for OCTR-1 and an important invertebrate neurotransmitter closely related to norepinephrine, is produced by RIC interneurons and seems to be upstream of this signaling cascade (84). How RIC interneurons are activated to release octopamine upon infection remains unclear.

OLRN-1

OLRN-1 is a GPCR required for the differentiation of AWC olfactory neurons during larval development. In this capacity, it acts cell-autonomously in AWC neurons to suppress the TIR-1/NSY-1/SEK-1, PMK-1/2 cascade, allowing for olfactory receptor

expression in AWC. Interestingly, *C. elegans* seems to also use OLRN-1 to cell non-autonomously to repress PMK-1/p38 MAPK signaling in the intestine (85). Loss of OLRN-1 activity leads to increased immune effector transcription and subsequently increased intestinal clearance and enhanced survival on *P. aeruginosa*.

Serotonin

Serotonin plays an important neuromodulatory role in pathogen avoidance (see next section) and, like NPR-1, also has a role in certain innate immune responses. Upon infection with *M. nematophilum*, ADF neurons release serotonin, which then acts via its receptors SER-1 and SER-7 to suppress the innate immune response in the rectal epithelium (86). This suppression requires the G-protein GOA-1 (Gαo), which interacts with another G-protein, EGL-30 (Gαq) to regulate the immune response.

Pathogen Detection and Avoidance

C. elegans seems to lack the majority of the canonical pathogen recognition receptors (PRRs), but maintains a robust detection system that senses external bacterial cues and internal physiological disturbances or patterns of pathogenesis. In plants and higher animals, pathogen recognition is mainly mediated by a set of PRRs that detect conserved pathogen-derived molecules, known as pathogen-associated molecular patterns (PAMPs) or microbe-associated molecular patterns (MAMPs). The best characterized PRRs are a family of conserved transmembrane Toll-like receptors (TLRs) that recognize various microbial products, such as bacterial cell-wall components and flagellin, and trigger multiple defense response pathways. The genome of *C. elegans* does not encode the majority of known PRRs and lacks genes of some key components of the TLR pathways such as NF-κB homologs and the TLR adaptor MyD88. Nematode orthologs of Toll-like receptor (TOL-1), TNF receptor-associated factor-1 (TRF-1), Pelle and IL-1R-associated kinases (PIK-1), and inhibitor of NF-κB

(IKB-1) do not seem to play major roles in immunity. However, it is worth noting that TOL-1 has been implicated in immune signaling during *S. enterica* infection (21) and that TIR-1, a scaffold protein containing Toll/IL-1R (TIR) protein–protein interaction domain, is involved in antimicrobial defense against a variety of *C. elegans* pathogens (44, 49). *C. elegans* is also capable of activating immune pathways when exposed to heat-killed *S. aureus* and *C. albicans*, suggesting that the nematode can detect pathogenic microbes via MAMP recognition (18, 46).

Lacking the traditional set of PRRs used to detect pathogens, *C. elegans* seems to rely on the sensation of external bacterial cues and endogenous pathways to initiate avoidance and the innate immune responses. Critical to this are GPCRs, which may play direct or indirect roles in pathogen detection in *C. elegans*. The nematode uses neuronal GPCR-mediated signaling to sense bacterial compounds, responding by avoiding pathogens and activating immune pathways (76, 81, 87, 88). Furthermore, dihydrocaffeic acid receptor (DCAR-1), a GPCR that functions in the epidermis, activates innate immunity by recognizing an endogenous ligand, 4-hydroxyphenyllactic acid. This ligand potentially acts as a danger signal to alert the animals of fungal infections (89). GPCRs, along with ion channels, neurotransmitters, and neuropeptides are integral to how *C. elegans* uses its repertoire of sensory modalities and small nervous system to detect pathogens, via both environmental and internal cues, and initiate avoidance behaviors. Reducing exposure to pathogens is a major line of defense found throughout the animal kingdom. The set of behaviors an animal deploys to protect against pathogen infection is often referred to as the behavioral immune response. For *C. elegans*, avoidance behaviors range from toxin-induced withdrawal reflexes to trans-generationally stable learned avoidance (**Fig. 6**). The following subsections describe these behaviors, with a focus on the neurons, GPCRs, ion

channels, and signaling pathways required for pathogen avoidance, and the internal cues the animal uses to sense danger.

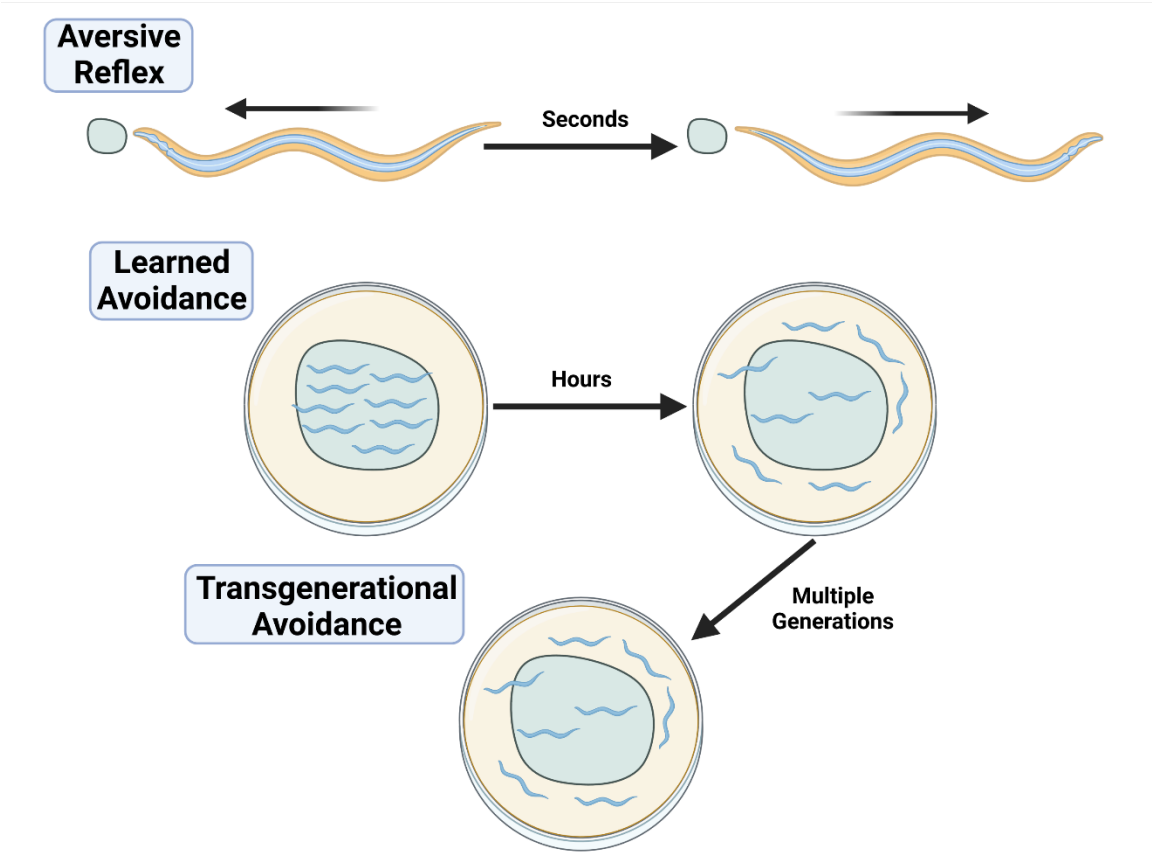

Fig. 6. Behavioral immune responses range from aversive reflexes to transgenerational learned avoidance behaviors. When *C. elegans* crawls forward and encounters a drop of a pathogenic bacteria or a substance produced by a pathogen, it can react by quickly initiating an omega turn to reverse its direction (top). The nematode can also learn to avoid certain pathogens over the course of several hours, with the exact dynamics varying for each pathogen (middle). Some pathogens also seem to initiate a transgenerationally stable avoidance memory in the nematode that persists for several generations. A single prolonged encounter with a pathogenic bacterium in adult *C. elegans* can result in an avoidance memory that lasts five generations (bottom).

Aversive reflexes

Some pathogens produce toxins that cause an aversive withdrawal when presented to moving animals. For example, many *Streptomyces* species produce antinematodal compounds, such as avermectin (90). The *Streptomyces* avoidance response requires the detection of bacterially secreted dodecanoic acid by the GPCR SRB-6. SRB-6 is expressed in five different amphid (head) and phasmid (tail) chemosensory neurons: ASH, ADL, ADF, PHA, and PHB. At least one of these, ASH, was shown to respond to both *S. avermitilis* supernatant and dodecanoic acid in an *srb-6*-dependent manner via calcium imaging. The role of the other neurons remains to be determined, as does the downstream neuronal circuitry required to produce the aversive response. While not the main focus, Chapter 3 of this dissertation lays out a potential circuit for this behavior.

S. marcescens also produces an aversive molecule, surfactant serrawettin W2, that induces aversive withdrawal (87). The AWB olfactory neurons mediate this behavior as evidenced by loss of aversive response in animals lacking functional AWB neurons. Mutations in cGMP-gated channels encoded by the *tax-2* and *tax-4* genes, expressed in AWB and other neurons, suppress aversion to *S. marcescens*. Additionally, mutants for *odr-3*, the *C. elegans* G_i-like protein-encoding gene, and the G protein receptor kinase encoded by *grk-2* are deficient in *S. marcescens* avoidance, implicating G-protein signaling. The GPCR responsible for the detection of serrawettin W2, however, remains unknown. Intriguingly, avoidance of *S. marcescens* takes place after a couple of hours of exposure, while aversion to high concentrations of serrawettin W2 takes place instantly in even naïve animals. This may result from either lower concentration of serrawettin produced by the bacterium than used in the chemical treatment or *S. marcescens* producing several molecules including attractants such as

acetone and butanone, in addition to serrawettin (91). The calcium signaling response of specific neurons to *S. marcescens* versus various doses of serrawettin would be necessary to decipher circuits involved in avoidance of *S. marcescens*.

Learned avoidance

Bacterial metabolites have also been implicated in the avoidance of *P. aeruginosa*. The secondary metabolites phenazine-1-carboxamide and pyochelin induce expression of the neuroendocrine signaling molecule DAF-7/TGF-β in ASI and ASJ chemosensory neurons (92). The TGF-β pathway is thought to modulate aerotaxis behavior and promote avoidance of *P. aeruginosa* via *daf-1* dependent communication with downstream RIM/RIC interneurons. The detection of these metabolites probably involves an unidentified GPCR, as *gpa-2* and *gpa-3*, which encode G protein α subunits, were implicated. It is important to note, however, that phenazine-1-carboxamide added to *E. coli* lawns does not induce avoidance, nor do *P. aeruginosa* mutants lacking phenazine synthesis pathways alter avoidance responses in *C. elegans* (93). Additionally, the induction of DAF-7 in ASJ neurons takes place within minutes of exposure, while avoidance of *P. aeruginosa* takes several hours. Thus, how DAF-7 induction in ASJ neurons by phenazines contributes to avoidance remains unclear.

Avoidance of *P. aeruginosa* takes hours because *C. elegans* is initially attracted to the pathogen (94). Given a choice between *P. aeruginosa* and *E. coli*, naïve animals will choose the former. Thus, a switch in preference such that *P. aeruginosa* goes from attractive to aversive must take place for avoidance to occur. A number of bacterial cues and neuronal pathways have been implicated in this preference switch, often described as learned avoidance. One of the first to be recognized was an olfactory preference. The olfactory neurons AWB and AWC establish the naïve olfactory preference for *P. aeruginosa* over *E. coli* (95). The choice between the two bacteria is mediated via a

sensorimotor circuit involving these two olfactory neurons along with the interneurons AIZ, AIY, and AIB, and the motor neurons RIM and SMD. Furthermore, neuromodulation of this circuit by the serotonergic ADF neurons and down- stream RIA interneurons may generate the learned olfactory preference (94, 95).

A recent study indicates that a volatile compound, 1-undecene, produced by *P. aeruginosa* is a repellent for *C. elegans* (37). The production of this MAMP is dependent on the bacterial non-heme iron oxidase UndA. The volatile induces a calcium response in AWB neurons in a dose-dependent manner, causing aversion as well as omega turns, a locomotory behavior seen only in the presence of aversive cues. 1-undecene appears to be a genuine MAMP, since the exposure of *C. elegans* to 1-undecene alone enhances expression of IRGs, *irg-1*, *irg-2*, *irg-3*, in a ZIP-2 transcription factor dependent manner. Chapter 2 will describe an additional olfactory-mediated learned avoidance response to *E. faecalis* infection.

In addition to olfaction, modulation of aerotactic behaviors may partly underly learned avoidance behaviors (92, 93). Both NPR-1 and DAF-7 pathways are important for aerotaxis and regulate hypoxia avoidance in *C. elegans*. Inhibition of these pathways elicits avoidance of high oxygen, while higher activity induces avoidance of low oxygen. *P. aeruginosa* infection is known to increase the activity of these pathways. Additionally, bacterial lawns have lower oxygen levels than the surrounding environment due to the consumption of oxygen by the growing bacteria (96). Thus, animals tend to avoid the lawns after infection because of a preference for higher oxygen levels induced by NPR-1 and DAF-7 activity. Interestingly, *E. coli* lawns were reported to have higher oxygen levels than *P. aeruginosa* lawns, which may explain the switch in lawn preference. Another possibility is that there is a threshold level of oxygen that negates aversion such that *E. coli* negates aversion but *P. aeruginosa* does not;

both explanations seem equally likely, with no experimental evidence ruling out either one thus far. NPR-1 is notably expressed in the oxygen sensing neurons AQR, PQR, and URX, which have their sensory cilia embedded in the pseudocoelomic space (76, 97), where they likely function to control pathogen avoidance (and innate immune regulation, see previous section). DAF-7 is expressed in ASI and ASJ neurons, as noted above. Interestingly, animals lacking ASI neurons were shown to have reduced avoidance of *P. aeruginosa* (83). Various studies have implicated other gases in pathogen avoidance, including ASJ neuron-mediated sensation of nitric oxide (98) and BAG neuron-mediated sensation of carbon dioxide (99). The latter takes place in the context of *S. marcescens* and involves TOL-1, demonstrating an interesting overlap between innate and behavioral immune pathways.

How various environmental cues are integrated in the nervous system to come to a decision to avoid a given pathogen remains unclear, though there is some evidence that there is a convergence of signals in interneurons downstream of the sensory neurons described above. For example, activation of ASI neurons leads to the release of the insulin-like peptide INS-6 (100). INS-6 inhibits *ins-7* ex- pression in URX neurons, which leads to upregulation of DAF-2 activity in the RIA interneurons. These interneurons, as noted above, are also involved in the olfactory learning circuit, and so may be an important integrator of distinct environmental cues influencing avoidance behaviors.

Chapter 3 will touch on an additional question: how do the chemosensory inputs described here get translated into the motor neuron outputs necessary for avoidance? There is very little research on this topic, but advances in computational modeling and the availability of whole-brain wiring diagrams for *C. elegans* will aid

research into this important topic. In the course of answering this question, Chapter 3 will also describe an interesting link between aversive reflexes and learned avoidance.

Transgenerational avoidance

Several recent studies have established that learned behaviors, including pathogen avoidance, can be passed down several generations in *C. elegans* (101–104). In the initial discovery of transgenerational pathogen avoidance, it was shown that *C. elegans* that have learned to avoid *P. aeruginosa* can pass this learning onto their progeny (103). This requires the Piwi/Argonaute homolog PRG-1 and the TGF-β ligand DAF-7 in ASI sensory neurons, and involves epigenetic and transcriptional changes that get passed down to progeny. A follow-up study showed that a small RNA from *P. aeruginosa*, P11, is capable of inducing avoidance in both hermaphrodite parents and progeny for up to four generations before a gradual decay back to parental levels (102). Detection and subsequent avoidance behaviors require RNA interference and PIWI-interacting RNA pathways in the intestine, the germline, and ASI neurons. The *C. elegans* homolog of the mammalian neuronal gene macoilin, *maco-1*, was also shown to regulate *daf-7* expression in ASI neurons in response to P11, and was interpreted to be the target of P11. The RNAi genes *sid-1, sid-2*, and *dcr-1* are required for the intestine-to-germline signaling, and *Cer1* retrotransposon-encoded virus-like particles were proposed to be the signaling molecule for germline-to-neuron communication (104). Microbial colonization of the intestine also seems to induce 14–3–3 chaperone protein PAR-5-dependent histone H4 Lys8 acetylation in the germline, which influences both learned avoidance and its transmission to the next generation (101). Chapter 2 will show that small RNAs do not account for avoidance of *E. faecalis*, and so these mechanisms may be specific to certain pathogens.

Endogenous pathogenesis surveillance mechanisms

C. elegans appears to have evolved cellular surveillance systems to monitor its core cellular activities and interpret disruption of specific activities as evidence of pathogen attack. The innate immunity elicited by this kind of indirect recognition is similar to effector-triggered immunity (ETI) that was originally demonstrated in plants (105) and later found conserved across invertebrate and vertebrate animals (106, 107). An example of ETI in *C. elegans* is its response to a virulence factor of *P. aeruginosa*, Exotoxin A (ToxA). Upon infection with *P. aeruginosa*, ToxA enters the intestinal epithelial cells, likely via endocytosis, and inhibits protein translation by modifying elongation factor 2 via ADP-ribosylation, which triggers the host to up-regulate immune defense genes (36, 108). Besides protein translation, disruption of many other cellular functions such as mitochondrial respiration, ubiquitin-proteasome system activity, or actin cytoskeleton and microtubule dynamics, results in activation of detoxification and immune responses in *C. elegans* (69, 109). Pore-forming toxins (PFTs), the single largest class of proteinaceous bacterial virulence factors that perforate host cell membranes, can also trigger ETI in the nematode, although the precise molecular mechanisms remain unknown (110). It has been suggested that the host cells can sense disruption of the cell membrane, potassium efflux, or calcium influx and respond with antimicrobial signaling and membrane repair pathways (111, 112).

Recently, it has also been shown that intestinal distention is an important trigger for *C. elegans* pathogen avoidance (93, 113). *P. aeruginosa* induces intestinal distention throughout the intestine. How intestinal distention is detected and the signal passed along to the nervous system to initiate avoidance is not fully understood. One

study showed that distention itself increases NPR-1 and DAF-7 activity, thus modulating aerotaxis as described above (113).

One of the main contributions of this dissertation is to show that *E. faecalis* also causes intestinal distention. The details of this distention, along with potential mechanisms for sensing the distention, are presented in Chapter 2. Mechanosensation likely plays also a role in sensing intestinal distention, though the only confirmed role for mechanosensation in pathogen avoidance is in the avoidance of *P. aeruginosa* via a conserved HECT domain-containing E3 ubiquitin ligase, HECW-1 (114). However, HECW-1 functions in the nervous system, specifically OLL neurons, to inhibit NPR-1 activity, and so the role of mechanosensation in the detection of intestinal distention remains unclear. The intestine is not directly innervated, so any signal that needs to be passed along must be extra-synaptic, perhaps via a neuropeptide like the insulin-like peptide INS-11 (115).

Overall, ETI offers *C. elegans* an effective and versatile strategy to detect and distinguish pathogens from surrounding microbes. This allows the nematode to combat a wide variety of microbes without evolving the full repertoire of PRRs. It remains to be addressed how the nematode can distinguish infecting microbes if different pathogens disrupt the same cellular processes, as immune responses are not only pathogen-shared but also pathogen-specific (18, 29, 57, 116, 117).

Thesis Overview

This dissertation somewhat touches on this issue of pathogen-specific responses, as the following research chapter details how *E. faecalis* causes a fast pathogen avoidance response due to intense intestinal distention, much faster than the response to *P. aeruginosa*. Anterior intestinal distention is most important for the *E. faecalis* avoidance response, again differentiating it from the intestine-wide distention caused by *P.*

aeruginosa. Further dissimilarities stem from the fact that this intestinal distention and avoidance occur before immune signaling pathways such as *pmk-1*-mediated pathways and immune effectors such as *clec-60* come online. Even further, bacterial small RNAs do not seem to play a role in the avoidance of *E. faecalis* as they do for *P. aeruginosa*. Instead, chemosensory neurons, especially olfactory neurons, are used to associate bacterial cues such as odors with the intestinal distention. It is this association between cues and infection that allows the animal to evade the bacteria after initial exposure. Two transient receptor potential melastatin (TRPM) channels expressed in the intestinal and excretory cells, GON-2 and GTL-2, are key in establishing the *E. faecalis* association.

Avoidance of *P. aeruginosa* also shares the olfactory aversive learning mechanism; however, the unique odor cue coming from the bacteria allows the animal to successfully evade the distention-inducing pathogen. This specificity is evident from the cross-training experiments presented in Chapter 3, where infection with *P. aeruginosa* does not lead to *E. faecalis* avoidance, and vice versa. Pairing the odor of one pathogen with infection by the other, however, does cause the animal to avoid the odor-paired pathogen. The main finding presented in this second research chapter, however, is the neural circuitry linking olfactory and motor neurons necessary for avoidance. Simulations of the entire *C. elegans* nervous system where specific neurons are stimulated and ablated *in silico* and network activity can be monitored allow for the identification of neurons that are crucial components of the avoidance circuit. Using these simulations, AUA and RMG interneurons are found to be part of a four-layer circuit for olfactory aversive learning. These interneurons form electrical synapses with AWB olfactory neurons, passing signals down to motor command neurons and eventually the motor neuron subtypes involved in backward locomotion. Further functional assays using animals with genetically ablated AUA and RMG interneurons confirm the predictions of the simulation. The last chapter of this dissertation represents

a marked shift in focus and tone. It contains a brief summary of the main research findings; however, the main goal of this concluding chapter is to scrutinize the techniques and methodology used in the dissertation in order to suggest promising future research directions.

CHAPTER 2: TRPM CHANNELS MEDIATE LEARNED PATHOGEN AVOIDANCE FOLLOWING INTESTINAL DISTENTION[2]

Background

The preceding chapter has hopefully convinced the reader that *C. elegans* is a useful model for pathogen avoidance. A full understanding of the complex behavioral survival mechanisms will obviously take an interdisciplinary approach, with inputs from fields ranging from molecular biology to sociology, but *C. elegans* models are quite adept at uncovering the molecular and cellular components of pathogen avoidance.

Many questions remain unanswered or understudied, however. For example, as mentioned in the preceding chapter it was recently proposed that bacterial colonization causes a distension of the *C. elegans* intestine that may be used as a general mechanism to activate immune pathways and pathogen avoidance (93, 113, 118). How intestinal distention leads to avoidance, though, remains unclear. One possibility is that mechanoreceptors on intestinal cells sense the pressure caused by distention and then send neuropeptide signals to the nervous system to initiate avoidance. While no mechanoreceptors have been found to be functional in the *C. elegans* intestine, the intestinal epithelial cells do express transient receptor (TRP) channels which could act as mechanoreceptors (119). However, TRP channels are known to play many other roles, including but not limited to taste, thermoregulation, ion homeostasis, and pacemaker activity (120). Indeed, while the TRP vanilloid (TRPV) channel genes *ocr-2* and *osm-9* are known to inhibit avoidance of the pathogen *Pseudomonas aeruginosa* (93), this inhibition is through their role on hyperoxia avoidance rather than direct sensing of bacteria or distention. Moreover, they are not expressed in the *C. elegans* intestine. One

[2]This chapter is largely based on A. Filipowicz, J. Lalsiamthara, and A. Aballay, TRPM channels mediate learned pathogen avoidance following intestinal distention. *eLife*, 10: e65935 (2021).

TRP channel that is expressed in the *C. elegans* intestine is the thermosensitive channel TRPA-1 (121). TRPA-1 also plays a role in sensory neuron-mediated nose-touch responses (122). Interestingly, the *Drosophila* homolog of this channel was shown to be involved in avoidance of bacterial lipopolysaccharide (LPS), though activity of this channel was localized to gustatory neurons (Soldano et al., 2016). The mammalian digestive system expresses many TRP channels, including members of the TRPA, TRP melastatin (TRPM) and TRPV families (120). Because nearly all of these channels are conserved across species, identification of their role in pathogen avoidance in *C. elegans* is likely to improve our understanding of pathogen avoidance in a range of organisms.

This chapter presents evidence that *C. elegans* avoids *Enterococcus faecalis* faster than *P. aeruginosa*. In contrast to the *P. aeruginosa*-mediated avoidance that requires small RNAs (sRNAs) (102), *E. faecalis* does not depend on sRNAs, nor does it require ASI neurons, full bacterial virulence, or innate immune activation. Instead, avoidance occurs after a rapid expansion of the anterior part of the intestine. This avoidance behavior, which exists in opposition to an NPR-1-mediated hyperoxia avoidance process, requires the ASE, AWB, and AWC chemosensory neurons. These latter two neuron pairs regulate an olfactory aversive learning process that underpins avoidance of *E. faecalis*. Finally, two novel regulators of intestinal distention-induced pathogen avoidance are identified: the TRP melastatin (TRPM) channels GON-2 and GTL-2.

Results

E. faecalis elicits fast avoidance in C. elegans

C. elegans is a free-living nematode that feeds on organic material rich in microorganisms, and therefore frequently encounters pathogenic bacteria. It has developed behavioral strategies to minimize exposure to these threats. For example, it

avoids the pathogenic *P. aeruginosa* bacteria slowly, taking between 12 to 24 hours to execute aerotactic and olfactory aversive learning processes depending on the bacterial growth conditions used (93, 94). In contrast, it was previously reported that animals quickly avoid the lawns of the Gram-positive pathogens *E. faecalis, E. faecium,* and *S. aureus* (113). Examining this in more detail, it was found that animals displayed strong, fast avoidance of monoaxenic lawns of *E. faecalis, E. faecium,* or *S. aureus* grown on brain heart infusion (BHI) media (**Fig. 7A and B**, and **Fig. S1**). While population avoidance levels peaked at 4 hours for *E. faecalis*, wild-type animals first leave *E. faecalis* lawns at around 19 minutes on average (**Fig. 7C**). Interestingly, animals were observed frequently exiting and entering the bacterial lawns over time. Quantification of these events revealed a slight imbalance favoring exiting events as early as 1 hour, with this difference growing larger in the 3–4-hour window due to a decrease in the entry events (**Fig. 7D**).

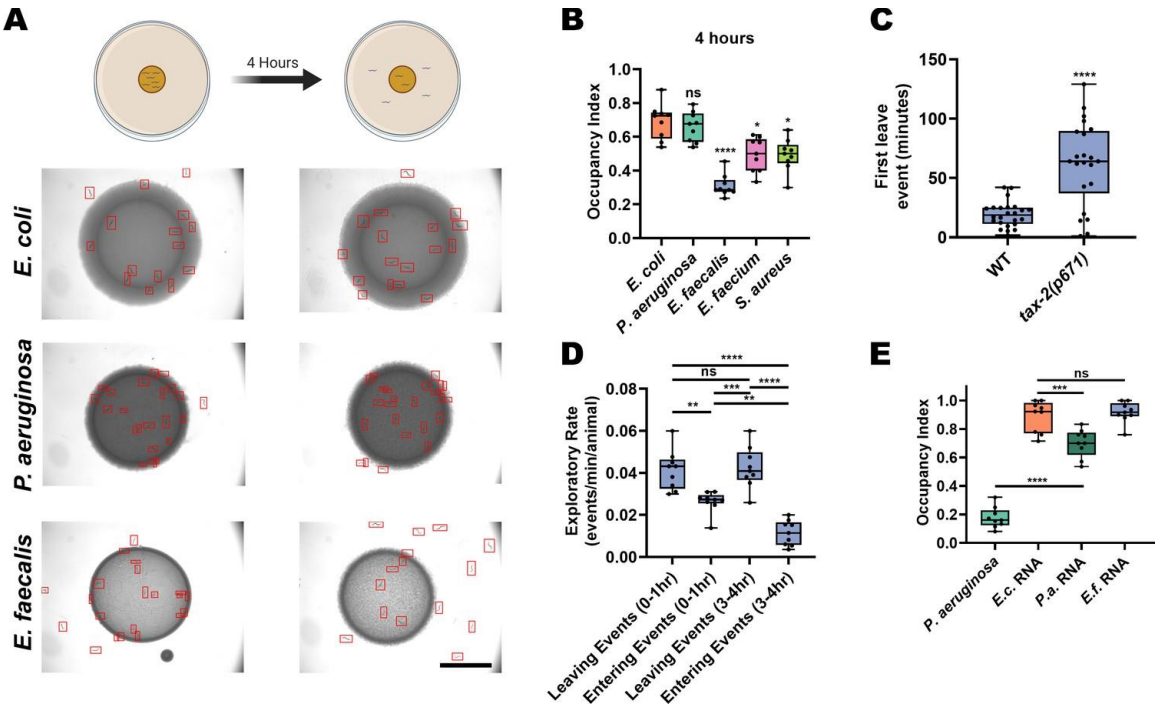

Fig. 7. *E. faecalis* elicits fast avoidance in *C. elegans*. (**A**) Schematic of avoidance assays (top) and representative photomicrographs (bottom) of *C. elegans* on lawns of *E. coli* OP50, *P. aeruginosa* PA14, or *E. faecalis* OG1RF at 0 hr (left) and 4 hr (right) on BHI media. Individual animals are outlined in red. Scale bar, 5 mm. (**B**) Occupancy index of N2 animals after 4 hr of incubation on *E. coli*, *P. aeruginosa*, *E. faecalis*, *E. faecium*, or *S. aureus*. One-way ANOVA with subsequent comparison to *E. coli* as the control group was performed. Occupancy Index = (number of animals on bacterial lawn)/(total number of animals). (**C**) Individual animals were tracked on lawns of *E. faecalis* and the time that they first left the lawn after transfer was recorded. Wild-type (WT, N2 Bristol) animals showed an average first leave time of 19.20 min while *tax-2(p671)* animals showed an average first leave time of 61.98 min. An unpaired t-test between the groups was performed. (**D**) N2 animals on standard avoidance assays plates with *E. faecalis* were observed for 10 min during two different time windows (0–1 hr and 3–4 hr) and the number of times the animals left and entered the bacteria lawns was counted. One-way ANOVA with subsequent comparisons between all groups was performed. (**E**) Occupancy index of N2 animals after 24 hr incubation on *P. aeruginosa* PA14 lawns or *E. coli* OP50 lawns supplemented with isolated total RNA from *E. coli* (*E.c.* RNA), *P. aeruginosa* (*P.a.* RNA), or *E. faecalis* (*E.f.* RNA). One-way ANOVA with subsequent comparison to *E. coli* RNA as the control group was performed.

The fast exiting events induced by *E. faecalis* are reminiscent of a *C. elegans* rapid aversive behavior elicited by exposure to a dry-drop of dodecanoic acid, a toxin secreted by *Streptomyces* (90). However, implementing this dry-drop assay with live *E. faecalis* or *E. faecium* did not induce an aversive response (**Fig. S1**), indicating that direct contact with live replicating bacteria is required for the rapid avoidance of *E. faecalis* or *E. faecium*. Rapid aversion alone also cannot explain the re-entry events. Instead, it is likely that there is a balance of attraction and aversion to *E. faecalis* that

changes over the course of exposure. Thus, the animals learn to avoid *E. faecalis* quickly after exposure. This process likely involves sensory pathways, as animals with loss-of-function mutations in *tax-2,* a subunit of a cGMP-gated-ion-channel important for sensory neuron function (124), show slowed avoidance (**Fig. 7C**). Because it has recently been suggested that the sensation of a bacterial sRNAs is at least partly responsible for learned *P. aeruginosa* avoidance (102), RNA from *E. faecalis* was examined to determine whether it also can elicit avoidance. Unlike RNA from *P. aeruginosa*, RNA from *E. faecalis* fails to induce avoidance (**Fig. 7E**). The fact that exposure to bacterial sRNAs only accounts for ~25% of the avoidance of *P. aeruginosa,* and that they have no role in avoidance of *E. faecalis,* suggests that another pathway is required to induce pathogen avoidance.

Avoidance of E. faecalis follows anterior intestinal distention and is independent of virulence

Two other potential pathways for induction of avoidance are sensation of intestinal distention or bacterial metabolites. The bacterial metabolite serrawettin W2 is responsible for the avoidance of *S. marcescens* (87). Even though secondary metabolites phenazine-1-carboxamide and pyochelin produced by *P. aeruginosa* are insufficient for the elicitation of pathogen avoidance (93), they are sensed by *C. elegans* as they elicit induction of DAF-7/TGF-β in ASJ neurons (125). However, *E. faecalis* does not increase expression of DAF-7 in the ASJ neurons (125), further strengthening the idea that direct contact with this pathogen rather than metabolite sensing induces avoidance.

To determine whether intestinal distention plays a role in avoidance of *E. faecalis*, measurements were conducted for the diameter of the intestinal lumen of animals fed either *E. coli, P. aeruginosa,* or *E. faecalis* grown on BHI. There was significant expansion of the anterior part of the intestine of animals feeding on *E.*

faecalis compared to *E. coli* even at 1 hour, with distention persisting at 4 hours (**Fig. 8A and B**). The medial part of the intestine was not significantly distended at 1 hour compared to animals fed *E. coli*, but was distended at 2 and 4 hours. The anterior part of the intestine was slightly distended in animals feeding on *P. aeruginosa* compared to *E. coli* at 4 hours, but was otherwise not distended. Both parts of the intestine, but especially the anterior portion, were filled with live *E. faecalis*, as determined through the use of an *E. faecalis* strain expressing GFP, while the intestine of animals fed *E. coli* or *P. aeruginosa* expressing GFP were relatively empty and not distended (**Fig. 8C**). Because the first measurement of the anterior intestinal diameter was at 1 hour, it was not clear whether distention preceded avoidance or vice versa. To explore this, animals were tracked until they left a lawn of *E. faecalis* and measurements of their anterior intestines were taken (**Fig. S2**). These animals had significantly larger anterior intestines compared to animals that remained on the *E. faecalis* lawn. It is therefore likely that fast accumulation of *E. faecalis* in the anterior intestine induces an aversive response to the pathogen, leading to avoidance.

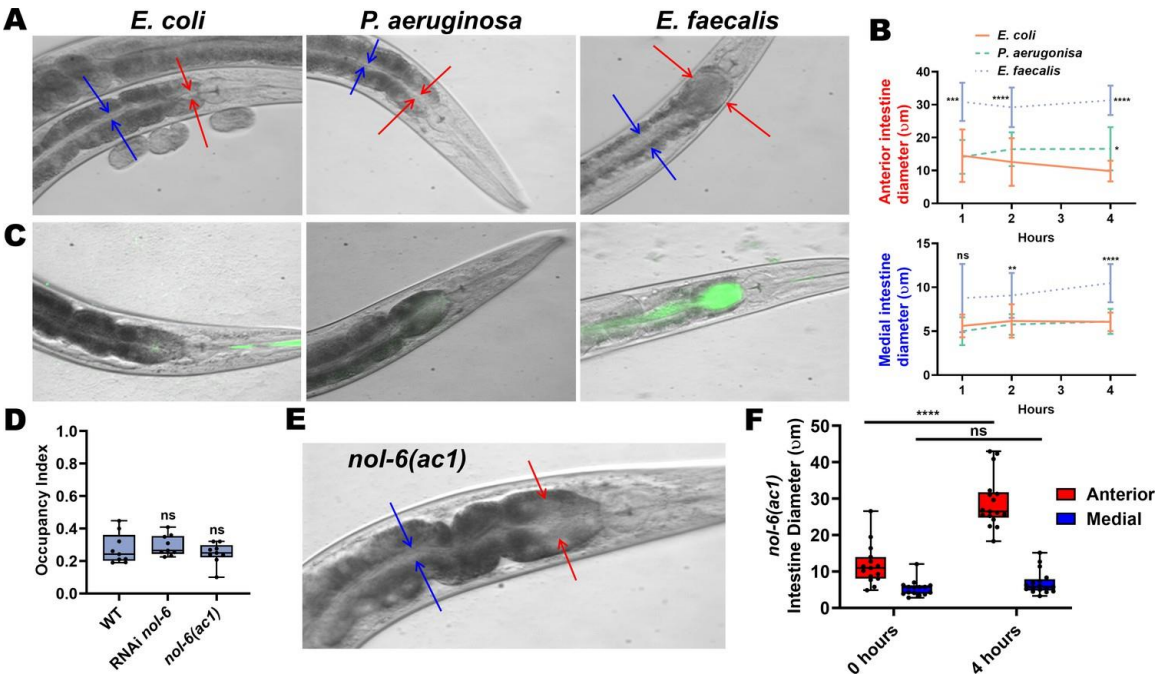

Fig. 8. Anterior intestinal distention elicits avoidance of *E. faecalis.* (**A**) Representative photomicrographs of animals at 4 hr on BHI media with *E. coli* (left), *P. aeruginosa* (middle), or *E. faecalis* (right). Red arrows point to the borders of the anterior intestine while blue arrows point the borders of the medial intestine. (**B**) Quantification of the anterior (top) and medial (bottom) intestinal lumen diameter of animals on *E. coli*, *P. aeruginosa*, or *E. faecalis* at 1, 2, and 4 hr. Two-way ANOVA was performed with comparison to the *E. coli* group at each time point. For *E. coli*, N = 11, 13, and 17 at 1, 2, and 4 hr, respectively. For *P. aeruginosa*, N = 18, 14, and 18. For *E. faecalis*, N = 13, 18, and 16. Points are the mean of each group and error bars are standard deviation. (**C**) Representative photomicrographs with fluorescent and brightfield images merged of *E. coli, P. aeruginosa*, and *E. faecalis* expressing GFP in the intestinal lumen of animals at 4 hr. (**D**) Occupancy index on *E. faecalis* at 4 hr of WT animals compared to either RNAi-mediated knockdown of *nol-6* or a loss-of-function mutation in *nol-6*. One-way ANOVA was performed with subsequent comparison to the WT group as the control. (**E**) A representative photomicrograph of a *nol-6(ac1)* animal after exposure to *E. faecalis* for 4 hr. Red arrows point to the borders of the anterior intestine, and blue arrows point to the borders of the medial intestine. (**F**) Quantification of anterior and medial intestinal lumen diameter of *nol-6(ac1)* animals at 0 and 4 hr on *E. faecalis*. Two-way ANOVA was performed with comparison to the 0 hr groups for both anterior and medial quantifications.

RNA interference (RNAi)-mediated knockdown of *nol-6*, a nucleolar RNA-associated protein, reduces colonization and distention of the intestine by microbial pathogens (126). Furthermore, knockdown of *nol-6* delays avoidance of *P. aeruginosa* by delaying intestinal distention(93) (**Fig. S3**). Therefore, testing of both *nol-6* RNAi and a *nol-6* loss-of-function (lf) mutant (*nol-6(ac1)*) for avoidance of *E. faecalis* was warranted. Avoidance for both the mutant and *nol-6* RNAi remained at wild-type levels (**Fig. 8D**). Interestingly, while anterior intestinal distension was observed in both *nol-*

6(ac1) and *nol-6* RNAi animals fed *E. faecalis* at 4 hours, the middle part of the intestine did not display significant distention (**Fig. 8E and F,** and **Fig. S3**). This suggests that the anterior, but not medial, intestinal distention triggers avoidance of *E. faecalis*.

To determine whether bacterial virulence is required for anterior intestine distention induced avoidance of *E. faecalis*, a strain of *E. faecalis* lacking the *fsrB* gene (*E. faecalis ΔfsrB*), a gene important for quorum sensing, which displays significantly reduced virulence across multiple animal models was used (17, 19, 127). Surprisingly, this avirulent strain also elicits avoidance (**Fig. 9A**) and causes anterior intestinal distention (**Fig. 9B**). Lending further evidence to the notion that virulence plays no role in avoidance, *E. faecium*, a related enterococcal species that is non-pathogenic to *C. elegans* (17, 128), also elicits avoidance (**Fig. 9B**). While *E. faecium* is non-pathogenic to *C. elegans* it does cause an innate immune response (128), raising the possibility that an early immune response may be responsible for alerting the animal to avoid *E. faecalis* and related species upon ingestion.

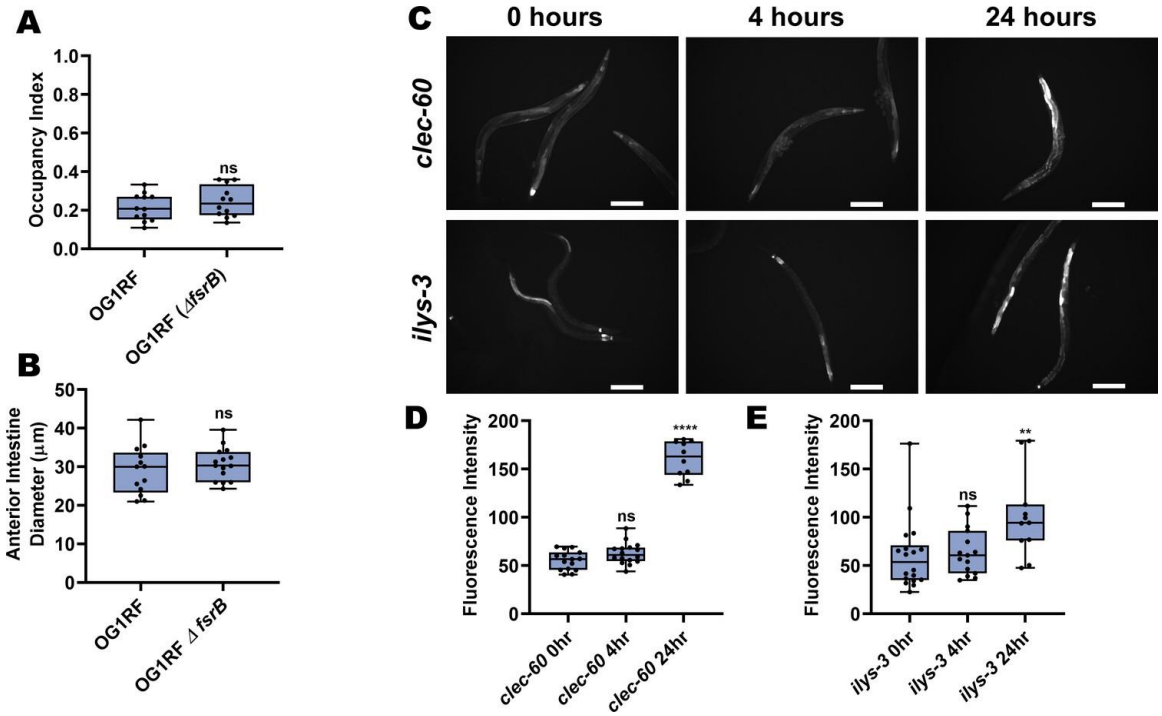

Fig. 9. Avoidance of *E. faecalis* is independent of virulence. (**A**) Occupancy index of N2 animals on virulent *E. faecalis* OG1RF and avirulent *E. faecalis* OG1RF *ΔfsrB* at 4 hr. An unpaired t-test was performed. (**B**) Quantification of anterior intestinal diameter of N2 animals on *E. faecalis* strain OG1RF or OG1RF Δ*fsrB* at 4 hr. An unpaired t-test was performed. (**C**) Representative fluorescent micrographs of *clec-60p::GFP* (top) and *ilys-3p::GFP* (bottom) animals at 0, 4, and 24 hr on *E. faecalis*. Scale bar, 200 μm. (**D**) Quantification of *clec-60::GFP* at 0, 4, and 24 hr on *E. faecalis*. One-way ANOVA was performed with comparisons to the 0 hr group as the control. (**E**) Quantification of *ilys-3p::GFP* at 0, 4, and 24 hr on *E. faecalis*. One-way ANOVA was performed with comparisons to the 0 hr group as the control.

Therefore, examination of the *in vivo* expression of two immune pathway markers, *clec-60* (18, 128) and *ilys-3* (18, 128, 129), was used to determine whether an immune response was mounted at these early timepoints. While a later immune response could be observed, there was no evidence of an immune response at timepoints where early avoidance of *E. faecalis* is observed (**Fig. 9C-E**). Furthermore, loss-of-function mutants for three key immune signaling genes, *pmk-1, fshr-1,* and *bar-1*, displayed wild-type levels of avoidance of *E. faecalis* (**Fig. S4**). Altogether, these results suggest that virulence and immune pathway activation is not necessary for anterior distension and avoidance of *E. faecalis*, differentiating this avoidance mechanism further from that induced by *P. aeruginosa*, which requires virulence and intestine-wide distension (93, 113, 118).

TAX-2/4 pathways regulate avoidance of E. faecalis and P. aeruginosa

NPR-1, known to play a role in *C. elegans* survival and behavior on pathogens (76, 88, 92), is responsible for the intestinal distention induced avoidance behavior on *P. aeruginosa*. One hypothesis is that NPR-1 also plays a role in avoidance of *E. faecalis*. As a first step to test this, measurement of the avoidance of *E. faecalis* in two *npr-1 (lf)*

mutants found that both displayed decreased avoidance compared to wild-type animals (**Fig. 10A**).

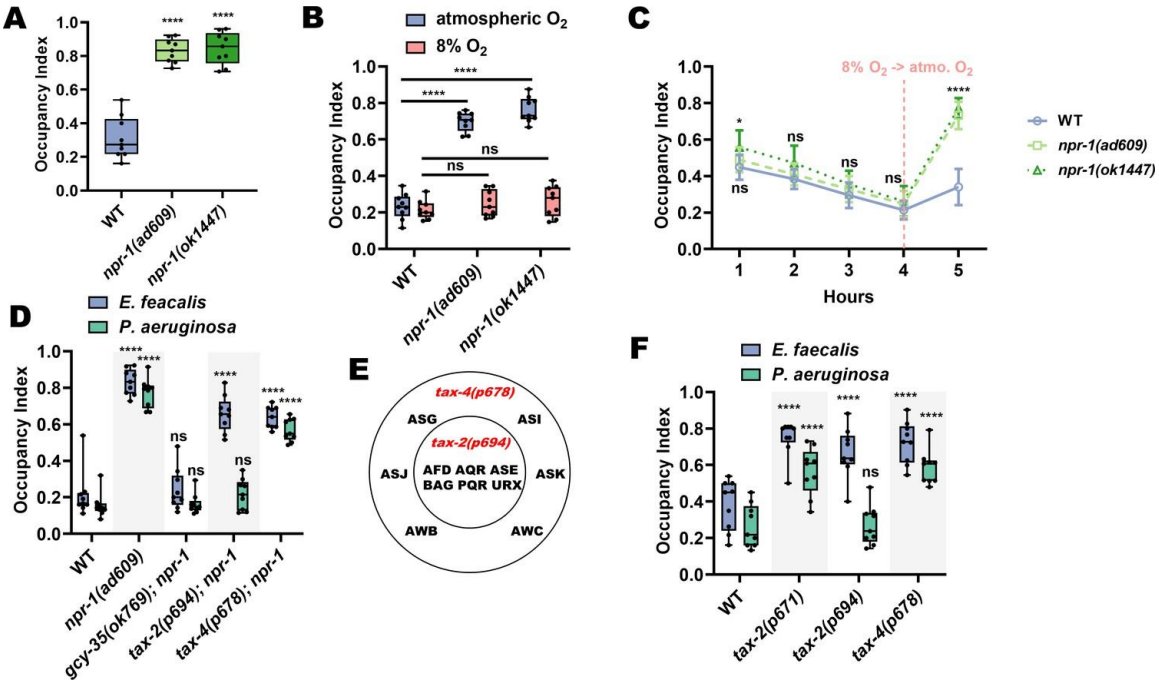

Fig. 10. TAX-2/4 pathways regulate avoidance of *E. faecalis* and *P. aeruginosa*. (**A**) Occupancy index of WT animals compared to *npr-1(ad609)* and *npr-1(ok1447)* after 4 hr on *E. faecalis.* One-way ANOVA with subsequent comparison to WT animals as the control group was performed. (**B**) Occupancy index of WT, *npr-1(ad609)* and *npr-1(ok1447)* on lawns of *E. faecalis* in atmospheric oxygen or a chamber containing 8% oxygen. Two-way ANOVA with subsequent comparison to WT animals of each respective oxygen condition was performed. (**C**) Occupancy index of WT, *npr-1(ad609)*, and *npr-1(ok1447)* in an 8% oxygen chamber at 1, 2, 3, and 4 hr, and 1 hr after removal from the chamber (vertical dashed line). Two-way ANOVA with subsequent comparison at each time point to WT animals was performed. N = 9 for all animals. Points are the mean of each group and error bars are standard deviation. (**D**) Occupancy index for WT and double loss-of-function mutants for *gcy-35*, *tax-2*, or *tax-4*, and *npr-1* on *E. faecalis* for 4 hr and *P. aeruginosa* for 24 hr. Two-way ANOVA with subsequent comparisons to WT animals for each

bacterium were performed. (**E**) Diagram of the neurons affected by *tax-2(p694)* and *tax-4(p678)*. The latter allele covers all *tax-2* expressing sensory neurons, while the former covers a subset. (**F**) Occupancy index for WT and single loss-of-function mutants for *tax-2* or *tax-4* on *E. faecalis* for 4 hr and *P. aeruginosa* for 24 hr. Two-way ANOVA as in with subsequent comparisons to WT animals for each bacterium were performed.

Inhibition of NPR-1 elicits avoidance of high oxygen (130–132), resulting in suppression of *P. aeruginosa* avoidance (76, 88), as the bacterial lawns have low oxygen due to microbial metabolism (96). To test whether that is the case with avoidance of *E. faecalis,* wild-type and *npr-1 (lf)* animals were placed into hypoxia (8% oxygen) chambers and scored for avoidance. In this low oxygen environment, both *npr-1(ad609)* and *npr-1(ok1447)* displayed wild-type levels of avoidance (**Fig. 10B**). Furthermore, when animals were taken out of the low oxygen environment and allowed to roam at atmospheric oxygen levels for one-hour, wild-type animals remained off the *E. faecalis* lawns while both *npr-1(lf)* strains migrated back onto the lawns (**Fig. 10C**), indicating that hyperoxia avoidance is a more potent aversive stimulus than *E. faecalis* in *npr-1(lf)* animals.

Hyperoxia avoidance in *npr-1(lf)* animals requires the transient receptor potential channel vanilloid (TRPV) genes *ocr-2* and *osm-9* (93, 131, 133). Loss-of-function mutations in these genes results in decreased hyperoxia avoidance, and should thus lead to increased pathogen avoidance. Indeed, while loss-of-function mutants in both genes displayed avoidance levels similar to wild-type animals at 4 hours, their rate of avoidance was faster than that of wild-type animals (**Fig. S5**). Hyperoxia avoidance of *npr-1(lf)* nematodes also depends on functional *gcy-35, tax-2,* and *tax-4* genes (131, 134). GCY-35 is a soluble guanylyl cyclase (sGC) that binds directly to molecular oxygen (135) while TAX-2 and TAX-4 are two subunits of a cGMP-gated-ion-channel (124)

thought to act downstream of GCY-35 (97, 134). Through the activity of GCY-35 and TAX-2/TAX-4, the sensory neurons AQR, PQR, and URX drive avoidance of high oxygen. Use of double loss-of-function mutants of *gcy-35*, *tax-2,* or *tax-4* and *npr-1* would test the hypothesis that *gcy-35*, *tax-2*, and *tax-4* mutations would suppress the lack of pathogen avoidance of *npr-1(ad609)* animals. While this was indeed the case for the *gcy-35* mutation, *tax-2* and *tax-4* mutations failed to suppress the lack of avoidance of *E. faecalis* exhibited by *npr-1(ad609)* animals (**Fig. 10D**). These results suggest that TAX-2 and TAX-4 are involved in the detection of avoidance cues in addition to their role in oxygen detection.

Next, the role of TAX-2 and TAX-4 in the NPR-1-mediated avoidance of *P. aeruginosa* was tested using double mutants for *tax-2* or *tax-4* and *npr-1*. Surprisingly, and in contrast to avoidance of *E. faecalis*, *tax-2* but not *tax-4* mutation suppressed the avoidance of *P. aeruginosa* of *npr-1(ad609)* animals (**Fig. 10D**). The discrepancy between the double mutants is that the *tax-2(p694)* allele used only affects a subset of the *tax-2* expressing neurons (95). The *tax-4(p678)* allele, in contrast, affects all *tax-4*-expressing neurons (**Fig. 10E**). Thus, the neurons affected by the *tax-4(p678)* allele, but spared by the *tax-2(p694)* allele, most likely play a role in avoidance of *P. aeruginosa* independent from the oxygen sensing pathway. The results from the *E. faecalis* experiments, on the other hand, suggest that the *tax-2(p694)* allele covers additional neurons that regulate avoidance of that bacteria. Single loss-of-function mutants for *tax-2* and *tax-4*, including a strain carrying an allele that affects expression in all *tax-2* expressing neurons (*tax-2(p671)*), were used to confirm this. Indeed, it was found that all strains tested displayed decreased avoidance of *E. faecalis* compared to wild-type animals, while only *tax-2(p671)* and *tax-4(p678)* mutants displayed decreased avoidance of *P. aeruginosa* (**Fig. 10F**).

ASE, AWB, and AWC neurons mediate avoidance of E. faecalis

Attention was turned to uncovering the specific neurons in the TAX-2/TAX-4-dependent pathway that regulate avoidance of both *E. faecalis* and *P. aeruginosa*. To identify the neuron(s) responsible for *E. faecalis* avoidance, two strategies were employed. The first approach was to ask whether *tax-2* expression in individual neurons would rescue the lack of pathogen avoidance of *tax-2(p694)* animals. This revealed that *tax-2* expression in ASE neurons was sufficient for pathogen avoidance, while *tax-2* expression in the AQR, PQR, and URX neurons, had no effect (**Fig. 11A**). The second approach used animals lacking ASE neurons and the individual AWB, AWC, and ASI neurons, which are spared by the *tax-2(p694)* allele. The results confirmed the involvement of ASE neurons in *E. faecalis* avoidance and showed that AWB and AWC neurons are also necessary (**Fig. 11B**).

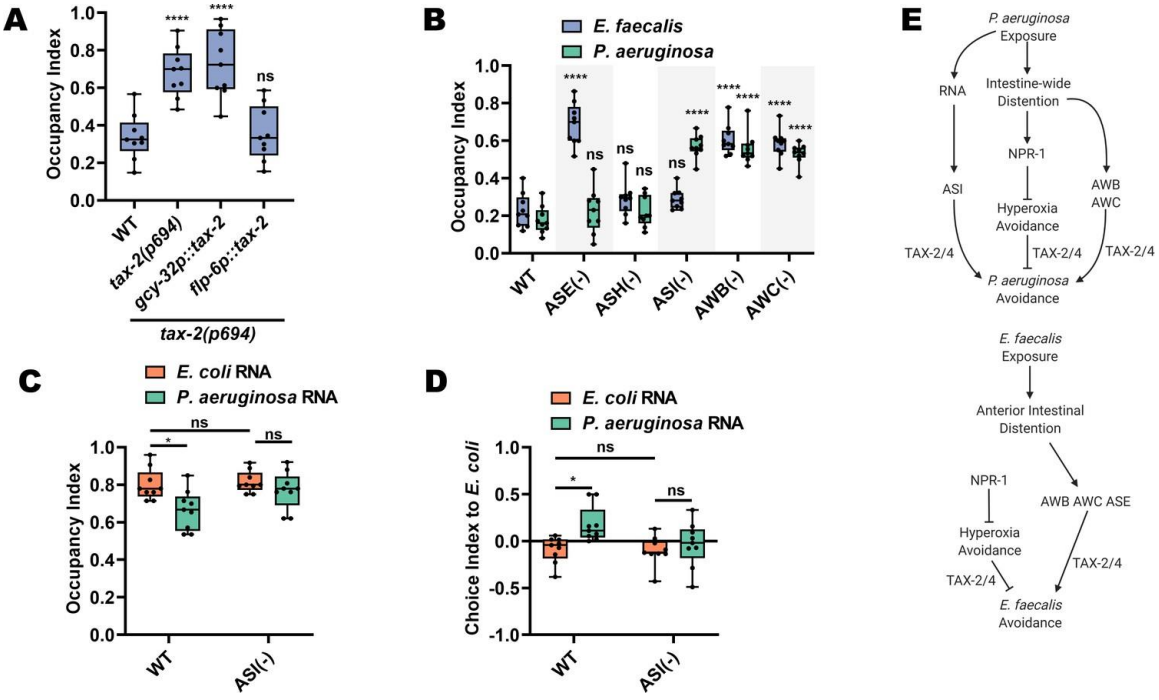

Fig. 11. ASE, AWB, and AWC neurons mediate avoidance of *E. faecalis*. (**A**) Occupancy index on *E. faecalis* at 4 hr for WT, *tax-2(p694)* and animals with *tax-2* expression in ASE neurons (*flp-*

6p::tax-2) or AQR, PQR, or URX neurons (*gcy-32p::tax-2*) in the *tax-2(p694)* background. One-way ANOVA with subsequent comparison to wild-type (WT) animals was performed. (**B**) Occupancy index of WT animals and animals with ablated neurons on *E. faecalis* at 4 hr and *P. aeruginosa* at 24 hr. Ablation of sensory neurons either by mutation (*che-1(p680)* = ASE(−)) or by caspase expression (*sra-6p::mCasp-1*=ASH(−); *gpa-4p::TU#813* + *gcy-27p::TU#814* = ASI(−); *str-1p::mCasp-1* = AWB(−); *ceh-36p::TU#813* + *ceh-36p::TU#814* = AWC(−)). Two-way ANOVA with subsequent comparisons to WT groups for each respective bacterium were performed. (**C**) Occupancy index at 1 hr for WT and ASI(−) animals on *P. aeruginosa* lawns. Animals were trained on *E. coli* OP50 lawns supplemented with either *E. coli* or *P. aeruginosa* RNA for 24 hr. Two-way ANOVA with subsequent comparison with WT control groups was performed. (**D**) Choice index after 1 hr for WT and ASI(−) animals choosing between *E. coli* and *P. aeruginosa* lawns. Two-way ANOVA with subsequent comparison with WT control groups was performed. Choice Index = (number of animals on *E. coli* – number of animals on *P. aeruginosa*)/(number of animals on *E. coli* + number of animals on *P. aeruginosa*). (**E**) Model for avoidance of *P. aeruginosa* (top) and *E. faecalis* (bottom) Avoidance of *P. aeruginosa* depends on both an ASI neuron-mediated bacterial sRNA pathway along with intestine-wide distention. The latter requires the NPR-1-dependent hyperoxia avoidance pathway along with AWB and AWC olfactory neurons. Avoidance of *E. faecalis* also depends on intestinal distention, though this is confined to the anterior intestine. This anterior intestinal distention-induced avoidance also requires AWB and AWC olfactory neurons, but also requires ASE chemosensory neurons. NPR-1-dependent hyperoxia avoidance opposes *E. faecalis* avoidance and depends on functional TAX-2/4.

For avoidance of *P. aeruginosa,* the genetic ablation strategy was also employed, which revealed the requirement of AWB and AWC neurons (**Fig. 11B**). Confirming the results of the *tax-2* experiments, ASE neurons were not required for avoidance of *P.*

aeruginosa. These experiments also confirmed a previous report that ASI neurons, but not ASH neurons, are required for avoidance of *P. aeruginosa* (83), while showing that neither is required for avoidance of *E. faecalis* (**Fig. 11B**). Using a two-choice assay where, unlike the pathogen avoidance assay that only uses *P. aeruginosa*, animals are given a choice between *E. coli* and *P. aeruginosa*, it was shown that ASI neurons respond to *P. aeruginosa* RNAs by eliciting avoidance (102). Using both avoidance and choice assays, animals lacking ASI neurons also fail to avoid *P. aeruginosa* after total RNA exposure (**Fig. 11C and D**). These results are consistent with the idea that ASI neurons are capable of sensing *P. aeruginosa* RNAs and that *E. faecalis* RNAs do not induce avoidance (**Fig. 7E**). Altogether, these results suggest that regulation of pathogen avoidance is pathogen-specific (**Fig. 11E**).

AWB and AWC neurons are necessary for aversive olfactory learning following ingestion of E. faecalis

The data suggested that avoidance of *E. faecalis* represented an aversive learning process (**Fig. 7D**), but a direct test was needed. AWB and AWC neurons are known to play a role in odor preference and olfactory aversive learning in *C. elegans* in the context of *P. aeruginosa* (95, 136). Because AWB and AWC neurons are also involved in avoidance of *E. faecalis*, it was hypothesized that odor preference and olfactory aversive learning may also play a role in avoidance of *E. faecalis*. As a first step to test this, the naïve preference of *C. elegans* when given the choice between *E. coli* and *E. faecalis* was established. A two-choice assay was used in which animals were able to roam for one hour on test plates containing *E. coli* and *E. faecalis* lawns on opposite sides of the plates before animals were scored based on lawn occupancy. Under this condition, animals showed a preference for *E. coli* over *E. faecalis*; however, if animals were instead paralyzed upon approaching the lawns, they displayed a preference for *E. faecalis* (**Fig. 12A**). From this,

it was hypothesized that there is an initial attraction to *E. faecalis* that is quickly overcome after feeding on it, such that animals go towards the familiar *E. coli* lawn instead. Paralyzing animals on lawn arrival captures the initial choice, while allowing them to freely roam captures the aversive learning behavior. A further hypothesis is that this attraction-aversion dynamic was at least partly olfactory, based on neuron ablation results (**Fig. 11**), and evidence that *tax-2(lf)* leads to significantly delayed lawn exiting (**Fig. 7C**).

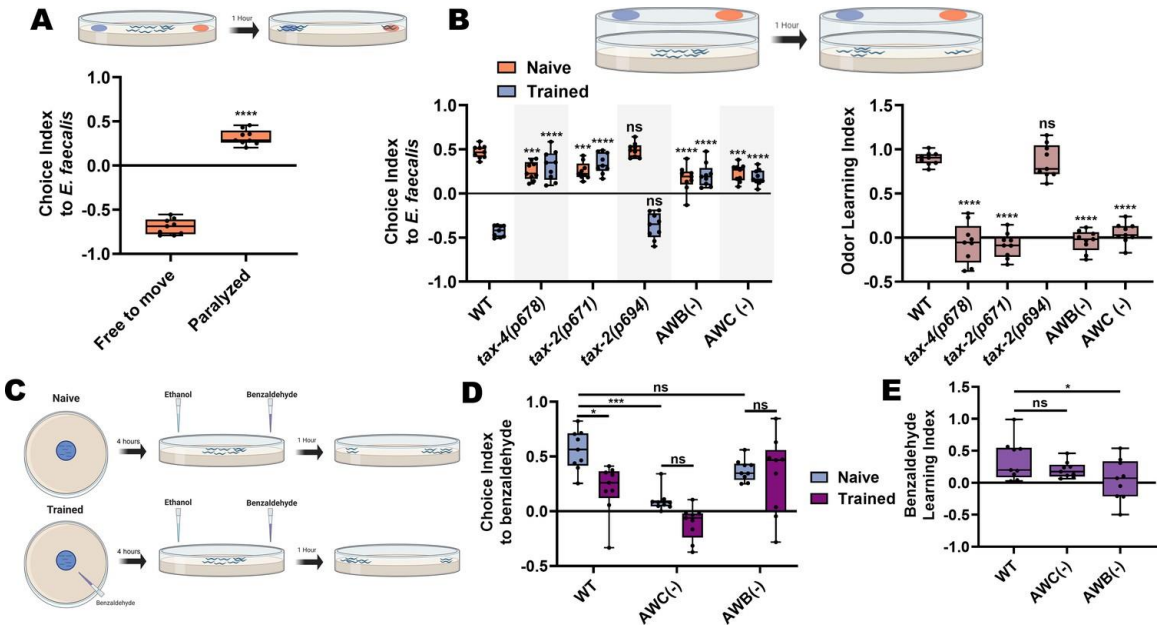

Fig. 12. AWB and AWC neurons are necessary for aversive olfactory learning following ingestion of *E. faecalis*. (**A**) Schematic of the choice assay (top) and quantification (bottom) of choice index for N2 animals choosing between *E. coli* and *E. faecalis* lawns and either free to move for 1 hr (Free to move) or paralyzed upon arrival at a bacterial lawn (Paralyzed). An unpaired t-test between the groups was performed. (**B**) Schematic of the lid choice assay (top) and quantification of naïve and trained choice index (bottom, left) and learning index (bottom, right) for WT, *tax-4(p678)*, *tax-2(p671)*, *tax-2(p694)*, AWB(−), and AWC(−) animals. To train animals, young adult animals were placed on *E. faecalis* lawns for 4 hr before the choice assay was

performed. For choice index, two-way ANOVA with subsequent comparisons to the naïve and trained WT groups as controls were performed. For learning index, one-way ANOVA with comparison to the WT group as control was performed. (**C**) Schematic of the paired olfactory choice assay. (**D**) Quantification of choice index for naïve and trained WT, AWC(−), and AWB(−) animals, choosing between 1:200 benzaldehyde and ethanol. Two-way ANOVA with subsequent comparisons between naïve and trained groups and between WT and neuron ablated animals was performed. (**E**) Quantification of the learning index for WT, AWC(−), and AWB(−) animals from (**D**). One-way ANOVA with comparison to the WT group as control was performed. Learning index = (naïve choice index) – (trained choice index).

To directly test the idea of an initial odor attraction, the choice assay was modified by attaching plugs of agar with bacterial lawns on opposite sides of the lids of empty test plates (**Fig. 12B**, schematic), preventing the animals from getting direct contact with the bacteria. The anesthetic sodium azide was then placed on the test plate surface underneath the bacteria plugs and placed animals in the center of the plate, allowing them to migrate towards one side or the other. This revealed a naïve preference for the odor of *E. faecalis* over *E. coli* (**Fig. 12B**, left). Both *tax-2(p671)* and *tax-4(p678)* mutants displayed decreased naïve odor preferences but *tax-2(p694)* did not. This result is consistent with the idea that the *tax-2* and *tax-4* expressing neurons AWB and AWC are responsible for establishing the naïve odor preference. Indeed, ablating them also resulted in a decreased preference (**Fig. 12B**, left). It was next asked whether trained animals that were allowed to ingest *E. faecalis* would switch their odor preference. The animals were trained by exposing them to *E. faecalis* for four hours using the same plate setup that had been used for the avoidance assays. Then, the trained animals were transferred to the lid-choice testing plates. A marked shift in preference was observed for trained wild-type animals that was not seen in *tax-2(p671)*, *tax-4(p678),* or AWB and

AWC ablated strains (**Fig. 12B**, left). The *tax-2(p694)* mutants, on the other hand, behaved like wild-type animals. The learning index for each strain also highlights that aversive olfactory learning takes place in wild-type and *tax-2(p694)* animals but not in *tax-2(p671)* or *tax-4(p678)* mutants or AWB and AWC ablated strains (**Fig. 12B**, right). Thus, the *tax-2* and *tax-4* expressing AWB and AWC neurons are necessary both for establishing a naïve preference and for aversive olfactory learning following ingestion of *E. faecalis* over a period of four hours.

To strengthen the idea that avoidance of *E. faecalis* involves aversive learning, an attractive odorant, benzaldehyde, was paired with lawns of *E. faecalis* and animals were to this pairing for four hours (**Fig. 12C**). Animals were then transferred to a choice plate, spotted with the attractive odorant on one side and ethanol on the other, and were allowed to roam for one hour before scoring. Results were compared to a naïve group that had no exposure to the odorant. Naïve animals displayed a strong attraction to benzaldehyde that was significantly reduced upon training (**Fig. 12D and E**). As benzaldehyde is primarily sensed by AWC neurons, ablation of these cells led to a decrease in naïve attraction, with training leading to no additional decrease. Interestingly, animals with ablated AWB neurons displayed wild-type levels of naïve attraction but did not show a decrease in attraction upon training, indicating that AWB neurons may be required for this aversive learning process.

The TRPM channels gon-2 and gtl-2 are required for distention-induced pathogen avoidance

It remains unclear how *C. elegans* senses intestinal distention in order to execute pathogen avoidance, either for *P. aeruginosa* or *E. faecalis*. Because TRP channels could be mechanoreceptors (119) capable of sensing the intestinal distension caused by microbial colonization, a screen for animals with loss-of-function mutations in 5 TRP-

encoding genes for avoidance of *E. faecalis* was conducted. This screen returned two members of the TRPM subfamily, *gon-2* and *gtl-2,* that negatively affected avoidance of *E. faecalis* (**Fig. S6**). Because *gon-2* mutants are known to have abnormal gonad development, and the germline has previously been shown to be involved in pathogen avoidance and immunity (102, 103, 137), it was tested whether the effect of *gon-2(lf)* mutations on pathogen avoidance was due to perturbed gonad development. Taking advantage of the fact that the Gon phenotype is temperature sensitive (high penetrance at 25°C and low penetrance at 15°C), a comparison of avoidance results for both *E. faecalis* and *P. aeruginosa* at both temperatures was conducted. For *P. aeruginosa*, *gon-2(lf)* animals raised at 25°C failed to avoid, while animals raised at 15°C avoided like wild-type animals (**Fig. 13A and B**). For *E. faecalis*, *gon-2(lf)* animals failed to avoid at both temperatures (**Fig. 13A and B**), suggesting that the germline does not play a role in the control of avoidance of this pathogen. Furthermore, *glp-1(e2141)* mutants, which lack most germline cells due to defects in mitotic and meiotic division (138, 139), behave similarly to *gon-2(lf)* mutant animals on both pathogens (**Fig. 13A and B**). This suggests that *gon-2(lf)* animals fail to avoid *P. aeruginosa* specifically because of a lack of gonad development, while for *E. faecalis* the effect on avoidance is independent of the germline. Unlike *gon-2(lf)*, *gtl-2(n2618)* animals failed to avoid *E. faecalis* but not *P. aeruginosa* (**Fig. 13A and B**).

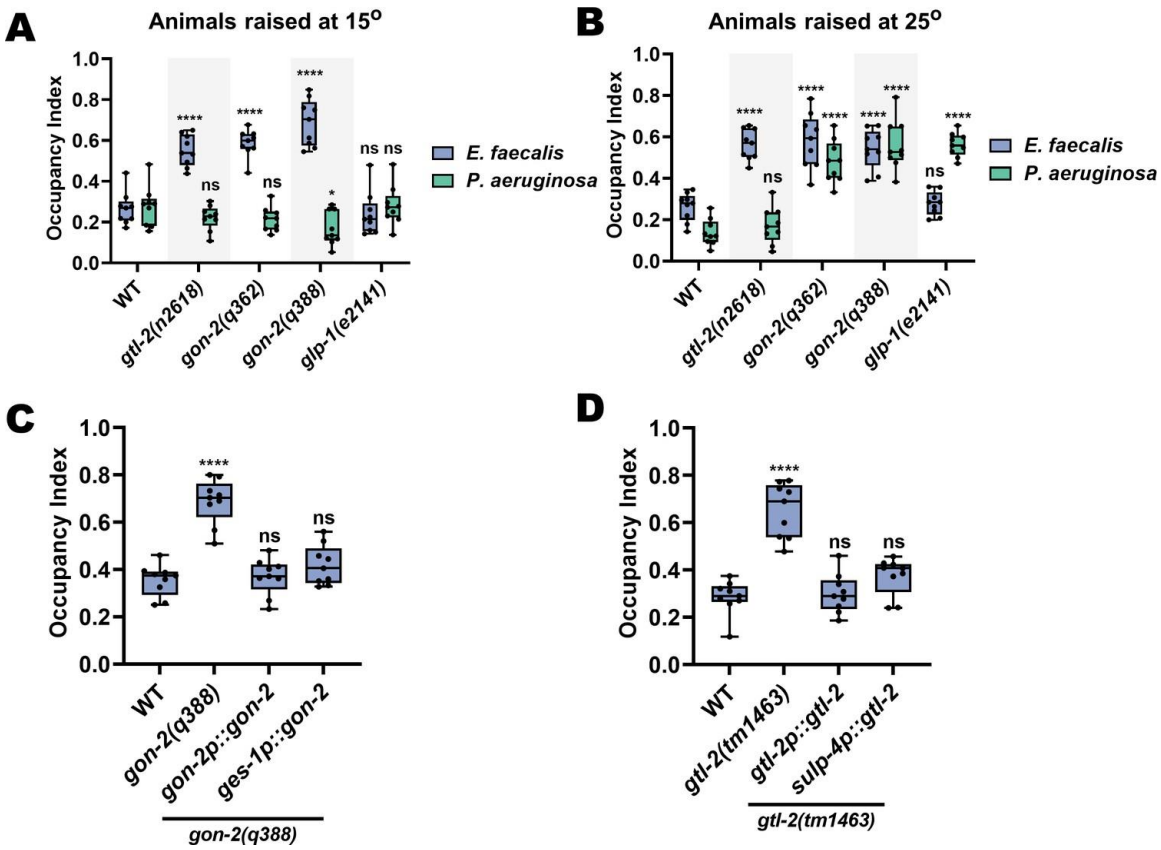

Fig. 13. The TRPM channels GON-2 and GTL-2 are required for distention-induced pathogen avoidance. (**A**) Occupancy index for wild-type, *gtl-2(n2618)*, *gon-2(q362)*, *gon-2(q388)*, and *glp-1(e2141)* animals on *E. faecalis* at 4 hr or *P. aeruginosa* at 24 hr. Animals were grown to the young adult stage at 15°C. Two-way ANOVA with comparisons to the respective WT group for each bacterium were performed. (**B**) Occupancy index for wild-type, *gtl-2(n2618)*, *gon-2(q362)*, *gon-2(q388)*, and *glp-1(e2141)* animals on *E. faecalis* at 4 hr or *P. aeruginosa* at 24 hr. Animals were grown to the young adult stage at 25°C. Two-way ANOVA with comparisons to the respective WT group for each bacterium were performed. (**C**) Occupancy index for wild-type, *gon-2(q388),* self-promoter rescue (*gon-2(q388);gon-2p::gon-2*), and intestine specific rescue (*gon-2(q388);ges-1p::gon-2*) animals on *E. faecalis* at 4 hr. One-way ANOVA with comparison to the wild-type group as control was performed. (**D**) Occupancy index for wild-type, *gtl-2(tm1463)*, self-promoter rescue (*gtl-2(tm1463);gtl-2p::gtl-2*), and excretory cell specific rescue

(*gtl-2(tm1463);sulp-4p::gtl-2*) animals on *E. faecalis* at 4 hr. One-way ANOVA with comparison to the wild-type group as control was performed.

In addition to gonadal expression, *gon-2* is known to exhibit intestinal expression (140). To confirm this, a strain expressing *gon-2::GFP* under the *gon-2* promoter was generated, which revealed expression in the gonads and intestine (**Fig. S7**). The hypothesis was that driving *gon-2* expression to the intestines of *gon-2(q388)* mutants would rescue the pathogen avoidance defect of the mutants. Indeed, *gon-2(q388)* animals expressing *gon-2* under its own promoter or an intestine specific promoter (*ges-1p*) displayed wild-type levels of avoidance of *E. faecalis* (**Fig. 13C**). The site of action of *gtl-2* for the pathogen avoidance behavior was also unknown. It was previously reported that *gtl-2* is functionally expressed in the excretory cell, with additional expression in the pharyngeal muscle (141, 142). A strain expressing *gtl-2::GFP* under its own promoter was constructed and revealed that this was indeed the case (**Fig. S7**). Furthermore, *gtl-2(tm1463)* mutants expressing *gtl-2* under its own promoter or under a promoter that drives expression only to the excretory cell (*sulp-4p*) displayed wild-type levels of avoidance (**Fig. 13D**). Together, these results indicate that *gon-2* expression in the intestine and *gtl-2* expression in the excretory cell is sufficient for *C. elegans* avoidance of *E. faecalis*.

Because *gon-2(lf)* and *gtl-2(lf)* animals display wild-type levels of anterior intestinal distention (**Fig. S8**), the hypothesis was that the effect observed in these animals was due to an inability to sense intestinal distention either directly or indirectly. It was previously shown that knockdown of *aex-5* leads to defects in the defecation motor program and subsequent intestinal distention by the accumulation of bacteria, resulting in increased avoidance of even non-pathogenic *E. coli* (93). Interestingly, *gon-2(lf)* mutants failed to exhibit such avoidance on *E. coli* strain HT115 after knockdown of

aex-5, while *gtl-2(n2618)* mutants behaved like wild-type animals (**Fig. 14A**). These results are consistent with the different types of distention caused by *E. faecalis* and *P. aeruginosa*, with the former causing a more severe but localized distention of the anterior intestine and the latter causing a distention along the entire length of the intestine, which seems to require the germline to elicit avoidance. Both *gon-2* and *gtl-2* mutants suppressed the *aex*-5 knockdown avoidance phenotype on *E. faecalis* (**Fig. 14B**), suggesting that both TRPM channels might be involved in the process of sensing the anterior intestinal distention caused by *E. faecalis*. However, TRPM channels display many distinct functions in various settings, including the absorption of calcium and magnesium ions by TRPM6 and TRPM7 in the human colon, TRPM7-mediated pacemaker activity of interstitial cells of Cajal, and colonic nociception by mouse TRPM8 (120, 143). Thus, it remains unclear how exactly GON-2 and GTL-2 function in pathogen avoidance.

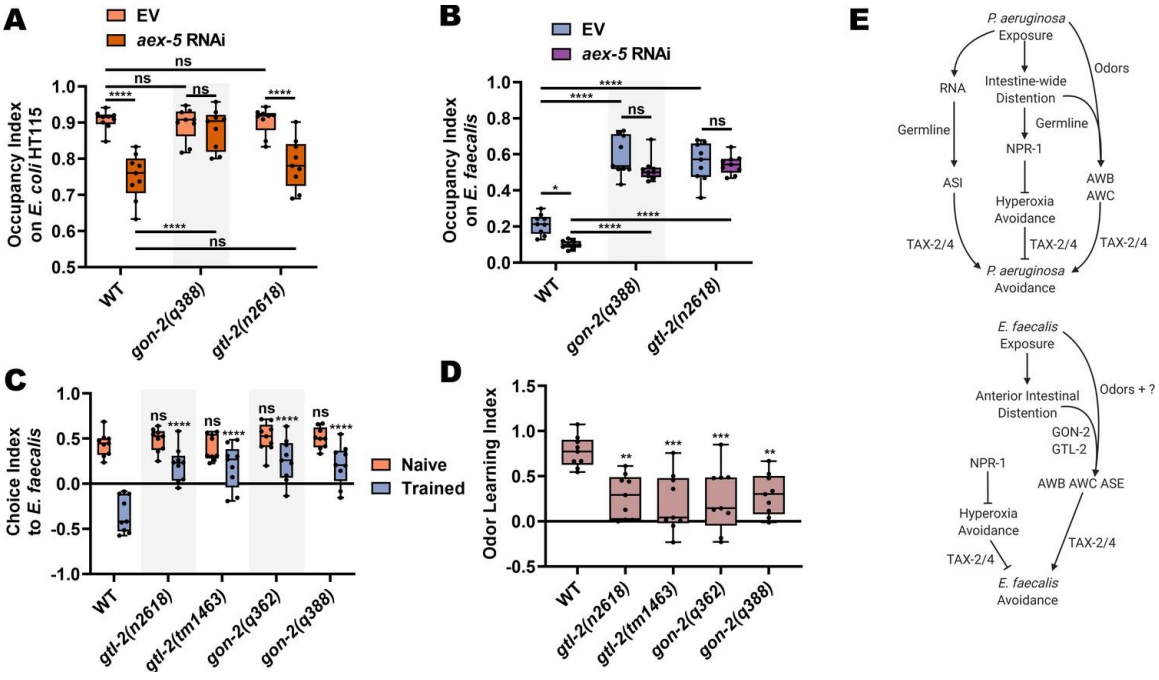

Fig. 14. GON-2 and GTL-2 diminish olfactory aversive learning following *E. faecalis* exposure. (**A**) Occupancy index for WT, *gon-2(q388)*, and *gtl-2(n2618)* animals with either RNAi-mediated

knockdown of *aex-5* or an empty vector (EV) control on the *E. coli* HT115 lawns these animals were raised on. Two-way ANOVA with subsequent comparison between all groups was performed. (**B**) Occupancy index for WT, *gon-2(q388),* and *gtl-2(n2618)* animals with either RNAi-mediated knockdown of *aex-5* or an EV control on *E. faecalis* lawns at 4 hr. Two-way ANOVA with subsequent comparison between all groups was performed. (**C**) Choice index for wild-type, *gtl-2(n2618), gtl-2(tm1463), gon-2(q362),* and *gon-2(q388)* animals between *E. faecalis* and *E. coli* using the lid choice assay. Two-way ANOVA with comparison to the naïve and trained WT group was performed. (**D**) Quantification of learning index for animals from (**C**). One-way ANOVA with comparison to the WT group was performed. (**E**) Model for avoidance of *P. aeruginosa* (top) and *E. faecalis* (bottom), as in **Fig. 10E**, with the addition of a germline role in avoidance of *P. aeruginosa*, GON-2 and GTL-2 regulation of avoidance of *E. faecalis*, and the contribution of odor sensing pathways to avoidance of both bacteria.

If these TRPM channels are somewhat involved in sensing anterior intestinal distention caused by *E. faecalis* infection, their loss should leave naïve olfactory preferences to *E. faecalis* intact while diminishing negative associative learning. Testing *gon-2(lf)* and *gtl-2(lf)* mutants on olfactory choice assays with and without prior exposure to *E. faecalis* revealed that this was indeed the case (**Fig. 14C and D**). All *gon-2* and *gtl-2* mutants displayed wild-type levels of naïve preference to *E. faecalis* versus *E. coli*. After training by exposure to *E. faecalis* for four hours, *gon-2(lf)* and *gtl-2(lf)* mutants displayed significantly reduced preference switching compared to wild-type animals (**Fig. 14C**). This results in significantly lower learning indices for the mutants (**Fig. 14D**). Altogether, these findings indicate that GON-2 and GTL-2 are required for the learned avoidance of *E. faecalis*, though their exact mechanistic role remains to be determined (**Fig. 14E**).

Chapter Discussion

This study establishes that *E. faecalis* infection in *C. elegans* leads to anterior intestinal distention which results in a rapid pathogen avoidance behavior, opposed by NPR-1-mediated hyperoxia avoidance, and regulated by TAX-2/4 expressing AWB, AWC, and ASE sensory neurons, and the TRPM channels GON-2 and GTL-2. In contrast, avoidance of *P. aeruginosa* uses different mechanisms that involve intestine-wide distention, germline mediated-signaling, and sensing of bacterial sRNAs via an ASI neuronal pathway (**Fig. 14E**). Thus, bacterial context is important for the elicitation of pathogen avoidance behaviors. This context-dependence makes it likely that using *C. elegans* may lead to the discovery of new components of sensory pathways involved in pathogen avoidance and help to elucidate how physiological information from the site of infection is relayed to the nervous system. This was indeed highlighted by the identification of ASE neurons and GTL-2 as being necessary for avoidance of *E. faecalis* but not *P. aeruginosa,* and the requirement of the germline in avoidance of *P. aeruginosa* but not *E. faecalis*.

The decision to leave a bacterial lawn represents a dynamic balance between risk and reward for *C. elegans*, with feeding and food choice being critical for survival and propagation (144–146). Initially, the balance may be towards staying on the lawn, as it could be an area of high reward in the form of food. However, depending on the quality of the food, its availability, and its potential noxious qualities, the balance may swing towards bacterial avoidance, as the lawn becomes either an area of low reward (depleted or low-quality) or an area of high risk (pathogenic). The frequent entering and exiting events of animals on lawns of *E. faecalis* (**Fig. 7C and D**) may be indicative of this dynamic balance. Multiple sensory inputs or physiological states such as oxygen level, odors, tastes, mechanosensation, pain, and hunger must be integrated in order to

evaluate the environment and come to a decision. These cues are most likely integrated in the interneurons of *C. elegans,* which are downstream of the sensory neurons (147–149).

The involvement of ASE neurons, largely described as gustatory neurons, in the avoidance of *E. faecalis* (**Fig. 11A and B**) suggests that taste may play a role in pathogen avoidance in *C. elegans* in certain contexts. ASE neurons have also been shown to be carbon dioxide sensors (150), and polymodal sensory neurons are common in *C. elegans* (147, 151), raising the possibility that ASE sensation of carbon dioxide, and not gustation, may elicit avoidance of *E. faecalis*. Additionally, a recent study implicated ASEL as a secondary sensory neuron in the detection of the food odor benzaldehyde (152). The results of the olfactory aversive learning experiments, however, suggest that ASE neurons are not involved in the olfactory component of *E. faecalis* avoidance. Whether they are involved in some other learning process underpinning avoidance remains unclear. Interestingly, AWC neurons are also recruited into a salt-sensing circuit via neuropeptide signaling from ASE neurons depending on salt concentration changes (153), leaving open the possibility that AWC neurons also play a role in avoidance of *E. faecalis* (**Fig. 11B**) not only through olfactory aversive learning (**Fig. 12C-E**) but through taste aversive learning. Further studies will need to be conducted to determine which possible sensory modality is important for ASE-dependent and AWC-dependent avoidance of *E. faecalis*. ASE neurons were also identified as part of the complex circuitry underlying the decision to leave a resource-depleted food patch, possibly via carbon dioxide sensing (145), suggesting an interesting link between pathogen avoidance and adaptive food leaving.

AWB and AWC involvement in odor preference and olfactory aversive learning is well-established in various contexts (95, 136, 154), and this study extends this to *C.*

elegans interactions with *E. faecalis* (**Fig. 12**) while providing direct evidence of their involvement in avoidance for both *E. faecalis* and *P. aeruginosa* (**Fig. 11B**). The olfactory circuitry in *C. elegans* has been described in detail (152, 155). AWC neurons also communicate and receive feedback from other interneurons through the use of neuropeptides, such as the NLP-1-NPR-11-INS-1 feedback loop between AWC and AIA interneurons (156). The circuitry for olfactory aversive learning has also received extensive study in the context of *P. aeruginosa* with serotonin and various neuropeptides playing crucial roles in learning and foraging states (94, 95, 100, 136, 157, 158). Interestingly, both AWB and AWC neurons were previously shown to play a role in avoidance of normally attractive food following undernourishment (159) providing another link between pathogen avoidance behavior and foraging. Indeed, for *C. elegans* feeding on any bacteria there is most likely a balance between nourishment and pathogenicity, with olfactory-mediated decisions constantly being made that affect foraging and avoidance. How information about this nutrition/infection dichotomy is integrated is currently unknown, though a recent study showed that the transcription factor Nrf2/*skn-1* was required in the AIY interneuron for the integration of information from ASE and AWC neurons during foraging (149). Whether this same AIY neuronal integration is required for pathogen avoidance remains to be seen. Previous work in *Drosophila* has also revealed olfactory-mediated avoidance of harmful microbes (160), illustrating that similar mechanisms are at play across different species.

The discovery of *gon-2* and *gtl-2* playing a role in pathogen avoidance is novel. The most well-known impact of loss of *gon-2* function is severe impairment of gonadogenesis due to disruption of gonadal cell divisions (161). This impairment is most likely responsible for the results observed for avoidance of *P. aeruginosa* (**Fig. 13A and B**), as the germline and associated tissues are necessary for this avoidance behavior (102, 103, 137). The results of the *glp-1* experiments (**Fig. 13A and B**) further support this

idea. However, the germline seems to play no role in avoidance of *E. faecalis,* and therefore other functions of *gon-2* and *gtl-2* may be responsible. The germline plays a role in a transgenerational learned avoidance of *P. aeruginosa* (103), but the lack of involvement of the germline (**Fig. 13A and B**), bacterial sRNAs (**Fig. 7E**), and ASI neurons (**Fig. 11B**) in avoidance of *E. faecalis* suggest that such a process may not exist in the case of *E. faecalis* infection. Because *gon-2* is known to be highly expressed in the intestine, where it is responsible for electrolyte homeostasis (140), and rescue of *gon-2* intestinal expression using the *ges-1* promoter rescues *E. faecalis* avoidance phenotypes, it may function as an intestinal receptor for the changes elicited by *E. faecalis* colonization. Magnesium excretion, and perhaps additional electrolytes, requires the activity of *gtl-2* in the excretory cell (142), and rescue of *gtl-2* excretory cell expression using the *sulp-4* promoter rescues *E. faecalis* avoidance phenotypes. Thus, it is possible that the role of *gon-2* and *gtl-2* in pathogen avoidance is related to sensation of an electrolyte perturbance caused by intestinal distention. Both *gon-2* and *gtl-1,* though not *gtl-2,* are also required for maintaining the rhythm of the *C. elegans* defecation motor program (141), which could also result in aberrant avoidance behaviors, though loss of *gtl-1* does not seem to affect avoidance (141). Finally, these TRPM channels could also be mechano-nociceptors, as described in other animal models (143), that sense intestinal distention directly, though the data presented here could also be consistent with a less direct role as described above. Indeed, TRPM channels display many distinct functions in various settings, including the absorption of calcium and magnesium ions by TRPM6 and TRPM7 in the human colon, TRPM7-mediated pacemaker activity of interstitial cells of Cajal, and colonic nociception by mouse TRPM8 (120, 143). Thus, it remains unclear how exactly GON-2 and GTL-2 function in pathogen avoidance. Because the intestine is not directly innervated, any signal coming from it must be extra-synaptic, such as an intestinal neuropeptide (115). All animals are under pressure to develop behaviors that

allow them to flee potential pathogens (2). Future work will continue to elucidate the mechanisms underlying avoidance of pathogenic threats.

CHAPTER 3: DISSECTION OF A SENSORIMOTOR CIRCUIT FOR PATHOGEN AVERSION BY WHOLE-BRAIN MODELING[3]

Background

While the chemosensory neurons responsible for some forms of pathogen avoidance have been at least partially worked out, the complete neural circuitry required to coordinate these avoidance behaviors remains unknown. Signals from the sensory neurons, such as those described in the previous chapter, likely converge on downstream interneurons. Activation of ASI neurons, for example, results in the release of the insulin-like-peptide INS-6, inhibiting *ins-7* expression in URX and subsequent upregulation of DAF-2 activity in RIA interneurons (100). These same interneurons are involved in the modulation of olfactory preference (136), and thus may be important integrators of distinct bacterial cues triggering avoidance behaviors.

Any chemosensory signal must eventually be propagated down not only to interneurons but also to the motor neurons required for avoidance-associated locomotion (162–164). The circuitry linking these neurons together is unknown, but the complete connectome of *C. elegans* (165) can be used to dissect the mechanisms involved in translating the detection of pathogenic cues into physical avoidance. In this chapter, the discovery that backward locomotion is a crucial component of pathogen avoidance is described. Animals trained on either *P. aeruginosa* or *E. faecalis* display reflexive aversion to these pathogens. To elucidate the reflexive aversion circuitry, simulations of the *C. elegans* nervous system, which have been shown to be useful in studying behaviorally relevant neural activity, were used (166, 167). In particular, using one

[3] This chapter is largely based on A. Filipowicz, J. Lalsiamthara, and A. Aballay, Dissection of a sensorimotor circuit that regulates aversion to odors and pathogenic bacteria in *C. elegans* by whole-brain simulation. *bioRxiv*, 489073 (2022).

simulation platform, the *C. elegans* Neural Interactome (167), the neural patterns resulting from stimulation of the chemosensory neurons known to be involved in different pathogen avoidance behaviors were investigated. It was found that oscillations in motor neurons critical for backward locomotion could be induced by AWB stimulation. AUA and RMG interneurons electrically coupled to AWB neurons also showed high activity upon AWB stimulation, and *in silico* ablation of these neurons resulted in the loss of motor neuron oscillations. Genetic ablation of these neurons demonstrated their involvement not only in pathogen avoidance, but 2-nonanone aversion as well. The olfactory neuron AWB, electrically synapses onto AUA and RMG interneurons, which themselves synapse onto motor command interneurons to control backward locomotion motor neurons, thus representing a novel sensorimotor circuit for pathogen and repulsive odor aversion.

Results

Intestinal infection by P. aeruginosa or E. faecalis induces a learned reflexive aversion requiring multiple chemosensory neurons

To investigate the neural circuitry governing the translation of pathogen chemosensory cues into the motor neuron activity necessary for avoiding said cues, a direct test of avoidance locomotion was conducted by making use of an assay that would allow for quick assessment of individual neuron requirements for reflexive aversion both before and after exposure to a pathogen (**Fig. 15A**). The pathogenic bacteria *P. aeruginosa* and *E. faecalis* (see previous chapter) are initially attractive to *C. elegans* and only induce an avoidance response after many hours of exposure (92, 94, 136). This learning process involves the association of infection and subsequent physiological responses, including intestinal distention, engagement of RNAi pathways, and immune activation, with bacterial cues, resulting in avoidance of the bacteria (93, 102). Using the reflexive

aversion assay, it was found that naïve animals do not respond to drops of *P. aeruginosa* (**Fig. 15B**) or *E. faecalis* (**Fig. 15C**); however, animals exposed to bacteria prior to testing showed reflexive aversion to the same bacteria. The response to *P. aeruginosa* required ASI, AWB, and AWC neurons, while the response to *E. faecalis* required ASE, AWB, and AWC neurons (**Fig. 15B and C**). These results indicate that intersecting neural circuits are required for learned reflexive aversion against different pathogens.

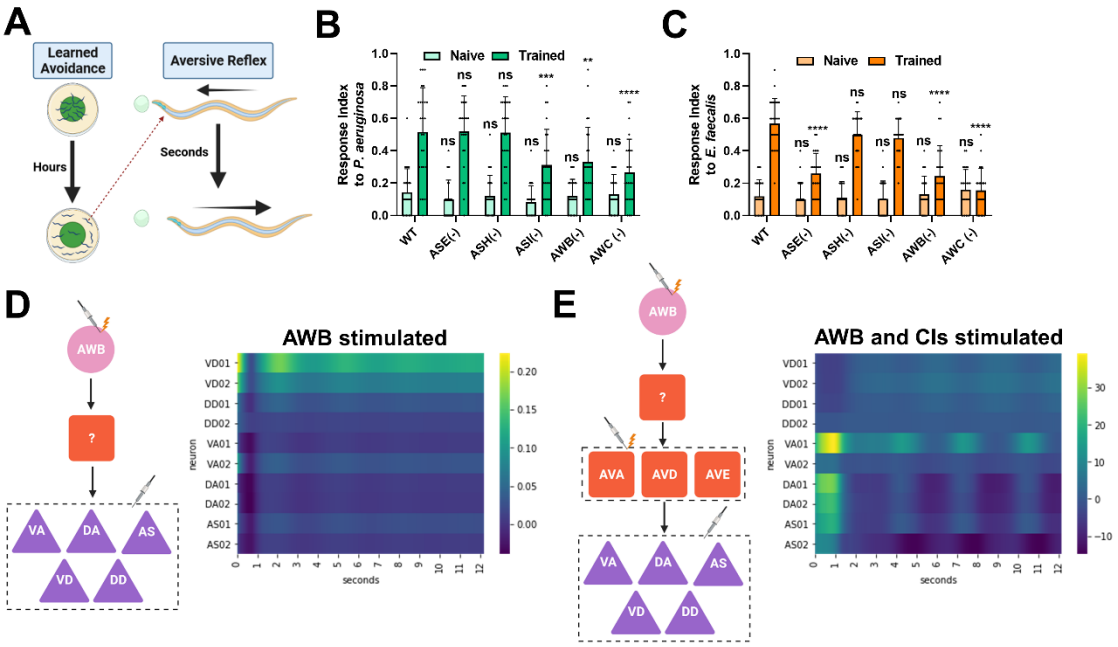

Fig. 15. Intestinal infection induces a learned reflexive aversion requiring multiple chemosensory neurons. (A) Diagram of the assays to determine learned avoidance (left) and naïve reflexive aversion (right). Details of assays can be found in the Materials and Methods. Briefly, for learned avoidance, animals are placed on a lawn of bacteria and allowed to roam freely for several hours (4 hr for *E. faecalis*, 24 hr for *P. aeruginosa*) before the number of animals inside and outside the bacterial lawn is counted. For reflexive aversion, a drop of bacterial culture is placed in front of a forward-moving animal, and a response is recorded if the animal initiates backward locomotion upon encountering the dried drop. Trained reflexive aversion involves taking from the avoidance plates and placing them onto a plate with no bacteria. Then, the reflexive aversion assay is carried

out. (B) Response index to *P. aeruginosa* for both naïve (light green) and trained (dark green) animals with either no neurons ablated (N2, WT) or ASE (PR680), ASH (JN1713), ASI (PY7505), AWB (JN1715), or AWC (PY7502) neurons ablated. (C) Response index to *E. faecalis* for the same groups as in **B**. For both **B** and **C**, two-way ANOVA with subsequent comparison to naïve or trained WT groups was performed. Error bars depict standard deviation. N = 25 (individual dots) for all groups. (D) Schematic of the sensorimotor circuit and protocol used in the Neural Interactome (left). AWB neurons were stimulated at 5.0 nA and the activity of VA, DA, AS, VD, and DD motor neurons (dashed-outline) was recorded. There is no direct connection between AWB neurons and the motor neurons, so an unknown interneuron must complete the circuit (question mark). Pink circle = sensory neuron; red square = interneuron; purple triangle = motor neuron. The recorded activity of the motor neurons is presented as a heatmap (right), with rows representing individual neuronal activity over time. The first two neurons of each motor neuron class were chosen for ease of visualization. (E) An updated schematic of the stimulation protocol (left). AVA, AVD, and AVE command interneurons (CIs) were stimulated at 0.9 nA along with the 5.0 nA stimulation of AWB neurons. This resulted in oscillations in the motor neurons (right). There is no direct connection between AWB neurons and the CIs, so another interneuron must complete the circuit (question mark).

Nervous system simulation predicts that AUA and RMG neurons are in the AWB neuron-mediated learned reflexive aversion circuit

To uncover the overall neural circuitry that integrates bacterial-related cues that result in learned reflexive aversion, the *C. elegans* Neural Interactome, a simple user-friendly simulation of the *C. elegans* nervous system that allows for stimulation and ablation of individual neurons and outputs total network activity, was used (167). The simulation takes advantage of the complete connectome of *C. elegans* and its neural dynamics, and was previously shown to assist in the study of neural response patterns associated with

locomotion and external stimuli such as nose touch. This makes the Neural Interactome a potentially useful tool in studying other aversive behaviors, including pathogen avoidance. To assess the neural activity of reflexive aversion, oscillations in VA, DA, VD, DD, and AS motor neurons were measured and used as a readout for backward locomotion, as it has previously been shown that these neurons are active during backward locomotion and function as oscillators (162, 163, 167, 168). Because AWB neurons are at the intersection of the circuits required for learned reflexive aversion against *P. aeruginosa* and *E. faecalis*, these neurons were first targeted for stimulation. However, no oscillations in the aforementioned motor neurons was found (**Fig. 15D**), indicating that additional neurons must participate in the circuit. Previous studies indicated that the command interneurons (CIs) AVA, AVD, and AVE are necessary reflexive aversion to nose touch (164, 167). Thus, the Neural Interactome was used to activate AWB together with CIs and oscillatory activity in the VA, DA, VD, DD, and AS motor neurons was observed (**Fig. 15E**). Stimulation of AWC and ASI neurons led to no oscillations in the motor neurons, while stimulation of ASE neurons led to very weak oscillations (**Fig. S9**). This indicates that AWB neurons are the primary mediator of reflexive aversion, while AWC, ASI, and ASE play some other roles in the learning process.

To confirm that motor neuron oscillations are a good readout for aversion behaviors, a behavior that has a known circuit correlate was examined: reflexive aversion to the common laboratory detergent sodium dodecyl sulfate (SDS; (169)). This behavior was confirmed to require the chemosensory neuron ASH, as animals lacking ASH neurons responded less strongly to SDS compared to wild-type animals (**Fig. S10A**). Aversion to SDS requires the command interneurons AVA, AVD, and AVE, and the motor neurons VA, DA, VD, DD, and AS (162, 163, 169). The connections between these neurons resolve as a three-layer circuit (**Fig. S10B**). Stimulation of ASH, AVA, AVD, and

AVE neurons within the Neural Interactome resulted in oscillatory activity in VA, DA, DD, and AS motor neurons, indicating that oscillations in these neurons were a suitable readout for aversion behaviors (**Fig. S10C**). Furthermore, this same circuitry is required for the response to dodecanoic acid (**Fig. S10A**). Dodecanoic acid is a toxin produced by the pathogenic bacteria *Streptomyces* (90), thus showing the simulation's ability to uncover circuits of pathogen avoidance.

AWB neurons have no direct connection to the motor command AVA, AVD, and AVE interneurons (**Fig. 15E**). Thus, another layer of interneurons is likely involved in the circuit. Looking at the activity of all the neurons in the interactome model after AWB stimulation, the AUA and RMG neurons stood out as having high oscillatory activity (**Fig. 16A and B**). According to the connectome of *C. elegans*, AUA and RMG form electrical synapses with AWB, and chemically synapse onto the AVA, AVD, and AVE neurons (**Fig. 16C**; (165)). This places them in a prime position to be regulators of the circuit for learned reflexive aversion. Indeed, *in silico* ablation of either AUA or RMG neurons resulted in the loss of oscillatory activity in VA, DA, VD, DD, and AS motor neurons upon AWB, AVA, AVD, and AVE stimulation (**Fig. 16D and E**). Other neurons, such as AIB, AVB, and SMB, also bridge the AWB and motor command interneurons, but *in silico* ablation of these neurons left the motor neuron oscillations intact (**Fig. S11**).

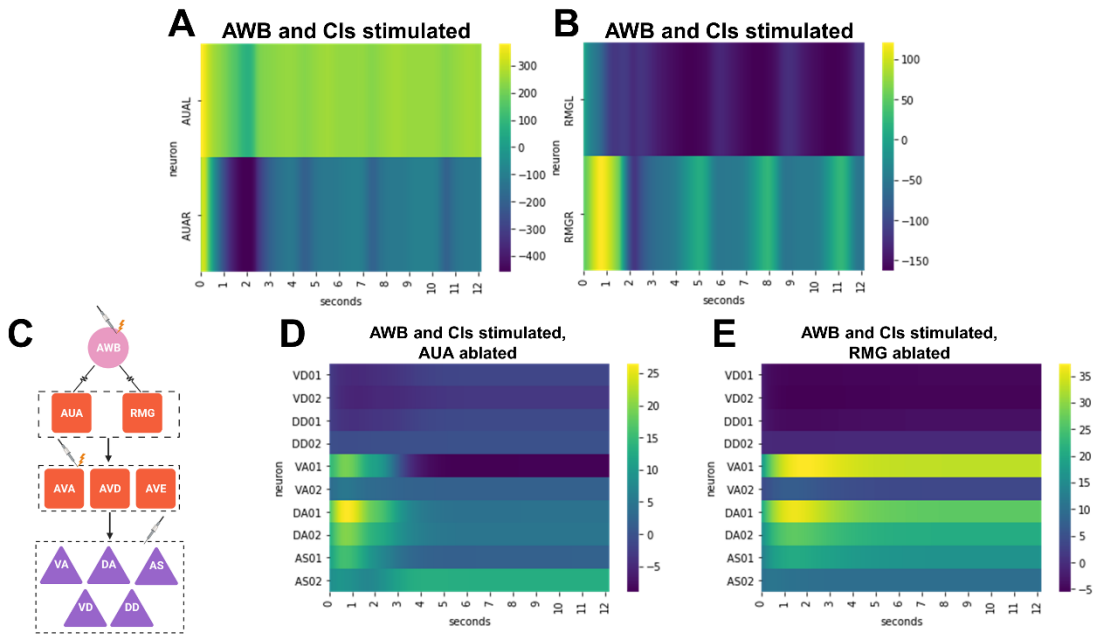

Fig. 16. Nervous system simulation predicts that AUA and RMG neurons are in the AWB neuron-mediated learned reflexive aversion circuit. (A) Activity of AUA left and right (AUAL/R) neurons (rows) upon 5.0 nA stimulation of AWB neurons and 0.9 nA stimulation of the CIs in the Neural Interactome. (B) Activity of RMG left and right (RMGL/R) neurons (rows) upon 5.0 nA stimulation of AWB neurons and 0.9 nA stimulation of the CIs in the Neural Interactome. (C) Updated circuit diagram and stimulation protocol schematic showing the connections between AWB, AUA, RMG, AVA, AVD, AVE, VA, DA, AS, VD, and DD neurons. The first neuron of each motor neuron class was chosen for ease of visualization. Arrows represent chemical synapses, while jagged lines represent electrical synapses. (D) Activity of motor neurons (rows) upon 5.0 nA stimulation of AWB neurons and 0.9 nA stimulation of the CIs with AUA neurons ablated in the Neural Interactome. (E) Activity of motor neurons (rows) upon 5.0 nA stimulation of AWB neurons and 0.9 nA stimulation of the CIs with RMG neurons ablated in the Neural Interactome.

A four-layer circuit underlies pathogen avoidance behaviors and aversion to 2-nonanone

To test whether AUA and RMG neurons affected learned reflexive aversion, AUA and RMG neurons were genetically ablated (**Fig. S12**) and the response of these animals to drops of *P. aeruginosa* and *E. faecalis* was measured. Ablation of either AUA or RMG left naïve responses to both bacteria intact, while trained responses showed a significant decrease (**Fig. 17A and B**). The occupancy index of animals lacking either AUA or RMG was also measured for both *P. aeruginosa* and *E. faecalis* and it was found that loss of either neuron resulted in increased lawn occupancy (**Fig. 17C and D**). This indicates that AUA and RMG neurons contribute to both learned reflexive aversion and learned pathogen avoidance of *P. aeruginosa* and *E. faecalis*.

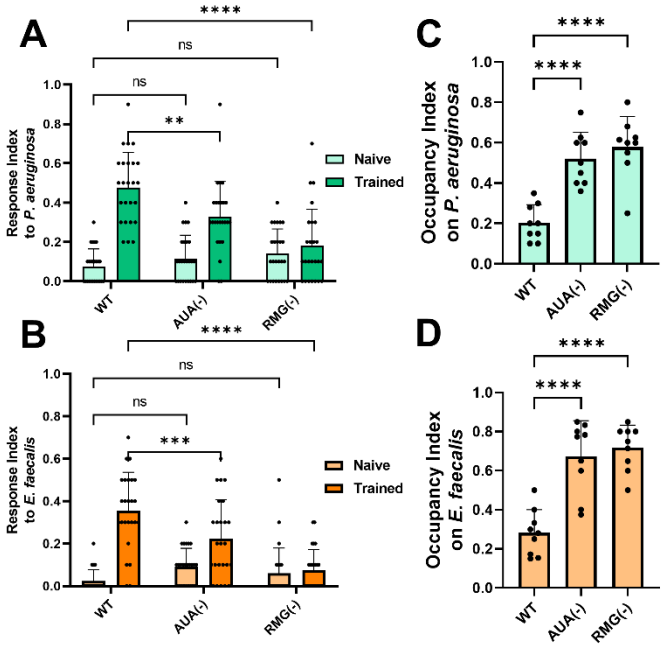

Fig. 17. A four-layer circuit underlies pathogen avoidance behaviors. (A) Response index to *P. aeruginosa* for both naïve (light green) and trained (dark green) animals with either no neurons ablated (WT) or AUA (AY178) or RMG (AY179) neurons ablated. (B) Response index to *E. faecalis* for the same groups as in **A**. For both **A** and **B**, two-way ANOVA with subsequent

comparison to naïve or trained WT groups was performed. Error bars depict standard deviation. N = 25 (individual dots) for all groups. (C) Occupancy index for *P. aeruginosa* after 24 hours for animals with no neurons ablated (WT) or AUA or RMG neurons ablated. (D) Occupancy index for *E. faecalis* after 4 hours for the same groups as in **C**. For both **C** and **D**, one-way ANOVA with subsequent comparison to the WT group was performed. Error bars depict standard deviation. N = 9 (individual dots) for all groups.

Was the learned reflexive aversion response specific to the bacteria used to train the animals or a general result of bacterial infection? Animals were cross-tested, trained on *E. faecalis* and then tested with drops of *P. aeruginosa* and vice versa. This revealed that animals did not show any reflexive aversion (**Fig. 18A and B**). However, if *E. faecalis* lawns were paired with the odor of *P. aeruginosa* during training, achieved by placing an agar plug of *P. aeruginosa* on the lid of the training plates, animals showed reflexive aversion (**Fig. 18A**). The same was true for the opposite pairing (**Fig. 18B**), suggesting that underlying learned reflexive aversion is a process whereby animals associate the odors of the bacteria with infection.

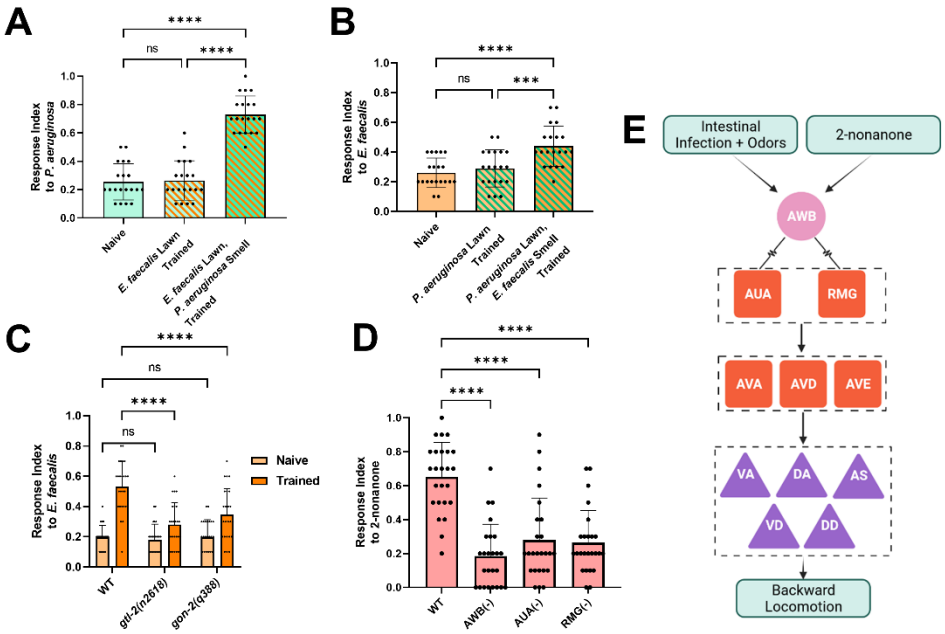

Fig. 18. The sensorimotor circuit involves olfaction and regulates aversion to 2-nonanone. (A) Response index to *P. aeruginosa* for wild-type animals either naïve to *P. aeruginosa*, trained on *E. faecalis* lawns, or trained on *E. faecalis* lawns with a lawn of *P. aeruginosa* on the lid, inaccessible to the animals. (B) Response index to *E. faecalis* for wild-type animals either naïve to *E. faecalis*, trained on *P. aeruginosa*, or trained on *P. aeruginosa* lawns with a lawn of *E. faecalis* on the lid. For both **A** and **B**, one-way ANOVA with subsequent comparisons between all groups was performed. Error bars depict standard deviation. N = 25 (individual dots) for all groups. (C) Naïve and trained response index to *E. faecalis* for wild-type (WT) and either *gtl-2* or *gon-2* loss-of-function mutants. Two-way ANOVA with subsequent comparison to the WT groups was performed. Error bars depict standard deviation. N = 25 (individual dots) for all groups. (D) Response index to 2-nonanone (1:10) for animals with no neuronal ablation (WT) or AWB, AUA, or RMG neurons ablated. One-way ANOVA with subsequent comparison to the WT group was performed. Error bars depict standard deviation. N = 25 (individual dots) for all groups. (E) Diagram of the odor-aversion sensorimotor circuit. AWB neurons sense an olfactory cue either from pathogenic bacteria or other repulsive odorants such as 2-nonanone. They pass this signal to AUA and RMG neurons via electrical synapses. AUA and RMG neurons form chemical synapses with AVA, AVD, and AVE command interneurons, which synapse with the motor neurons important for backward locomotion, VA, DA, VD, DD, and AS neurons. These neurons execute the backward locomotion necessary for odor avoidance.

Because a significant variation in the reflexive aversion of trained animals was noticed, it was theorized that varying levels of intestinal distention, which can trigger learned avoidance (93), may account for the variation in the responses. Intestinal distention on *P. aeruginosa*, measured by either PA14-GFP signal in the intestinal lumen or intestine diameter, correlated with the trained response index to a weak, but significant, amount (**Fig. S13A and B**). However, intestinal distention on *E. faecalis*

showed no such correlation, perhaps due to the fact that distention was much more prevalent and severe in animals exposed to *E. faecalis* (**Fig. S13C and D**). As shown in the previous chapter, the association of intestinal distention and *E. faecalis* cues requires the TRPM channels GON-2 and GTL-2. It was found that these channels were also required for the learned reflexive aversion to *E. faecalis*, as animals with loss-of-function mutations in the genes encoding for GON-2 and GTL-2 displayed mitigated responses to *E. faecalis* after training (**Fig. 18C**). Although intestinal distention may not explain the variation in aversion observed, this data suggests that the association of intestinal distention and bacterial cues is required for the trained reflexive aversion to at least *E. faecalis,* indicating that the mechanisms of learned reflexive aversion and learned avoidance share similar connections.

Finally, it remained to be seen whether this circuit was specific to the pathogen response or if it governed a general reflexive aversion to repulsive odors. It was found that animals lacking AWB neurons showed reduced reflexive aversion to 2-nonanone, a volatile organic compound that is known to be repulsive to *C. elegans* (**Fig. 18D**). This confirms previous reports that AWB is the primary senor of 2-nonanone (8, 170). Importantly, animals lacking either AUA or RMG also showed reduced reflexive aversion to 2-nonanone (**Fig. 18D**). Altogether, these results indicate that learned reflexive aversion involves the formation of an association between intestinal infection and bacterial odors, with the behavior executed by a four-layer neural circuit composed of AWB olfactory neurons electrically synapsed to AUA and RMG interneurons, which themselves are connected chemically to the motor-command interneurons AVA, AVD, and AVE (**Fig. 18E**). These interneurons control the motor neurons, VA, DA, VD, DD, and AS, which execute backward locomotion. Backward locomotion and the underlying circuit seem to be crucial for learned reflexive aversion to *P. aeruginosa* and *E. faecalis,* learned avoidance of lawns of these pathogens, and aversion to a repulsive volatile

organic compound, 2-nonanone, in *C. elegans*. Taken together, the results implicate the sensorimotor circuit in the control of an innate reflexive aversion to a repulsive odor and a learned aversion to pathogenic bacteria.

Chapter Discussion

The discovery of a sensorimotor circuit involved in learned reflexive aversion to the pathogenic bacteria *P. aeruginosa* and *E. faecalis* and naïve aversion to 2-nonanone demonstrates the utility of the *C. elegans* Neural Interactome as a tool for hypothesis generation. AUA and RMG neurons had not previously been implicated in either pathogen avoidance or aversion to 2-nonanone. Interestingly, both had been implicated in the regulation of social feeding behavior (97, 171). AUA is a synaptic target of URX, and expression of *npr-1* in *npr-1(ad609)* mutants in AQR, PQR, URX, and AUA neurons results in suppression of aggregation and bordering behaviors (97). RMG is at the center of a gap junction hub-and-spoke circuit, connected to many sensory neurons, including ASK, URX, ASH, ADL, and AWB (171). High activity in RMG is essential for all aspects of social behavior, including aggregation, bordering, and, with input from ASK neurons, attraction to hermaphrodite pheromones. The innexin gene *unc-9* was shown to be required in RMG neurons to drive social behavior (172). As AWB and AUA neurons also express *unc-9* (173), it is possible that *unc-9*-based gap junctions are also required for AWB-mediated pathogen and odor avoidance behaviors.

A crucial step to study sensorimotor circuits necessary for learned pathogen avoidance was to find a behavior that matched the seconds-long timescale necessary to perform simulations. Learned pathogen avoidance takes hours and was therefore not a suitable behavior. The discovery that *C. elegans* avoids drops of *P. aeruginosa* and *E. faecalis* within seconds, following hours-long pre-exposure on bacterial lawns, allowed us to match the behavior and the simulated data from the Interactome on similar

timescales. Ultimately the neurons involved in learned reflexive aversion and learned pathogen avoidance were the same for both *P. aeruginosa* and *E. faecalis*, with AUA and RMG neurons required for both (**Fig. 17**). Thus, it is speculated that learned reflexive aversion to pathogenic bacteria is a crucial component of the general learned pathogen avoidance behavior. In general avoidance, the reflex to avoid pathogenic bacteria is most likely countered by attraction to the bacteria as a food source. This attraction is likely driven by AWC neurons, which are known to shape the olfactory response to pathogenic bacteria and food odors (94, 95). It was found that AWC neurons were required for the learned reflexive aversion response, further implicating them in the associative learning process required for avoidance of *P. aeruginosa* and *E. faecalis* (**Fig. 15B and C**). The cross-training experiments performed with the two pathogens make clear that this process is driven by olfaction (**Fig. 18A and B**). Exactly how this learning takes place, and what the changes in the neural dynamics are that allow for a shift from attraction to aversion over time remains unclear, though modulation via serotonin likely plays a role (94, 136). ASI and ASE neurons also seem to play a role in the learned aversion to *P. aeruginosa* and *E. faecalis*, respectively (**Fig. 16B and C**). The simulated data suggest that such a role is not through the engagement of the backward-movement motor neuron circuitry, as stimulation of AWC, ASE, or ASI neurons does not lead to strong oscillations in the motor neurons (**Fig. S9**). This is in contrast to the stimulation of AWB neurons, which induces motor neuron oscillations (**Fig. 15E**). What bacterial cue actually stimulates the AWB neurons remains unknown, though it is likely a bacterial odor (or blend of odors). This could be an initially attractive odor that becomes aversive with bacterial infection, or an innately aversive odor such as 1-undecene (37). If I had to speculate, I would guess that bacterial odors are most likely a blend of attractive and aversive odors. *C. elegans* odor valence perception seems to be affected by nutritional and infection status, possibly through neuromodulation of circuits downstream of the

olfactory neurons. I suspect that the responses of olfactory neurons such as AWB and AWC remain the same regardless of nutritional or infection status, but that the strength of the signal passed to downstream neurons is modulated by feeding and infection. This hypothesis could be tested by looking at the activity of downstream neurons, such as RMG or AUA, in response to bacterial odor stimulation before and after infection or starvation.

While the Interactome allowed me to accurately predict which neurons would be necessary for pathogen avoidance and 2-nonanone aversion, the actual neural dynamics at play in these behaviors may be quite different. An important next step would be to experimentally uncover the dynamics at play and compare them to the Interactome model. This would allow for further refinement of the model, and would be possible using tools such as NeuroPAL, which allows for neuronal identification of all *C. elegans* neurons via a multicolor fluorescence map, and genetically encoded calcium indicators (174). Further combinations of experimental manipulation and computational modeling will be crucial in deepening our understanding of behaviorally relevant neural circuits.

CHAPTER 4: SUMMARY AND CONCLUSIONS

Summary of Findings

The main findings of this dissertation are that the TRPM channels GON-2 and GTL-2 mediate learned pathogen avoidance following intestinal distention, and that AUA and RMG interneurons are crucial components of a four-layer sensorimotor circuit important for olfactory-induced, avoidance-associated locomotion. Together, these findings further our understanding of the gut-brain axis and its influence on behavior in the context of host-pathogen interactions. This chapter begins with a brief summary of the results.

After giving a brief overview of innate immunity and pathogen avoidance in Chapter 1, it was shown that *E. faecalis* quickly elicits avoidance in *C. elegans*. Population avoidance levels peaked at four hours, but individual animals left lawns of *E. faecalis* in 19.2 minutes on average. This leaving was balanced by re-entry events that became diminished over time.

Avoidance was not the result of bacterial RNA as is the case with *P. aeruginosa*-induced avoidance, but was instead elicited by intestinal distention. Anterior intestinal distention in particular lined up with avoidance levels, differentiating *E. faecalis*-induced distention from the more medial intestinal distention induced by *P. aeruginosa*. This anterior intestinal distention was also not able to be blocked by loss of *nol-6* function, further differentiating it from the *P. aeruginosa* case. Intestinal distention seemed to be the sole cause of *E. faecalis*-induced avoidance, as avoidance was independent of both pathogen virulence and immune effectors or pathways.

The avoidance response to *E. faecalis* was shown to be counteracted by hyperoxia avoidance through loss of function of the GPCR NPR-1. Mutant animals for *npr-1* failed

to avoid lawns of *E. faecalis*. The avoidance phenotype could be rescued by placing animals in 8% oxygen environments. The mutant phenotype re-emerged upon the transfer of animals from 8% to atmospheric oxygen. The *npr-1* mutant phenotype depended upon the guanylyl cyclase GCY-35. The cGMP-gated-ion-channel subunits TAX-2 and TAX-4 were also required independently from NPR-1, and their expression patterns pointed to potential neurons that could play a role in avoidance of *E. faecalis*.

Rescuing *tax-2* expression in a *tax-2* mutant background revealed that ASE neurons play a role in avoidance of *E. faecalis*. This was confirmed by genetic ablation of ASE neurons. These genetic ablations also confirmed the involvement of AWB and AWC neurons in avoidance of both *E. faecalis* and *P. aeruginosa*. ASI neurons were also shown to be involved in avoidance of *P. aeruginosa*, with animals lacking ASI neurons failing to avoid *E. coli* lawns supplemented with *P. aeruginosa* derived RNA and failing to discriminate between *E. coli* lawns with and without supplementation of *P. aeruginosa* RNA.

The AWB and AWC neurons were shown to be important components for aversive olfactory learning following ingestion of *E. faecalis*. Wild-type animals naïve to *E. faecalis* preferred the smell of the pathogen over the smell of *E. coli*, but after ingestion this preference switched. Both the naïve preference and the preference switch required AWB and AWC neurons. Pairing an odor that is attractive to naïve wild-type animals, benzaldehyde, with *E. faecalis* caused the animals to avoid benzaldehyde after *E. faecalis* ingestion. This strengthened the argument that what was observed was truly a form of associative learning. The naïve preference for benzaldehyde required AWC neurons, while the preference switch required AWB neurons.

The above summarized results revealed how *E. faecalis* induces learned pathogen avoidance, but what about the gut-brain axis? Screening animals with loss of various

TRP channels for *E. faecalis*-induced avoidance revealed that GON-2 and GTL-2 TRPM channels were necessary for avoidance. Expression of *gon-2* in intestinal cells and *gtl-2* in the excretory cell was sufficient to rescue the avoidance phenotype. Tying these channels into learned pathogen avoidance, it was shown that these channels did not affect the naïve preference to *E. faecalis* but were necessary for the odor preference switch upon *E. faecalis* ingestion.

While the precise mechanism by which these TRPM channels contribute to learned pathogen avoidance remains unknown, it was shown that it is not through reduced anterior intestinal distention. Instead, it was speculated that these channels either sensed a perturbance in ion concentrations caused by intestinal distention or that they sensed the mechanical force caused by distention directly. The signal from the intestinal and excretory cells to the nervous system that allows for intestinal distention and bacterial cues to be associated remains also remains unknown.

Having established that olfactory aversive learning is a crucial component the animal's response to *E. faecalis* and *P. aeruginosa*, Chapter 3 detailed the experiments and computational modeling done to uncover a circuit that transforms olfactory cues into the locomotion necessary for avoidance. It started with an explanation of the assay used to test both naïve and trained aversive reflexes to *P. aeruginosa* and *E. faecalis*. No naïve aversive reflex was recorded for any animal, but a trained reflex did emerge after infection with either pathogen. This trained reflex required ASI, AWB, and AWC neurons for *P. aeruginosa* and ASE, AWB, and AWC neurons for *E. faecalis*. These were the same neurons shown to be necessary for learned avoidance of pathogen lawns in Chapter 2, indicating that the lawn avoidance assay and aversive reflex assay may be different ways of testing the same behavior.

Using the Neural Interactome, it was shown that stimulation of AWB and a set of command interneurons led to oscillations in motor neurons known to be important for backward locomotion. Stimulation of these neurons also led to high activity in AUA and RMG neurons. Ablation of these neurons within the Neural Interactome revealed that these neurons were crucial in generating the motor neuron oscillations. Genetic ablation of these neurons and behavioral testing confirmed the computational prediction, as animals with AUA or RMG neurons ablated showed decreased trained reflexive aversion to both *P. aeruginosa* and *E. faecalis*. These same animals also failed to avoid lawns of either pathogen. This suggested that AUA and RMG neurons were important parts of a four-layer neural circuit for reflexive aversion to pathogenic bacteria.

To show that this circuit was involved in an olfactory aversive learning process, animals were infected with one pathogen and then tested with the other. This resulted in no reflexive aversion; however, if animals were instead infected with one pathogen paired with the odor of the other and then tested with the latter, they displayed high levels of reflexive aversion. Furthermore, aversion to 2-nonanone, an odorant that is repulsive to naïve animals, was diminished in animals lacking AWB, AUA, or RMG neurons. This suggested a model whereby AWB neurons respond to odors paired with intestinal infection or naïvely repulsive odors. The AWB signal gets passed down gap junctions to the AUA and RMG neurons. Synaptic connection with the command interneurons allows the signal to pass through to the motor neurons necessary for backward locomotion.

An Aside on Philosophy

Moving on from this summary of findings, this dissertation closes with an examination of the philosophical underpinnings of the research. It may seem odd for a scientist to venture into philosophical argumentation, despite the fact that graduate research

culminates in a doctorate of philosophy. Indeed, scientists are often rather blasé about philosophy and philosophers; however, as Alex Rosenberg points out, it is impossible for scientists to escape philosophy (175). Every scientific endeavor makes a number of philosophical claims which reveal ontological, epistemological, and methodological priorities and inclinations. While a scientist may be unaware that they are making these claims when carrying out an experiment, philosophical complications still sneak in. A scientist's deep-seated, tacit beliefs, formed not just through scientific reasoning but also ideological construction, have profound influences on the questions that scientist asks and how they go about answering them (176–181). Thus, instead of ignoring philosophy, the claims should be acknowledged, justified, and analyzed in order to improve the theorizing and experimentation taking place. The rest of this chapter attempts to do just that, examining the research presented in the preceding chapters from a philosophical perspective, with the hope that this analysis will point towards promising future research directions.

Reductionist Explanations in Neuroscience

To begin, it is helpful to examine the title of this dissertation more closely: *Neural and Molecular Mechanisms of Pathogen Avoidance in Caenorhabditis elegans*. From the title, it is clear that the goal of the research was to attempt to explain how a certain type of behavior is generated by the nervous system of a simple model organism. The explanation was to be at the cellular, molecular, and circuit levels. To arrive at these explanations, the molecular, cellular, and circuit components of *C. elegans* were manipulated genetically and *in silico* in order to assess causality. For the sake of this dissertation, David Hume's infamous problem of induction will be set aside—it will be assumed that we can safely move from observations of particular events to general causal

explanations via inductive reasoning (182). If we do not assume this, the whole scientific enterprise would be on dubious footing.

While the problem of induction may not be solvable, convention dictates what valid inductive reasoning looks like. In neuroscience, and in biology in general, the convention is to label explanations as causal if they satisfy necessary and sufficient conditions. A necessary condition is a condition that must be present for an event to occur, while a sufficient condition is a condition that will produce the event. For this dissertation, experiments were done to prove the necessity and sufficiency of components for pathogen avoidance. The data presented thus far hopefully convinces the reader that the experiments performed did indeed allow for, or at least point towards, conventional causal explanations. Genetically ablating neurons and using loss-of-function mutants are conventional tests of necessity, for example, while rescuing components in specific tissues and stimulating neurons *in silico* are tests of sufficiency.

An interesting conundrum arises, as pointed out by Motojiro and Motoyuki Yoshihara, though: using formal logic, saying "Gene X is necessary and sufficient for a biological phenomenon" literally means that no other gene is required for the biological phenomenon (183). Logically, something being necessary means that if the thing is not present, the process does not happen. The contrapositive is also true—if the process happens, the thing is present. Sufficiency, on the other hand, is the converse of that last statement—if the thing is present, the process does happen. It is important to emphasize that, again logically, sufficiency means that all that has to be present for the process to happen is the thing *on its own*. But this is almost never what biologists and especially neuroscientists mean when they use the words "necessary and sufficient". The convention in biology, and the convention used in this dissertation, is that a component's necessity and sufficiency does not preclude the possibility of other component's necessity

and sufficiency. Indeed, all biological phenomenon are the result of multiple components functioning together to execute the whole process. In other words, it is more akin to saying "if the thing is *in this particular system with these particular conditions*, the process happens". Biology is further complicated by the fact that a thing may be sufficient for a process, but not biologically necessary, as in the case of artificial expression of the *eyeless* gene being enough to induce retinal development but other genes also being capable of inducing development (183). To correct this conundrum, the Yoshiharas suggest either abolishing the usage of "necessary and sufficient", or using "indispensable and inducing" when talking about experimental manipulations that strive to establish causality (183). Thus, a gene or neuron can be indispensable for or induce a behavior without satisfying the rigid formal logic rules implied by necessary and sufficient conditions. Other authors argue for other conventions including defining causality as the condition in which "if, with all else being equal, an event's presence or absence affects the probability of an outcome" (184), or understanding causes as factors that can be manipulated to control effects (185).

This all may seem like pedantic quibbling over language, but the language researchers use can have quite dramatic consequences. Language, after all, is part of how data is presented, interpretations argued, funding asked for, experiments requested from supervisors, results explained to the public, and all the other activities that comprise science. Just as there is no escape from philosophy, there is no escape from language. The language researchers use influences how they view results, what experiments they will perform, what questions they are asking, and ultimately the direction of whole research programs. Four types of potential pitfalls of using necessary and sufficient conditions in biological research were identified by the Yoshihara paper; however, it is their last type that is particularly concerning: application of the necessary and sufficient conditions framework leads to research with no scientific insight (183). Instead of using

knowledge of biology to ask important questions and develop experiments that may lead to new insights, researchers often fall into the trap of just manipulating something and seeing if it has a biological effect. For example, research conducted to see if calcium has an effect on long-term memory formation is misguided and wasteful when it is already known ahead of time that calcium plays a crucial role in synapse transmission. This is also the danger of doing forward genetic screens—their beauty lies in the fact that the experimenter is using nature/the organism to tell them what is going on. A forward screen in the hands of an informed, critical experimenter may reveal unexpected but interesting "hits". If the experimenter does not have an idea of what could be biologically interesting, however, they might get lost in uninteresting "hits" with little biological insight. A similar risk plagues "omics" profiling, where the profile in itself has no interesting information outside of the researcher's ability to interpret the profile and go on to perform further manipulations (186). This isn't to say that research into the specific roles of calcium in different processes, forward genetic screens, or profiling shouldn't be done, but care must be taken to set up conditions carefully in order to increase the likelihood of returning something actually biologically important. Only the human researcher, trained in the intricate details of their chosen topic can determine what is biologically worthwhile.

Using "indispensable and inducing" instead of "necessary and sufficient" language in biological research may be worthwhile; however, the particular language used is a symptom of a much larger problem that will require more than mere word switching: a bias towards reductionist explanations. It is important to take some time to examine what reductionist explanations are and why they can be a problem.

Here is a question to start: does demonstration of components that are indispensable and inducing for a given behavior allow one to gain deeper insight into the

behavior? For example, did this current dissertation lead to a deeper understanding of pathogen avoidance? One way of answering this is to look at the language used to describe the results. Several words, which Krakauer et al. call "filler verbs" (178), show up whenever an attempt was made to move from experimental manipulation to causal explanation. These include "reveal" (16 times), "involve" (50 times), "regulate" (73 times), "mediate" (43 times), "underlies" (10 times), and "play a role in" (18 times), to name a few. This is not just a quirk of my writing style, either. The scientific literature is rife with such verbs. This is not necessarily a bad thing: as I pointed out earlier, language is an essential component to explaining and understanding scientific research, and the choice of verb may convey subtle aspects of the research's meaning. What is important to make clear, however, is that their use does not add explanatory power to results but restates the causal explanation already arising from the experimental demonstration of indispensable and inducing components.

If nothing is learned besides a causal explanation for a behavior, one must ask if a causal account is enough on its own? At first blush it seems rather silly to say that it is not. If causes for a behavior are found, then it seems obvious that we have moved closer to understanding how the behavior was generated. But as Krakauer et al. point out, rephrasing a critique put forth by David Marr among others, this is just one level of analysis, the implementation level (178). Behaviors are also composed of what they call computational and algorithmic levels. Analyses at the computational level ask why a behavior is occurring, or what problem is being solved by the nervous system. The algorithmic level asks what rules are being used to realize the computational solution. The implementation level is made up of the physical features that allow for the algorithm to function. Take a bird flapping its wings to fly. Flying is the computational goal, and flapping its wings is the algorithmic realization. For the bird, wings depend upon feathers, the physical implementation of flying. By looking at only feathers, a full

understanding of flight is impossible. What is more, feathers may not be the only implementation that allows for flight, as bats fly but do not have feathers. By analogy, looking at only neurons or molecules can never give a full understanding of behavior, and even if one discovers a molecular mechanism for a behavior, it may not be *the* mechanism. Further, it is not clear whether an explanation of the implementation level of a behavior is anything more than a description of the physical components of that behavior. That is to say, mechanisms can be thought of as descriptions of physical components. Does knowing the physical components of a system add to understanding of that system? In a certain sense it does. As one of the reviewers of this dissertation rightly pointed out in the initial draft, knowing how something works computationally and algorithmically does not mean much, especially when we are looking at something like neurons, if we do not know the physical substrate on which the computations and algorithms are running. In other cases the physical substrate may not be as important, as in the case of something like playing chess, where the physical properties of the chess board do not matter for understanding how chess is played (178). What understanding at the implementation level does allow for is knowledge of how to break and, perhaps, fix the system if something goes wrong at that level. Thus, knowing molecular and cellular mechanisms of a behavior allows for molecular and cellular therapeutics. This is indeed valuable, but it is by no means the whole picture.

The reductionist bias, then, is the favoring of the implementation level of analysis over computational and algorithmic levels. While neuroscientists may shy away from ontological reductionism, or the idea that all there really exists are combinations of smaller and smaller entities, they increasingly commit themselves to methodological reductionism which favors manipulations at molecular, cellular, and circuit levels. This leads to epistemological reductionism, where descriptions of molecular and cellular events are compiled, with understanding at other levels falling by the wayside. Of course,

this is not the case across all neuroscience-related researchers; indeed, there are neuroscientists who focus on natural behaviors, cognitive neuroscientists who investigate the algorithmic levels, and computational scientists who work on models of nervous systems. However, it is increasingly hard for research working at levels of analysis above the reductionist one to get funded by a society that approaches problems in a more and more positivistic, reductionist way. If we are going to solve the problems of the brain, we need multiple levels of analysis, from molecular reductionist to cognitive. Unfunded research proposals and rejected articles are often criticized for being too descriptive and not mechanistic enough; this is ironic given that a mechanism is nothing but a description of how something is done. Answering this question will never give a complete story: in biology, it also needs to be asked what function something serves, what its evolution was, and how it developed.

It is admittedly hard to do everything, everywhere, all at once. For one person, it is impossible. The division of labor and hyper-specialization that is a hallmark of capitalist society, and the source of much alienation between the worker and their work, has also rendered the "Renaissance man" obsolete. In his stead we must work to support those doing work at multiple levels of study, build bridges between them, and foster a community that incorporates and makes accessible findings from all levels of study of the brain.

Putting the Focus on Behavior

Some neuroscientists often avoid studying behavior altogether. A structural biologist, for example, may study the structure and dynamics of an ion channel expressed in the human brain without any thought towards its contribution to behavior. Having some researchers ignore behavior is most likely fine on its own; however, situated in the actuality of neuroscientific research as a human endeavor with its accompanying

historical, sociological, and political ramifications, a larger abandonment of behavioral research by the field could be a major hindrance to furthering neuroscientific understanding. The previous section explained the loss in understanding that comes with methodological and epistemological reductionism, but in general the danger with any approach gaining dominance is that rather than the approach winning out because it is the best way to answer biological questions, it gains outsized influence because of larger sociopolitical trends. The rapid ascent of molecular biology, for example, was largely tied to partnerships between scientists and technologically-minded entrepreneurs looking to expand the reach of their newly developed technologies (187). That is not to say that molecular biology is not a worthwhile approach. It has been wildly successful in coming up with explanations of biological phenomena, and this dissertation relies heavily on molecular biology techniques. In his account, Rosenberg lists some of the achievements of molecular biology, including detailed molecular understanding of respiration, heredity and somatic gene regulation, sensory transduction in the visual system, photosynthesis, and the Krebs cycle (175).

Neuroscience has a similar relationship with technology and its accomplishments are many. New techniques drive some of the highest profile research, including optogenetics, genome engineering, single-cell profiling, calcium imaging, genetically-encoded voltage indicators, and so on. All of these technologies promise to further neuroscientific understanding, which is ultimately concerned with understanding nervous systems. The focus on these technologies, though, may result in answering an easier question rather than a harder one. The hard problem for neuroscience is to figure out nervous system functioning. The easier problems to solve, though still difficult, are technological hurdles that allow for finer and finer control over the implementation level of nervous systems. In other words, to achieve control over their physical hardware. This hardware does not exist absent animals, however, but instead is situated in animals

behaving in their environments. Understanding nervous systems, then, will only be accomplished if a similar level of research is devoted to the study of animal behavior. This type of research already exists to some extent, but broader support and funding is needed.

This dissertation did not avoid behavior; instead, it focused on a particular type of behavior—pathogen avoidance. Nevertheless, it mostly stayed at the implementation level, describing neural and molecular mechanisms of pathogen avoidance. The behavior was, in most cases, used as a mere readout for the molecular and neural manipulations taking place. There were some instances where the behavior was studied in a more detailed manner. For example, in Chapter 2, the *E. faecalis* lawn leaving and entering events were measured for individual animals over time, leading to the realization that population lawn avoidance numbers were not the result of increased leaving events but decreased re-entry events. One of the novel findings of Chapter 3 was the realization that backward locomotion events are a crucial component of pathogen lawn avoidance controlled by the same neural architecture. Further, the Neural Interactome is a model of *C. elegans* nervous system at the algorithm level, and was used in this dissertation to predict mechanisms at the implementation level.

It would be easy, in coming up with future directions building off of this dissertation, to suggest the application of new technologies to further clarify the neural and molecular mechanisms of pathogen avoidance in *C. elegans*. Chapter 3 ended with such a suggestion, laying out how NeuroPAL and genetically encoded calcium indicators could be used to refine the Neural Interactome model (174). Other applicable technologies include those listed above. Optogenetics could be used to simulate the AWB neuron in a similar manner to its *in silico* stimulation in the Neural Interactome, which would confirm its role in olfactory-induced learned reflexive aversion. Additional

neurons besides AUA and RMG could be ablated or stimulated experimentally to lend further evidence to the circuit model presented in Chapter 3. Expression of the TRPM channels in cell lines that do not express mechanosensitive ion channels followed by electrophysiological recordings of these cells following mechanical stimulation would test whether those TRPM channels were truly mechanosensitive. The list of potential implementation level manipulations goes on. The point of the dive into philosophical argumentation presented here, though, was to show that compiling a list implementation level mechanisms is not enough on its own to truly understand any given behavior. Thus, if understanding pathogen avoidance is truly the goal, these manipulations should be accompanied by detailed analyses of the avoidance itself. Well-designed behavioral experiments would reveal details of avoidance that could suggest algorithms for how that avoidance is accomplished, which in turn could predict hardware level implementation of those algorithms. Uncovering that hardware will allow for confirmation and refinement of the algorithms, ultimately resulting in fuller explanations of pathogen avoidance.

Detailed behavioral work in *C. elegans* is already under way. A recent study using whole-organism behavioral profiling, for example, found a role for dopamine in state-dependent motor program coupling (188). Such works demonstrates how detailed analyses of behaviors can lead to new appreciation of the role of molecules in behaviors. To advance the understanding of pathogen avoidance, behavioral analysis should make use of hardware and software tracking platforms that allow for detailed computational breakdowns of locomotion, feeding, and reproduction (189, 190). In addition, new environments beyond the petri dish setup with single lawns of pathogens may need to be developed, as an animal's environment can have profound consequences for the behavioral strategies it employs (191).

Interpretation of Observations

The previous section argued that a complete understanding of pathogen avoidance requires that more effort be spent working on computational and algorithmic problems of avoidance. This does not, however, mean that manipulations at the physical level cannot reveal something about the behavior. On a basic level, this dissertation adds to our understanding of the neural and molecular mechanisms of pathogen avoidance in *C. elegans*, revealing the involvement of TRPM channels in intestinal distention-induced avoidance and a complete sensorimotor circuit for learned reflexive aversion. While the previous section situates this research in a tradition of reductionist explanations of nervous system functioning, and points towards how to move beyond these reductionist explanations to achieve a fuller understanding of animal behavior, the manipulations at the physical level done here are important not only in understanding how *C. elegans* implements pathogen avoidance, but how animals in general implement aversive behaviors, and what may cause them. In a broader sense, this dissertation suggests ways in which other animals may detect and avoid infectious agents and noxious chemicals.

The hallmark of *C. elegans* infection by *E. faecalis* and *P. aeruginosa*, as shown by this dissertation, is intestinal distention. Gastrointestinal disorders, such as irritable bowel syndrome and Crohn's Disease, are common across many animal species and have diverse causes, including too much gas in the intestine, abnormal levels of bacteria in the small intestine, an imbalance of microorganisms in the bowel, food intolerance, increased sensitivity to digestive tract discomfort, and decreased abdominal muscle motility. Intestinal bacterial infection and subsequent distention in *C. elegans* may, therefore, be a good model to study the mechanisms of these gastrointestinal disorders. In particular, the finding that TRPM channels play a role in sensing intestinal distention points to potentially important roles for TRPM channels in other gastrointestinal

disorders. TRPM channels, as was pointed out in Chapter 2, are expressed in the human intestine, where they have been shown to function as calcium and magnesium ion absorbers and pacemaker activators, while in mice they play a role in colonic nociception. It seems very likely, then, that TRPM channels may contribute to sensing the pain that accompanies many gastrointestinal disorders, though this remains to be proven.

Infection by *E. faecalis* caused particularly extreme anterior intestinal distention in *C. elegans*. I was not able to find why this was the case, but it is worth speculating here on possible causes, as they may point to ways in which other animals become bloated. *C. elegans* initially breaks down the bacteria it eats using a thick, ridged cuticle called the grinder in its pharynx. Bacteria are ground up and passed to the intestine through the pharyngeal-intestinal valve. The anterior portion of the intestine, the segment that becomes distended upon *E. faecalis* infection, sits right behind this valve. I therefore think it is likely that *C. elegans* is not able to properly grind *E. faecalis*, which as a Gram-positive bacterium has a thicker peptidoglycan cell wall than gram-negative bacteria. *E. faecalis* likely then becomes stuck in this anterior portion of the intestine and eventually causes distention. If correct, this suggests that other Gram-positive bacteria may also cause similar distention, which the data on *S. aureus* and *E. faecalis* presented in Chapter 2 also seems to suggest. More broadly, hard to digest food may eventually set off intestinal pain sensors in many animals, leading them to avoid the hard-to-eat food. Humans avoid food that does not "sit well" with them all the time, and it is interesting to note that this is the case even in very simple organisms such as *C. elegans*.

This "hard-to-eat" property of *E. faecalis* ties into another point worth reiterating here: pathogen avoidance in *C. elegans* falls under the umbrella of foraging behaviors. This is primarily the case because *C. elegans* is a bacterivore, and thus the bacterial

pathogens and potential food sources it encounters are the same types of organisms, but the point is true for non-bacterivore animals as well: every animal food source has the potential to cause harm, either through its inability to be digested, its harboring of dangerous microorganisms, or even its proximity to predators. In choosing to feed on a particular food source, there is always a balance between risk and reward. For example, I could eat a piece of Epoisse de Bourgogne cheese now, but I may have stomach discomfort later. When *C. elegans* leaves a lawn of bacteria that it was feeding on it is, in a sense, making a calculation and determining that the risk of eating the bacteria any further outweighs the nutrition that can be derived from it. Studying the mechanisms of pathogen avoidance is important, therefore, not only for working out how pathogen avoidance works in animals, but how animals determine risks and rewards as they move about their environment, satisfying their need to feed.

The nervous system of *C. elegans*, which controls this decision-making process, is extremely simple and far different than even the simplest mammalian nervous system; and yet, the ways in which the neurons function and the types of circuits that it makes between sensory neurons, interneurons, and motor neurons are also found in humans. What's more, its simplicity allows for direct manipulation in a way that will probably never be possible in humans or mammalian species. These manipulations allow us to understand how simple circuits can govern associative learning, aversion, and foraging decisions. Chapter 3 of this dissertation in particular showed how a simple model of the *C. elegans* nervous system paired with neuron-specific manipulations can be used to predict and verify how aversive behaviors are governed by a four-layer sensorimotor circuit, identifying particular neurons at every layer that are necessary for a trained aversive reflex to *P. aeruginosa*. While this circuit is much simpler than the complex cortical circuits found in humans, it is similar to reflex circuits found in all animals, consisting of afferent sensory neurons, interneurons, and efferent motor neurons.

In Chapter 3 it was pointed out that the simulation probably does not capture the actual dynamics of the circuit, but is instead a close enough approximation that accurate predictions of the effect of experimental circuit manipulations on animal behavior could be made. Another important caveat to mention here is that this simulation is static in nature, and thus cannot capture how the circuitry is actually changing to give rise to different behaviors before and after learning has taken place. Thus, when I stimulated AWB neurons in the simulation I always recorded the same motor neuron output. This obviously would not be the case in a living animal where the strengths of the connections between different neurons is constantly changing based on prior experience, and where the animal is receiving many types of inputs all the time. In the particular case of pathogen avoidance under examination in this dissertation, it is likely that bacteria give off both attractive and aversive odors that are sensed by different olfactory neurons (likely AWC for attractive and AWB for aversive). During aversive learning, the strength of the AWC connection to downstream interneurons (and eventually motor neurons that control forward movement) likely decreases while the AWB connection discovered in Chapter 3 increases in strength. This increase and decrease in connection strength, also called long-term potentiation and depression (LTP and LTD), was not modeled in the Interactome simulation. Instead, possible connections that could be at play after aversive learning took place were probed to work out the sensorimotor connections that are important for execution of the learned behavior. It may be possible, however, to build a dynamic model of the *C. elegans* nervous system. In this dynamic model, the user could tweak the strengths of the connections over time, simulating what happens during LTP and LTD. For example, to test the hypothesis that learned reflexive aversion to *P. aeruginosa* involves LTD of AWC-mediated signals and LTP of AWB-mediated signals, one could stimulate AWC and AWB neurons and recording from motor neurons important for both backward and forward locomotion. Then, they could modify the

connection strength to individual neurons downstream of both neurons to see how the motor neuron output is affected. The results of these simulations could also be validated by using calcium-imaging to look at the activity of downstream interneurons, such as AUA and RMG, to see if their activities differ before and after learning. As was pointed out in Chapter 3, simulation models could be refined further by using whole-brain recording methods in behaving animals. Such technology is now being used in *C. elegans*, along with large-area imaging in other species such as *Drosophila* and zebrafish. These models will have to also take into account connectomes other than synaptic links, such as monoamine and neuropeptide maps, in order to more accurately predict nervous system activity, modulation, and function.

MATERIALS AND METHODS

Key resources table

Reagent type (species) or resource	Designation	Source or reference	Identifiers	Additional information
Strain, strain background (*Escherichia coli*)	OP50	*Caenorhabditis* Genetics Center (CGC)	OP50	
Strain, strain background (*E. coli*)	OP50-GFP	CGC	OP50-GFP	
Strain, strain background (*E. coli*)	HT115	Source BioScience	HT115	
Strain, strain background (*Pseudomonas aeruginosa*)	PA14	Frederick M. Ausubel laboratory	PA14	
Strain, strain background (*P. aeruginosa*)	PA14-GFP	Frederick M. Ausubel laboratory	PA14-GFP	
Strain, strain background (*Enterococcus faecalis*)	OG1RF	Danielle A. Garsin laboratory	OG1RF	
Strain, strain background (*E. faecalis*)	OG1RF-GFP	Danielle A. Garsin laboratory	OG1RF-GFP	
Strain, strain background (*E. faecalis*)	OG1RF Δ*fsrB*	Danielle A. Garsin laboratory	OG1RF Δ*fsrB*	
Strain, strain background (*E. faecium*)	E007	Danielle A. Garsin laboratory	E007	
Strain, strain background (*Staphylococcus aureus*)	NCTC8325	National Collection of Type Cultures	NCTC8325	
Strain, strain background (*Caenorhabditis elegans*)	N2 Bristol	CGC	N2	
Strain, strain background (*C. elegans*)	*npr-1(ad609)*	CGC	DA609	
Strain, strain background (*C. elegans*)	*npr-1(ok1447)*	CGC	RB1330	
Strain, strain background (*C. elegans*)	*ocr-2(ak47)*	CGC	CX4544	
Strain, strain background (*C. elegans*)	*osm-9(ky10)*	CGC	CX10	

Strain, strain background (*C. elegans*)	*gcy-35(ok769); npr-1(ad609)*	Aballay laboratory		
Strain, strain background (*C. elegans*)	*tax-2(p694); npr-1(ad609)*	Aballay laboratory		
Strain, strain background (*C. elegans*)	*tax-4(p678); npr-1(ad609)*	Aballay laboratory		
Strain, strain background (*C. elegans*)	*tax-2(p671)*	CGC	PR671	
Strain, strain background (*C. elegans*)	*tax-2(p694)*	CGC	PR694	
Strain, strain background (*C. elegans*)	*tax-4(p678)*	CGC	PR678	
Strain, strain background (*C. elegans*)	*tax-2(p694); lin-15 and lin-15A(n765); dbEx723[gcy-32p::tax-2(cDNA)::SL2::GFP + lin-15(+)]*	CGC	AX2159	
Strain, strain background (*C. elegans*)	*tax-2(p694); lin-15 and lin-15A(n765); dbEx724[flp-6p::tax-2(cDNA)::SL2::GFP + lin-15(+)]*	CGC	AX2161	
Strain, strain background (*C. elegans*)	*che-1(p680)*	CGC	PR680	ASE(-)
Strain, strain background (*C. elegans*)	*peIs1713 [sra-6p::mCasp-1+unc-122p::mCherry]*	CGC	JN1713	ASH(-)
Strain, strain background (*C. elegans*)	*oyIs84 [gpa-4p::TU#813 + gcy-27p::TU#814 + gcy-27p::GFP + unc-122p::DsRed]*	CGC	PY7505	ASI(-)
Strain, strain background (*C. elegans*)	*peIs1715 [str-1p::mCasp-1+unc-122p::GFP]*	CGC	JN1715	AWB(-)
Strain, strain background (*C. elegans*)	*oyIs85 [ceh-36p::TU#813 + ceh-36p::TU#814 + srtx-1p::GFP + unc-122p::DsRed]*	CGC	PY7502	AWC(-)
Strain, strain background (*C. elegans*)	*agIs26 [clec-60p::GFP + myo-2p::mCherry]*	CGC	JIN810	
Strain, strain background (*C. elegans*)	*unc-119(ed3); eEx650 [ilys-3p::GFP + unc-119(+)]*	CGC	CB6710	
Strain, strain background (*C. elegans*)	*pmk-1(km25)*	CGC	KU25	

Strain, strain background (*C. elegans*)	*fshr-1(ok778)*	CGC	RB911	
Strain, strain background (*C. elegans*)	*bar-1(ga80)*	CGC	EW15	
Strain, strain background (*C. elegans*)	*nol-6(ac1)*	CGC	AY1	
Strain, strain background (*C. elegans*)	*gtl-2(n2618)*	CGC	CZ9957	
Strain, strain background (*C. elegans*)	*gon-2(q362)*	CGC	EJ26	
Strain, strain background (*C. elegans*)	*gon-2(q388)*	CGC	EJ1158	
Strain, strain background (*C. elegans*)	*glp-1(e2141)*	CGC	CB4037	
Strain, strain background (*C. elegans*)	*gtl-1(ok375)*	CGC	VC244	
Strain, strain background (*C. elegans*)	*gtl-2(tm463)*	CGC	LH202	
Strain, strain background (*C. elegans*)	*trpa-1(ok999)*	CGC	RB1052	
Strain, strain background (*C. elegans*)	*trpa-2(ok3189)*	CGC	TQ233	
Strain, strain background (*C. elegans*)	ynIs78 [*flp-8p::GFP*]	CGC	NY2078	
Strain, strain background (*C. elegans*)	ynIs87 [*flp-21p::GFP*]	CGC	NY2087	
Strain, strain background (*C. elegans*)	*gon-2(q388); gon-2p::gon-2(cDNA)::SL2::GFP*	This Dissertation	AY157	*gon-2* expression, own promoter
Strain, strain background (*C. elegans*)	*gon-2(q388); ges-1p::gon-2(cDNA)::SL2::GFP*	This Dissertation	AY158	*gon-2* expression, intestine specific promoter
Strain, strain background (*C. elegans*)	*gtl-2(n2618); gtl-2p::gtl-2(cDNA)::SL2::GFP*	This Dissertation	AY159	*gtl-2* expression, own promoter
Strain, strain background (*C. elegans*)	*gtl-2(n2618); sulp-4p::gtl-2(cDNA)::SL2:GFP*	This Dissertation	AY160	*gtl-2* expression, excretory cell promoter
Strain, strain background (*C. elegans*)	ynIs78 *[flp-8p::GFP]; flp-8p::ced-3 (p15)::nz + flp-32::cz::ced-3 (p17) + unc-122p::rfp*	This Dissertation	AY178	AUA(-)

Strain, strain background (*C. elegans*)	ynIs87 *[flp-21p::GFP]; flp-21p::ced-3 (p15)::nz + ncs-1p::cz::ced-3 (p17) + unc-122p::rfp*	This Dissertation	AY179	RMG(-)
Software, algorithm	GraphPad Prism 8/9	GraphPad Software		https://www.graphpad.com/scientific-software/prism/
Software, algorithm	ImageJ	NIH		https://imagej.nih.gov/ij/
Software, algorithm	Leica LAS v4.6	Leica		https://www.leica-microsystems.com/
Software, algorithm	Neural Interactome	Eli Shlizerman laboratory		https://github.com/shlizee/C-elegans-Neural-Interactome
Software, algorithm	PowerPoint	Microsoft		https://www.microsoft.com/en-us/microsoft-365/powerpoint
Software, algorithm	BioRender	BioRender		https://biorender.com/
Other	Hypoxia chamber	STEMCELL Technologies	CAT# 27310	

Bacterial strains

The following bacterial strains were used: *Enterococcus faecalis* OG1RF, *E. faecalis* OG1RF Δ*fsrB*, *E. faecalis* OG1RF-GFP, *E. faecium* E007, *Escherichia coli* OP50, *E. coli* OP50-GFP, *E. coli* HT115(DE3), *Pseudomonas aeruginosa* PA14, *P. aeruginosa* PA14-GFP, and *Staphylococcus aureus* NCTC8325. *E. coli* and *P. aeruginosa* bacterial strains were grown in Luria-Bertani (LB) broth at 37°C, while the rest were grown in brain-heart infusion (BHI) broth at 37°C. All sources are listed in the Key Resources Table.

C. elegans strains and growth conditions

C. elegans hermaphrodites were maintained on *E. coli* at 20°C unless otherwise indicated. Bristol N2 was used as the wild-type control unless otherwise indicated. All other strains and their sources are listed in the Key Resources Table. Some strains used in this dissertation were provided by the *Caenorhabditis* Genetics Center (CGC), which is funded by the NIH Office of Research Infrastructure Programs (P40 OD010440).

Construction of transgenic strains

The following transgenic lines were generated for this dissertation:

AY157 – *gon-2(q388); gon-2p::gon-2(cDNA)::SL2::GFP*

AY158 – *gon-2(q388); ges-1p::gon-2(cDNA)::SL2::GFP*

AY159 – *gtl-2(n2618); gtl-2p::gtl-2(cDNA)::SL2::GFP*

AY160 – *gtl-2(n2618); sulp-4p::gtl-2(cDNA)::SL2::GFP*

AY178 – ynIs78*[flp-8p::GFP]; flp-8::ced-3(p15)::nz + flp-32::cz::ced-3(p17) + unc-122::rfp*

AY179 – ynIs87*[flp-21p::GFP]; flp-21p::ced-3(p15)::nz + ncs-1p::cz::ced-3(p17) + unc-122p::rfp*

The *gon-2* and *gtl-2* transgenic strains were generated by micro-injecting the DNA of an expression plasmid (50 ng/µL for the first three and 5 ng/µL for the last), along with a co-injection marker plasmid (*coel::RFP*, 50 ng/µL). The plasmids were maintained as extrachromosomal arrays. The expression plasmids consisted of a promoter region and full-length cDNA subcloned into pPD95.77 (Fire Lab *C. elegans* Vector Kit; Addgene) containing an SL2::GFP region (83) via *SphI-XmaI* restriction sites. The *gon-2* promoter region used was 3.5 kbp upstream from the *gon-2* gene, the *ges-1* promoter region used was 3.3 kbp upstream from the *ges-1* gene, the *gtl-2* promoter region used was 2.9 kbp upstream from the start codon of F54D1.5, and the *sulp-4* promoter was 4.4 kbp upstream from the start codon of K12G11.1. Full-length *gon-2* and *gtl-2* cDNA were 6099 and 4221 bp, respectively.

AY178 (AUA ablation) and AY179 (RMG ablation) were generated by first constructing pJL12 (pPD95.75 *flp-8p::ced-3 (p15)::nz*), pJL13 (pPD95.75 *flp-*

32p::cz::ced-3 (p17)), pJL14 (pPD95.75 *flp-21p::ced-3 (p15)::nz*), and pJL15 (pPD95.75 *ncs-1p:: cz::ced-3 (p17)*) plasmids. The pJL12 plasmid was constructed by cloning a 2019 bp upstream-promoter region of the *flp-8* gene into a *ced-3 (p15)::nz* backbone vector, via SphI-BamHI restriction sites. The pJL13 plasmid was constructed by cloning a 2085 bp upstream-promoter region of the *flp-32* gene into a cz::ced-3 (p17) backbone vector, via SphI-BamHI restriction sites. The pJL14 plasmid was constructed by cloning a 4109 bp upstream-promoter region of the *flp-21* gene into a *ced-3 (p15)::nz* backbone vector, via SphI-BamHI restriction sites. The pJL15 plasmid was constructed by cloning a 3116 bp upstream-promoter region of the *ncs-1* gene into a *cz::ced-3 (p17)* backbone vector, via SphI-BamHI restriction sites. recCaspase plasmids were a gift from Martin Chalfie, Addgene plasmids # 16080 and # 16081, Addgene, MA (192). A cocktail of pJL12 (10ng/µl), pJL13 (10ng/µl), co-injection marker *unc-122p::RFP* (50ng/µl) and empty vector PUC18 (50ng/µl) plasmids was co-injected into NY2078 animals to generate AY178 animals. A cocktail of pJL14 (10ng/µl), pJL15 (10ng/µl), co-injection marker *unc-122p::RFP* (50ng/µl) and empty vector PUC18 (50ng/µl) plasmids was co-injected into NY2087 animals to generate AY179 animals. Transgenic animals showing successful ablation of AUA or RMG neurons were selected and used for further assays. Plasmids were maintained as extrachromosomal arrays.

RNA interference

RNAi was used to generate loss-of-function RNAi phenotypes by feeding nematodes *E. coli* strain HT115(DE3) expressing double-stranded RNA (dsRNA) homologous to a target gene (193, 194). RNAi was carried out as described previously (195). Briefly, *E. coli* with the appropriate vectors were grown in LB broth containing ampicillin (100 µg/mL) and tetracycline (12.5 µg/mL) at 37°C overnight and plated onto NGM plates containing 100 µg/mL ampicillin and 3 mM isopropyl β-d-thiogalactoside (RNAi plates). RNAi-

expressing bacteria were allowed to grow for 2 days at 20°C. Gravid adults were transferred to RNAi-expressing bacterial lawns and allowed to lay eggs for 5 hr. The gravid adults were removed, and the eggs were allowed to develop at 20°C to young adults for subsequent assays. The RNAi clones were from the Ahringer RNAi library.

Lawn avoidance assays

Bacterial cultures were grown by inoculating individual bacterial colonies into 2 mL of either LB or BHI broth and growing them for 5–6 hr on a shaker at 37°C. Then, 20 μL of the culture was plated onto the center of 3.5-cm-diameter BHI or standard slow-killing (SK) plates (modified NGM agar plates [0.35% instead of 0.25% peptone]) as indicated. The plates were then incubated overnight at 37°C. The plates were cooled to room temperature for at least 30 min before seeding with animals. Synchronized young gravid adult hermaphroditic animals grown on *E. coli* OP50 were transferred outside the indicated bacterial lawns, and the numbers of animals on and off the lawns were counted at the specified times for each experiment. Three 3.5-cm-diameter plates were used per trial in every experiment. Occupancy index was calculated as (N_{on} lawn/N_{total}). For first exiting events, individual animals were monitored and the time that the animal first left the lawn was recorded. For exploratory events, entry and exiting events were recorded for 10 min at 50 min and 3 hr and 50 min after transfer.

Avoidance assays at 8% oxygen

Avoidance assays as described above were carried out in a hypoxia chamber. Briefly, after young gravid adult hermaphroditic animals were transferred to the avoidance plates, the plates were placed in the hypoxia chamber and the lids of the plates were removed. The chamber was purged with 8% oxygen (balanced with nitrogen) for 5 min at a flow rate of 25 L/min. The chamber was then sealed, and assays were carried out. Control plates were incubated at ambient oxygen.

Avoidance assays with bacterial RNA

RNA from bacterial pellets was isolated and used for avoidance assays as previously described (102). Briefly, bacteria for RNA collection were grown on SK or BHI plates overnight at 37°C. Bacterial lawns were collected from the surface of the plates using 1 mL of M9 buffer and a cell scraper. The resulting suspension was transferred to a 15 mL conical tube. PA14, OG1RF, or OP50 from 15 lawns was pooled in each tube and pelleted at 5000 g for 10 min at 4°C. The supernatant was discarded, and the pellet was resuspended in 1 mL of Trizol LS for every 100 µL of bacterial pellet recovered. The pellet was resuspended by vortexing and subsequently frozen at −80°C until RNA isolation. Two hundred and forty micrograms of total RNA was placed directly onto OP50 lawns and allowed to dry at room temperature before transferring worms over for avoidance assays.

Aversive training

Training plates of 3.5 cm diameter containing either *E. coli* OP50 on SK agar or *E. faecalis* OG1RF on BHI agar were made as described above for avoidance assays. For RNA training assays, SK plates containing *E. coli* OP50 were spotted with the appropriate isolated RNA. Young gravid adult hermaphroditic animals grown on *E. coli* OP50 were transferred to the training plates and allowed to roam for 4 hr for *E. faecalis* training or 24 hr for RNA training. They were then transferred to the appropriate assay plates. For cross-training with odors, agar plugs with bacterial lawns were cut from growth plates and transferred to the lids of the training plates with the appropriate training bacteria, as described in the “Two-choice odor preference assays” protocol below.

Two-choice preference assays

Bacterial cultures were grown as indicated in the lawn avoidance assays above. Then, 20 µL of each inoculum was plated on opposite sides of a 6-cm-diameter BHI or SK plate and incubated overnight at 37°C. The plates were cooled to room temperature for at least 30 min before seeding with animals. For the 'Paralyzed' condition, 1 µL of 1M sodium azide was spotted onto each bacterial lawn. Young gravid adult hermaphroditic animals grown on *E. coli* OP50 were transferred to the center of plates equidistant from both the lawns. The numbers of animals on both lawns were counted at the specified times for each experiment. Three 6-cm-diameter plates were used per trial in every experiment. The *E. faecalis* choice index (*E. faecalis* CI) was calculated as follows:

$$E.faecalis\ \text{CI} = \frac{\text{Worms on } E.faecalis - \text{Worms on } E.coli}{\text{Worms on } E.faecalis + \text{Worms on } E.coli}$$

Choice indices to other bacteria were similarly calculated.

Two-choice odor preference assays (lid choice assays)

A modified version of the two-choice preference assays was carried out as previously described (91) to assess odor preference alone. To do this, bacterial cultures were grown and plated as indicated in the two-choice preference assays above. Then, agar plugs with the bacterial lawns were cut from the plates and transferred to the lids of new 6-cm-diameter BHI agar plates without any bacteria, so that the bacteria on the agar plugs faced down toward the plate surface on opposite sides of the plate. Two microliters of 1 M sodium azide were spotted on the surface below each agar plug. Young gravid adult hermaphroditic animals grown on *E. coli* OP50 (naïve) or from *E. faecalis* OG1RF training plates were transferred to the center of plates equidistant from both agar plugs. The numbers of animals paralyzed under each agar plug were counted after 1 hr. Three 6-cm-diameter plates were used per trial in every experiment. The choice index was calculated as indicated above.

Dry-drop assay

The dry-drop assay was carried out as previously described (90). Using a capillary, a drop of the appropriate stimulus was placed on a dry SK plate (for SDS, LB, dodecanoic acid, 2-nonanone, and *P. aeruginosa*) or BHI plate (for *E. faecalis* and *E. faecium*) in front of a forward-moving animal. A response was counted if an animal initiated backward movement upon encountering the dried drop. Response Index = number of responses/total number of drops. Ten drops were used per animal, and a total of 25 animals of each strain were used for each experiment. The stimuli were prepared as follows: 0.6mM SDS, 1mM dodecanoic acid, 1:10 2-nonanone, and a 5-6 hr liquid culture of either *P. aeruginosa* or *E. faecalis*.

Imaging and quantification

Fluorescence imaging was carried out as described previously (195) with slight modifications. Briefly, the animals were anesthetized using an M9 salt solution containing 50 mM sodium azide and mounted onto 2% agar pads. The animals were then visualized using a Leica M165 FC fluorescence stereomicroscope. For quantification of intestinal lumen distention, brightfield images were acquired at each time point using the Leica LAS v4.6 software, and the diameter of the intestinal lumen was measured using ImageJ software. For quantification of fluorescent immune reporters, fluorescent images were acquired using the Leica LAS v4.6 software in grayscale as presented, and the fluorescence intensity was measured and averaged across three points in the intestine of each animal at the indicated time points using ImageJ software. For quantification of fluorescent bacteria, fluorescent images were acquired and the ImageJ software was used to first draw a region of interest around the bacteria in the intestines of animals and then to measure the fluorescence intensity in the region.

Neural interactome simulations and visualizations

Simulations of the *C. elegans* nervous system were carried out using a local copy of the Neural Interactome, pulled from https://github.com/shlizee/C-elegans-Neural-Interactome. Simulations were run for at least 12 seconds and neuronal activity for each simulation was saved into a numpy file. Simulated data was loaded directly with the Python Numpy package into a Jupyter Notebook and converted to a Pandas DataFrame. Python scripts were written to visualize individual neuronal activity over time as rows on a heatmap and graphs were generated using the Matplotlib and Seaborn libraries. The first two neurons of the VD, DD, VA, DA, and AS motor neuron classes were chosen as representatives of each class to aid visualization.

Statistical analysis

The statistical analysis was performed with Prism 8/9 (GraphPad). For box-and-whisker plots, the center line depicts the median, and the box range depicts the first and third quartile, while the whiskers depict the minimum and maximum data points. For all box plots, individual dots represent individual trials. For time course figures, the mean and standard deviation of nine trials is depicted at each time point. All bar graphs depict the mean of the population, with individual dots representing individual trials. Error bars represent the standard deviation of the population. For x-y correlation plots, individual dots represent measurements for individual animals, and the red line depicts a simple linear regression. All experiments were performed in triplicate on three separate days, resulting in the sample sizes listed in the figure legends. Unpaired t-tests, one-way or two-way ANOVA with subsequent group comparisons were performed as indicated in the figure legends. In the figures, ns denotes not significant, and asterisks (*) denote statistical significance as follows: *p≤0.05; **p≤0.01; ***p≤0.001; ****p≤0.0001, as compared with the appropriate controls.

Figure creation

Figures were created using Microsoft PowerPoint, Biorender.com, and the Python programming language.

REFERENCES

1. R. H. Straub, M. Cutolo, F. Buttgereit, G. Pongratz, Energy regulation and neuroendocrine-immune control in chronic inflammatory diseases. *J Intern Med* **267**, 543–560 (2010).

2. C. Sarabian, V. Curtis, R. McMullan, Evolution of pathogen and parasite avoidance behaviours. *Philos Trans R Soc Lond B Biol Sci* **373** (2018).

3. S. Mansourian, *et al.*, Fecal-Derived Phenol Induces Egg-Laying Aversion in *Drosophila*. *Curr Biol* **26**, 2762–2769 (2016).

4. M. Boillat, *et al.*, The vomeronasal system mediates sick conspecific avoidance. *Curr Biol* **25**, 251–255 (2015).

5. C. Sarabian, R. Belais, A. J. J. MacIntosh, Feeding decisions under contamination risk in bonobos. *Philos Trans R Soc Lond B Biol Sci* **373**, 20170195 (2018).

6. H. Schulenburg, M.-A. Félix, The Natural Biotic Environment of *Caenorhabditis elegans*. *Genetics* **206**, 55–86 (2017).

7. M.-A. Félix, F. Duveau, Population dynamics and habitat sharing of natural populations of *Caenorhabditis elegans* and *C. briggsae*. *BMC Biology* **10**, 59 (2012).

8. E. R. Troemel, B. E. Kimmel, C. I. Bargmann, Reprogramming Chemotaxis Responses: Sensory Neurons Define Olfactory Preferences in *C. elegans*. *Cell* **91**, 161–169 (1997).

9. C. J. Franz, *et al.*, Orsay, Santeuil and Le Blanc viruses primarily infect intestinal cells in *Caenorhabditis* nematodes. *Virology* **448**, 255–264 (2014).

10. M.-A. Félix, *et al.*, Natural and Experimental Infection of *Caenorhabditis* Nematodes by Novel Viruses Related to Nodaviruses. *PLOS Biology* **9**, e1000586 (2011).

11. C. Couillault, P. Fourquet, M. Pophillat, J. J. Ewbank, A UPR-independent infection-specific role for a BiP/GRP78 protein in the control of antimicrobial peptide expression in *C. elegans* epidermis. *Virulence* **3**, 299–308 (2012).

12. H. B. Jansson, Adhesion of Conidia of *Drechmeria coniospora* to *Caenorhabditis elegans* Wild Type and Mutants. *J Nematol* **26**, 430–435 (1994).

13. I. Engelmann, *et al.*, A Comprehensive Analysis of Gene Expression Changes Provoked by Bacterial and Fungal Infection in *C. elegans*. *PLoS One* **6** (2011).

14. S. Mahajan-Miklos, M. W. Tan, L. G. Rahme, F. M. Ausubel, Molecular mechanisms of bacterial virulence elucidated using a *Pseudomonas aeruginosa-Caenorhabditis elegans* pathogenesis model. *Cell* **96**, 47–56 (1999).

15. M.-W. Tan, S. Mahajan-Miklos, F. M. Ausubel, Killing of *Caenorhabditis elegans* by *Pseudomonas aeruginosa* used to model mammalian bacterial pathogenesis. *Proc Natl Acad Sci U S A* **96**, 715–720 (1999).

16. C. Darby, J. W. Hsu, N. Ghori, S. Falkow, *Caenorhabditis elegans*: plague bacteria biofilm blocks food intake. *Nature* **417**, 243–244 (2002).

17. D. A. Garsin, *et al.*, A simple model host for identifying Gram-positive virulence factors. *PNAS* **98**, 10892–10897 (2001).

18. J. E. Irazoqui, *et al.*, Distinct Pathogenesis and Host Responses during Infection of *C. elegans* by *P. aeruginosa* and *S. aureus*. *PLoS Pathog* **6** (2010).

19. E. Mylonakis, *et al.*, The *Enterococcus faecalis fsrB* Gene, a Key Component of the fsr Quorum-Sensing System, Is Associated with Virulence in the Rabbit Endophthalmitis Model. *Infect Immun* **70**, 4678–4681 (2002).

20. Y. Kato, *et al.*, *abf-1* and *abf-2*, ASABF-type antimicrobial peptide genes in *Caenorhabditis elegans*. *Biochem J* **361**, 221–230 (2002).

21. J. L. Tenor, A. Aballay, A conserved Toll-like receptor is required for *Caenorhabditis elegans* innate immunity. *EMBO Rep.* **9**, 103–109 (2008).

22. O. Zugasti, J. J. Ewbank, Neuroimmune regulation of antimicrobial peptide expression by a noncanonical TGF-β signaling pathway in *Caenorhabditis elegans* epidermis. *Nat Immunol* **10**, 249–256 (2009).

23. T. Roeder, *et al.*, Caenopores are antimicrobial peptides in the nematode *Caenorhabditis elegans* instrumental in nutrition and immunity. *Dev Comp Immunol* **34**, 203–209 (2010).

24. L. Bányai, L. Patthy, Amoebapore homologs of *Caenorhabditis elegans*. *Biochim Biophys Acta* **1429**, 259–264 (1998).

25. A. Hoeckendorf, M. Stanisak, M. Leippe, The saposin-like protein SPP-12 is an antimicrobial polypeptide in the pharyngeal neurons of *Caenorhabditis elegans* and participates in defence against a natural bacterial pathogen. *Biochem J* **445**, 205–212 (2012).

26. A. Hoeckendorf, M. Leippe, SPP-3, a saposin-like protein of *Caenorhabditis elegans*, displays antimicrobial and pore-forming activity and is located in the intestine and in one head neuron. *Dev Comp Immunol* **38**, 181–186 (2012).

27. K. Drickamer, R. B. Dodd, C-Type lectin-like domains in *Caenorhabditis elegans*: predictions from the complete genome sequence. *Glycobiology* **9**, 1357–1369 (1999).

28. T. Takeuchi, *et al.*, A C-type lectin of *Caenorhabditis elegans*: its sugar-binding property revealed by glycoconjugate microarray analysis. *Biochem Biophys Res Commun* **377**, 303–306 (2008).

29. H. Schulenburg, M. Hoeppner, J. Weiner, E. Bornberg-Bauer, Specificity of the innate immune system and diversity of C-type lectin domain (CTLD) proteins in the nematode *Caenorhabditis elegans*. *Immunobiology* (2008) https:/doi.org/10.1016/j.imbio.2007.12.004.

30. D. O'Rourke, D. Baban, M. Demidova, R. Mott, J. Hodgkin, Genomic clusters, putative pathogen recognition molecules, and antimicrobial genes are induced by infection of *C. elegans* with M. nematophilum. *Genome Res.* **16**, 1005–1016 (2006).

31. K. T. Simonsen, *et al.*, Quantitative proteomics identifies ferritin in the innate immune response of *C. elegans*. *Virulence* **2**, 120–130 (2011).

32. S. M. Miltsch, P. H. Seeberger, B. Lepenies, The C-type lectin-like domain containing proteins Clec-39 and Clec-49 are crucial for *Caenorhabditis elegans* immunity against Serratia marcescens infection. *Dev Comp Immunol* **45**, 67–73 (2014).

33. P. Bork, G. Beckmann, The CUB domain. A widespread module in developmentally regulated proteins. *J Mol Biol* **231**, 539–545 (1993).

34. K. T. Simonsen, S. F. Gallego, N. J. Færgeman, B. H. Kallipolitis, Strength in numbers: "Omics" studies of *C. elegans* innate immunity. *Virulence* **3**, 477–484 (2012).

35. K. A. Estes, T. L. Dunbar, J. R. Powell, F. M. Ausubel, E. R. Troemel, bZIP transcription factor *zip-2* mediates an early response to *Pseudomonas aeruginosa* infection in *Caenorhabditis elegans*. *PNAS* (2010) https:/doi.org/10.1073/pnas.0914643107 (October 15, 2021).

36. T. L. Dunbar, Z. Yan, K. M. Balla, M. G. Smelkinson, E. R. Troemel, *C. elegans* detects pathogen-induced translational inhibition to activate immune signaling. *Cell Host Microbe* **11**, 375–386 (2012).

37. D. Prakash, *et al.*, 1-Undecene from *Pseudomonas aeruginosa* is an olfactory signal for flight-or-fight response in *Caenorhabditis elegans*. *EMBO J* **40**, e106938 (2021).

38. H. Schulenburg, C. Boehnisch, Diversification and adaptive sequence evolution of *Caenorhabditis* lysozymes (Nematoda: Rhabditidae). *BMC Evol Biol* **8**, 114 (2008).

39. M. Dasgupta, *et al.*, NHR-49 Transcription Factor Regulates Immunometabolic Response and Survival of *Caenorhabditis elegans* during *Enterococcus* faecalis Infection. *Infect Immun* **88**, e00130-20 (2020).

40. V. L. Jensen, K. T. Simonsen, Y.-H. Lee, D. Park, D. L. Riddle, RNAi screen of DAF-16/FOXO target genes in *C. elegans* links pathogenesis and dauer formation. *PLoS One* **5**, e15902 (2010).

41. G. V. Mallo, *et al.*, Inducible Antibacterial Defense System in *C. elegans*. *Current Biology* **12**, 1209–1214 (2002).

42. E. K. Marsh, M. C. W. van den Berg, R. C. May, A two-gene balance regulates *Salmonella typhimurium* tolerance in the nematode *Caenorhabditis elegans*. *PLoS One* **6**, e16839 (2011).

43. A. N. Nathoo, R. A. Moeller, B. A. Westlund, A. C. Hart, Identification of neuropeptide-like protein gene families in *Caenorhabditis elegans* and other species. *PNAS* **98**, 14000–14005 (2001).

44. C. Couillault, *et al.*, TLR-independent control of innate immunity in *Caenorhabditis elegans* by the TIR domain adaptor protein TIR-1, an ortholog of human SARM. *Nat. Immunol.* **5**, 488–494 (2004).

45. M. A. Ermolaeva, B. Schumacher, Insights from the worm: the *C. elegans* model for innate immunity. *Semin Immunol* **26**, 303–309 (2014).

46. R. Pukkila-Worley, F. M. Ausubel, Immune defense mechanisms in the *Caenorhabditis elegans* intestinal epithelium. *Curr Opin Immunol* **24**, 3–9 (2012).

47. D. H. Kim, *et al.*, A conserved p38 MAP kinase pathway in *Caenorhabditis elegans* innate immunity. *Science* **297**, 623–626 (2002).

48. D. H. Kim, *et al.*, Integration of *Caenorhabditis elegans* MAPK pathways mediating immunity and stress resistance by MEK-1 MAPK kinase and VHP-1 MAPK phosphatase. *PNAS* **101**, 10990–10994 (2004).

49. N. T. Liberati, *et al.*, Requirement for a conserved Toll/interleukin-1 resistance domain protein in the *Caenorhabditis elegans* immune response. *Proc. Natl. Acad. Sci. U.S.A.* **101**, 6593–6598 (2004).

50. M. Ren, H. Feng, Y. Fu, M. Land, C. S. Rubin, Protein kinase D is an essential regulator of *C. elegans* innate immunity. *Immunity* **30**, 521–532 (2009).

51. K. Ziegler, *et al.*, Antifungal innate immunity in *C. elegans*: PKCdelta links G protein signaling and a conserved p38 MAPK cascade. *Cell Host Microbe* **5**, 341–352 (2009).

52. R. P. Shivers, *et al.*, Phosphorylation of the Conserved Transcription Factor ATF-7 by PMK-1 p38 MAPK Regulates Innate Immunity in *Caenorhabditis elegans*. *PLOS Genetics* **6**, e1000892 (2010).

53. E. R. Troemel, *et al.*, p38 MAPK Regulates Expression of Immune Response Genes and Contributes to Longevity in *C. elegans*. *PLOS Genetics* **2**, e183 (2006).

54. H. R. Nicholas, J. Hodgkin, The ERK MAP kinase cascade mediates tail swelling and a protective response to rectal infection in *C. elegans*. *Curr Biol* **14**, 1256–1261 (2004).

55. C.-Y. Kao, *et al.*, Global Functional Analyses of Cellular Responses to Pore-Forming Toxins. *PLOS Pathogens* **7**, e1001314 (2011).

56. K. Lin, H. Hsin, N. Libina, C. Kenyon, Regulation of the *Caenorhabditis elegans* longevity protein DAF-16 by insulin/IGF-1 and germline signaling. *Nat Genet* **28**, 139–145 (2001).

57. R. P. Shivers, M. J. Youngman, D. H. Kim, Transcriptional responses to pathogens in *Caenorhabditis elegans*. *Curr Opin Microbiol* **11**, 251–256 (2008).

58. C. T. Murphy, P. J. Hu, Insulin/insulin-like growth factor signaling in *C. elegans*. *WormBook*, 1–43 (2013).

59. S. M. Anderson, *et al.*, The fatty acid oleate is required for innate immune activation and pathogen defense in *Caenorhabditis elegans*. *PLOS Pathogens* **15**, e1007893 (2019).

60. J. D. Nhan, *et al.*, Redirection of SKN-1 abates the negative metabolic outcomes of a perceived pathogen infection. *PNAS* **116**, 22322–22330 (2019).

61. O. Visvikis, *et al.*, INNATE HOST DEFENSE REQUIRES TFEB-MEDIATED TRANSCRIPTION OF CYTOPROTECTIVE AND ANTIMICROBIAL GENES. *Immunity* **40**, 896–909 (2014).

62. E. J. O'Rourke, G. Ruvkun, MXL-3 and HLH-30 transcriptionally link lipolysis and autophagy to nutrient availability. *Nat Cell Biol* **15**, 668–676 (2013).

63. L. J. Bischof, *et al.*, Activation of the unfolded protein response is required for defenses against bacterial pore-forming toxin in vivo. *PLoS Pathog* **4**, e1000176 (2008).

64. K. A. Haskins, J. F. Russell, N. Gaddis, H. K. Dressman, A. Aballay, Unfolded protein response genes regulated by CED-1 are required for *Caenorhabditis elegans* innate immunity. *Dev Cell* **15**, 87–97 (2008).

65. C. E. Richardson, T. Kooistra, D. H. Kim, An essential role for XBP-1 in host protection against immune activation in *C. elegans*. *Nature* **463**, 1092–1095 (2010).

66. J. B. George-Raizen, K. R. Shockley, N. F. Trojanowski, A. L. Lamb, D. M. Raizen, Dynamically-expressed prion-like proteins form a cuticle in the pharynx of *Caenorhabditis elegans*. *Biol Open* **3**, 1139–1149 (2014).

67. K. M. Glover-Cutter, S. Lin, T. K. Blackwell, Integration of the unfolded protein and oxidative stress responses through SKN-1/Nrf. *PLoS Genet* **9**, e1003701 (2013).

68. E. R. Troemel, M.-A. Félix, N. K. Whiteman, A. Barrière, F. M. Ausubel, Microsporidia are natural intracellular parasites of the nematode *Caenorhabditis elegans*. *PLoS Biol.* **6**, 2736–2752 (2008).

69. M. A. Bakowski, *et al.*, Ubiquitin-Mediated Response to Microsporidia and Virus Infection in *C. elegans*. *PLOS Pathogens* **10**, e1004200 (2014).

70. S. A. Labed, *et al.*, Intestinal Epithelial Wnt Signaling Mediates Acetylcholine-Triggered Host Defense against Infection. *Immunity* **48**, 963-978.e3 (2018).

71. L. Pereira, *et al.*, A cellular and regulatory map of the cholinergic nervous system of *C. elegans*. *eLife* **4**, e12432 (2015).

72. M. Mochii, S. Yoshida, K. Morita, Y. Kohara, N. Ueno, Identification of transforming growth factor-beta- regulated genes in *Caenorhabditis elegans* by differential hybridization of arrayed cDNAs. *Proc Natl Acad Sci U S A* **96**, 15020–15025 (1999).

73. X. Zhang, Y. Zhang, DBL-1, a TGF-β, is essential for *Caenorhabditis elegans* aversive olfactory learning. *PNAS* **109**, 17081–17086 (2012).

74. X. Cao, A. Aballay, Neural Inhibition of Dopaminergic Signaling Enhances Immunity in a Cell-Non-autonomous Manner. *Current Biology* **26**, 2329–2334 (2016).

75. E. A. Evans, T. Kawli, M.-W. Tan, *Pseudomonas aeruginosa* Suppresses Host Immunity by Activating the DAF-2 Insulin-Like Signaling Pathway in *Caenorhabditis elegans*. *PLoS Pathog* **4** (2008).

76. K. L. Styer, *et al.*, Innate Immunity in *Caenorhabditis elegans* Is Regulated by Neurons Expressing NPR-1/GPCR. *Science* **322**, 460–464 (2008).

77. E. C. Andersen, J. S. Bloom, J. P. Gerke, L. Kruglyak, A Variant in the Neuropeptide Receptor *npr-1* is a Major Determinant of *Caenorhabditis elegans* Growth and Physiology. *PLOS Genetics* **10**, e1004156 (2014).

78. B. Otarigho, A. Aballay, Immunity-longevity tradeoff neurally controlled by GABAergic transcription factor PITX1/UNC-30. *Cell Rep* **35**, 109187 (2021).

79. D. Sellegounder, *et al.*, Neuronal GPCR NPR-8 regulates *C. elegans* defense against pathogen infection. *Science Advances* **5**, eaaw4717 (2019).

80. Y. Yu, L. Zhi, Q. Wu, L. Jing, D. Wang, NPR-9 regulates the innate immune response in *Caenorhabditis elegans* by antagonizing the activity of AIB interneurons. *Cell Mol Immunol* **15**, 27–37 (2018).

81. J. Sun, V. Singh, R. Kajino-Sakamoto, A. Aballay, Neuronal GPCR controls innate immunity by regulating noncanonical unfolded protein response genes. *Science* **332**, 729–732 (2011).

82. J. Sun, Y. Liu, A. Aballay, Organismal regulation of XBP-1-mediated unfolded protein response during development and immune activation. *EMBO Rep* **13**, 855–860 (2012).

83. X. Cao, R. Kajino-Sakamoto, A. Doss, A. Aballay, Distinct Roles of Sensory Neurons in Mediating Pathogen Avoidance and Neuropeptide-Dependent Immune Regulation. *Cell Reports* **21**, 1442–1451 (2017).

84. D. Sellegounder, C.-H. Yuan, P. Wibisono, Y. Liu, J. Sun, Octopaminergic Signaling Mediates Neural Regulation of Innate Immunity in *Caenorhabditis elegans*. *mBio* **9**, e01645-18 (2018).

85. K. J. Foster, *et al.*, Innate Immunity in the *C. elegans* Intestine Is Programmed by a Neuronal Regulator of AWC Olfactory Neuron Development. *Cell Rep* **31**, 107478 (2020).

86. A. Anderson, H. Laurenson-Schafer, F. A. Partridge, J. Hodgkin, R. McMullan, Serotonergic Chemosensory Neurons Modify the *C. elegans* Immune Response by Regulating G-Protein Signaling in Epithelial Cells. *PLOS Pathogens* **9**, e1003787 (2013).

87. E. Pradel, *et al.*, Detection and avoidance of a natural product from the pathogenic bacterium Serratia marcescens by *Caenorhabditis elegans*. *Proc Natl Acad Sci U S A* **104**, 2295–2300 (2007).

88. K. C. Reddy, E. C. Andersen, L. Kruglyak, D. H. Kim, A Polymorphism in *npr-1* Is a Behavioral Determinant of Pathogen Susceptibility in *C. elegans*. *Science* **323**, 382–384 (2009).

89. O. Zugasti, *et al.*, Activation of a G protein-coupled receptor by its endogenous ligand triggers the innate immune response of *Caenorhabditis elegans*. *Nat Immunol* **15**, 833–838 (2014).

90. A. Tran, *et al.*, *C. elegans* avoids toxin-producing *Streptomyces* using a seven transmembrane domain chemosensory receptor. *eLife* **6**, e23770 (2017).

91. S. E. Worthy, G. L. Rojas, C. J. Taylor, E. E. Glater, Identification of Odor Blend Used by *Caenorhabditis elegans* for Pathogen Recognition. *Chemical Senses* **43**, 169–180 (2018).

92. J. D. Meisel, D. H. Kim, Behavioral avoidance of pathogenic bacteria by *Caenorhabditis elegans*. *Trends in Immunology* **35**, 465–470 (2014).

93. J. Singh, A. Aballay, Intestinal infection regulates behavior and learning via neuroendocrine signaling. *eLife* **8**, e50033 (2019).

94. Y. Zhang, H. Lu, C. I. Bargmann, Pathogenic bacteria induce aversive olfactory learning in *Caenorhabditis elegans*. *Nature* **438**, 179–184 (2005).

95. G. Harris, *et al.*, Dissecting the Signaling Mechanisms Underlying Recognition and Preference of Food Odors. *J Neurosci* **34**, 9389–9403 (2014).

96. K. C. Reddy, R. C. Hunter, N. Bhatla, D. K. Newman, D. H. Kim, *Caenorhabditis elegans* NPR-1–mediated behaviors are suppressed in the presence of mucoid bacteria. *Proc Natl Acad Sci U S A* **108**, 12887–12892 (2011).

97. J. C. Coates, M. de Bono, Antagonistic pathways in neurons exposed to body fluid regulate social feeding in *Caenorhabditis elegans*. *Nature* **419**, 925–929 (2002).

98. Y. Hao, *et al.*, Thioredoxin shapes the *C. elegans* sensory response to *Pseudomonas* produced nitric oxide. *eLife* (2018) https:/doi.org/10.7554/eLife.36833 (July 27, 2018).

99. J. P. Brandt, N. Ringstad, Toll-like Receptor Signaling Promotes Development and Function of Sensory Neurons Required for a *C. elegans* Pathogen-Avoidance Behavior. *Current Biology* **25**, 2228–2237 (2015).

100. Z. Chen, *et al.*, Two Insulin-like Peptides Antagonistically Regulate Aversive Olfactory Learning in *C. elegans*. *Neuron* **77**, 572–585 (2013).

101. C. Hong, J. Lalsiamthara, J. Ren, Y. Sang, A. Aballay, Microbial colonization induces histone acetylation critical for inherited gut-germline-neural signaling. *PLOS Biology* **19**, e3001169 (2021).

102. R. Kaletsky, *et al.*, *C. elegans* interprets bacterial non-coding RNAs to learn pathogenic avoidance. *Nature*, 1–7 (2020).

103. R. S. Moore, R. Kaletsky, C. T. Murphy, Piwi/PRG-1 Argonaute and TGF-β Mediate Transgenerational Learned Pathogenic Avoidance. *Cell* **177**, 1827-1841.e12 (2019).

104. R. S. Moore, *et al.*, The role of the Cer1 transposon in horizontal transfer of transgenerational memory. *Cell* **184**, 4697-4712.e18 (2021).

105. J. D. G. Jones, J. L. Dangl, The plant immune system. *Nature* **444**, 323–329 (2006).

106. L. Boyer, *et al.*, Pathogen-derived effectors trigger protective immunity via activation of the Rac2 enzyme and the IMD or Rip kinase signaling pathway. *Immunity* **35**, 536–549 (2011).

107. A. Kleino, N. Silverman, UnZIPping mechanisms of effector-triggered immunity in animals. *Cell Host Microbe* **11**, 320–322 (2012).

108. D. L. McEwan, N. V. Kirienko, F. M. Ausubel, Host translational inhibition by *Pseudomonas aeruginosa* Exotoxin A Triggers an immune response in *Caenorhabditis elegans*. *Cell Host Microbe* **11**, 364–374 (2012).

109. J. A. Melo, G. Ruvkun, Inactivation of conserved genes induces microbial aversion, drug detoxification, and innate immunity in C.elegans. *Cell* **149**, 452–466 (2012).

110. I. Engelmann, N. Pujol, Innate immunity in *C. elegans*. *Adv Exp Med Biol* **708**, 105–121 (2010).

111. F. C. O. Los, *et al.*, RAB-5 and RAB-11-dependent vesicle-trafficking pathways are required for plasma membrane repair after attack by bacterial pore-forming toxin. *Cell Host Microbe* **9**, 147–157 (2011).

112. F. C. O. Los, T. M. Randis, R. V. Aroian, A. J. Ratner, Role of pore-forming toxins in bacterial infectious diseases. *Microbiol Mol Biol Rev* **77**, 173–207 (2013).

113. J. Singh, A. Aballay, Microbial Colonization Activates an Immune Fight-and-Flight Response via Neuroendocrine Signaling. *Developmental Cell* **49**, 89-99.e4 (2019).

114. H. C. Chang, J. Paek, D. H. Kim, Natural Polymorphisms in *C. elegans* HECW-1 E3 Ligase Affect Pathogen Avoidance Behaviour. *Nature* **480**, 525–529 (2011).

115. K. Lee, E. Mylonakis, An Intestine-Derived Neuropeptide Controls Avoidance Behavior in *Caenorhabditis elegans*. *Cell Reports* **20**, 2501–2512 (2017).

116. S. Alper, S. J. McBride, B. Lackford, J. H. Freedman, D. A. Schwartz, Specificity and complexity of the *Caenorhabditis elegans* innate immune response. *Mol Cell Biol* **27**, 5544–5553 (2007).

117. D. Wong, D. Bazopoulou, N. Pujol, N. Tavernarakis, J. J. Ewbank, Genome-wide investigation reveals pathogen-specific and shared signatures in the response of *Caenorhabditis elegans* to infection. *Genome Biol* **8**, R194 (2007).

118. S. Kumar, *et al.*, Lifespan Extension in *C. elegans* Caused by Bacterial Colonization of the Intestine and Subsequent Activation of an Innate Immune Response. *Developmental Cell* **49**, 100-117.e6 (2019).

119. R. Xiao, X. Z. S. Xu, *C. elegans* TRP channels. *Adv Exp Med Biol* **704**, 323–339 (2011).

120. P. Holzer, TRP channels in the digestive system. *Curr Pharm Biotechnol* **12**, 24–34 (2011).

121. R. Xiao, *et al.*, A Genetic Program Promotes *C. elegans* Longevity at Cold Temperatures via a Thermosensitive TRP Channel. *Cell* **152**, 806–817 (2013).

122. K. S. Kindt, *et al.*, *Caenorhabditis elegans* TRPA-1 functions in mechanosensation. *Nature Neuroscience* **10**, 568–577 (2007).

123. A. Soldano, *et al.*, Gustatory-mediated avoidance of bacterial lipopolysaccharides via TRPA1 activation in *Drosophila*. *eLife* **5**.

124. C. M. Coburn, C. I. Bargmann, A Putative Cyclic Nucleotide–Gated Channel Is Required for Sensory Development and Function in *C. elegans*. *Neuron* **17**, 695–706 (1996).

125. J. D. Meisel, O. Panda, P. Mahanti, F. C. Schroeder, D. H. Kim, Chemosensation of Bacterial Secondary Metabolites Modulates Neuroendocrine Signaling and Behavior of *C. elegans*. *Cell* **159**, 267–280 (2014).

126. L. E. Fuhrman, A. K. Goel, J. Smith, K. V. Shianna, A. Aballay, Nucleolar Proteins Suppress *Caenorhabditis elegans* Innate Immunity by Inhibiting p53/CEP-1. *PLoS Genet* **5** (2009).

127. C. D. Sifri, *et al.*, Virulence effect of *Enterococcus faecalis* protease genes and the quorum-sensing locus *fsr* in *Caenorhabditis elegans* and mice. *Infect. Immun.* **70**, 5647–5650 (2002).

128. G. J. Yuen, F. M. Ausubel, Both live and dead Enterococci activate *Caenorhabditis elegans* host defense via immune and stress pathways. *Virulence* **9**, 683–699 (2018).

129. M. J. Gravato-Nobre, F. Vaz, S. Filipe, R. Chalmers, J. Hodgkin, The Invertebrate Lysozyme Effector ILYS-3 Is Systemically Activated in Response to Danger Signals and Confers Antimicrobial Protection in *C. elegans*. *PLoS Pathog* **12** (2016).

130. M. de Bono, C. I. Bargmann, Natural variation in a neuropeptide Y receptor homolog modifies social behavior and food response in *C. elegans*. *Cell* **94**, 679–689 (1998).

131. A. J. Chang, N. Chronis, D. S. Karow, M. A. Marletta, C. I. Bargmann, A Distributed Chemosensory Circuit for Oxygen Preference in *C. elegans*. *PLOS Biology* **4**, e274 (2006).

132. C. Rogers, *et al.*, Inhibition of *Caenorhabditis elegans* social feeding by FMRFamide-related peptide activation of NPR-1. *Nature Neuroscience* **6**, 1178–1185 (2003).

133. M. de Bono, D. M. Tobin, M. W. Davis, L. Avery, C. I. Bargmann, Social feeding in *Caenorhabditis elegans* is induced by neurons that detect aversive stimuli. *Nature* **419**, 899–903 (2002).

134. J. M. Gray, *et al.*, Oxygen sensation and social feeding mediated by a *C. elegans* guanylate cyclase homologue. *Nature* **430**, 317–322 (2004).

135. B. H. H. Cheung, F. Arellano-Carbajal, I. Rybicki, M. de Bono, Soluble Guanylate Cyclases Act in Neurons Exposed to the Body Fluid to Promote *C. elegans* Aggregation Behavior. *Current Biology* **14**, 1105–1111 (2004).

136. H. Ha, *et al.*, Functional organization of a neural network for aversive olfactory learning in *Caenorhabditis elegans*. *Neuron* **68**, 1173–1186 (2010).

137. M. TeKippe, A. Aballay, *C. elegans* Germline-Deficient Mutants Respond to Pathogen Infection Using Shared and Distinct Mechanisms. *PLoS One* **5** (2010).

138. J. Austin, J. Kimble, *glp-1* is required in the germ line for regulation of the decision between mitosis and meiosis in *C. elegans*. *Cell* **51**, 589–599 (1987).

139. S. L. Crittenden, E. R. Troemel, T. C. Evans, J. Kimble, GLP-1 is localized to the mitotic region of the *C. elegans* germ line. *Development* **120**, 2901–2911 (1994).

140. T. Teramoto, E. J. Lambie, K. Iwasaki, Differential regulation of TRPM channels governs electrolyte homeostasis in the *C. elegans* intestine. *Cell Metabolism* **1**, 343–354 (2005).

141. C. S. Kwan, R. P. Vázquez-Manrique, S. Ly, K. Goyal, H. A. Baylis, TRPM channels are required for rhythmicity in the ultradian defecation rhythm of *C. elegans*. *BMC Physiology* **8**, 11 (2008).

142. T. Teramoto, *et al.*, Magnesium Excretion in *C. elegans* Requires the Activity of the GTL-2 TRPM Channel. *PLOS ONE* **5**, e9589 (2010).

143. S. M. Mueller-Tribbensee, *et al.*, Differential Contribution of TRPA1, TRPV4 and TRPM8 to Colonic Nociception in Mice. *PLoS One* **10** (2015).

144. Y. Kiyama, K. Miyahara, Y. Ohshima, Active uptake of artificial particles in the nematode *Caenorhabditis elegans*. *Journal of Experimental Biology* **215**, 1178–1183 (2012).

145. K. Milward, K. E. Busch, R. J. Murphy, M. de Bono, B. Olofsson, Neuronal and molecular substrates for optimal foraging in *Caenorhabditis elegans*. *PNAS* **108**, 20672–20677 (2011).

146. B. B. Shtonda, L. Avery, Dietary choice behavior in *Caenorhabditis elegans*. *J. Exp. Biol.* **209**, 89–102 (2006).

147. A. Metaxakis, D. Petratou, N. Tavernarakis, Multimodal sensory processing in *Caenorhabditis elegans*. *Open Biol* **8** (2018).

148. P. J. Summers, *et al.*, Multiple Sensory Inputs Are Extensively Integrated to Modulate Nociception in *C. elegans*. *J. Neurosci.* **35**, 10331–10342 (2015).

149. M. A. Wilson, *et al.*, *skn-1* is required for interneuron sensory integration and foraging behavior in *Caenorhabditis elegans*. *PLoS One* **12** (2017).

150. A. J. Bretscher, *et al.*, Temperature, Oxygen, and Salt-Sensing Neurons in *C. elegans* Are Carbon Dioxide Sensors that Control Avoidance Behavior. *Neuron* **69**, 1099–1113 (2011).

151. J. M. Kaplan, H. R. Horvitz, A dual mechanosensory and chemosensory neuron in *Caenorhabditis elegans*. *Proc Natl Acad Sci U S A* **90**, 2227–2231 (1993).

152. S. G. Leinwand, *et al.*, Circuit mechanisms encoding odors and driving aging-associated behavioral declines in *Caenorhabditis elegans*. *eLife* **4**, e10181 (2015).

153. S. G. Leinwand, S. H. Chalasani, Neuropeptide signaling remodels chemosensory circuit composition in *Caenorhabditis elegans*. *Nat Neurosci* **16**, 1461–1467 (2013).

154. K. Yoshida, *et al.*, Odour concentration-dependent olfactory preference change in *C. elegans*. *Nature Communications* **3**, 739 (2012).

155. S. H. Chalasani, *et al.*, Dissecting a circuit for olfactory behaviour in *Caenorhabditis elegans*. *Nature* **450**, 63–70 (2007).

156. S. H. Chalasani, *et al.*, Neuropeptide feedback modifies odor-evoked dynamics in *Caenorhabditis elegans* olfactory neurons. *Nature Neuroscience* **13**, 615–621 (2010).

157. M. Fadda, *et al.*, NPY/NPF-Related Neuropeptide FLP-34 Signals from Serotonergic Neurons to Modulate Aversive Olfactory Learning in *Caenorhabditis elegans*. *J. Neurosci.* **40**, 6018–6034 (2020).

158. S. W. Flavell, *et al.*, Serotonin and the Neuropeptide PDF Initiate and Extend Opposing Behavioral States in *C. elegans*. *Cell* **154**, 1023–1035 (2013).

159. B. Olofsson, The olfactory neuron AWC promotes avoidance of normally palatable food following chronic dietary restriction. *Journal of Experimental Biology* **217**, 1790–1798 (2014).

160. M. C. Stensmyr, *et al.*, A Conserved Dedicated Olfactory Circuit for Detecting Harmful Microbes in *Drosophila*. *Cell* **151**, 1345–1357 (2012).

161. A. Y. Sun, E. J. Lambie, Gon-2, a Gene Required for Gonadogenesis in *Caenorhabditis elegans*. *Genetics* **147**, 1077–1089 (1997).

162. S. Gao, *et al.*, Excitatory motor neurons are local oscillators for backward locomotion. *eLife* **7**, e29915 (2018).

163. G. Haspel, M. J. O'Donovan, A. C. Hart, Motoneurons Dedicated to Either Forward or Backward Locomotion in the Nematode *Caenorhabditis elegans*. *J Neurosci* **30**, 11151–11156 (2010).

164. M. Chalfie, *et al.*, The neural circuit for touch sensitivity in *Caenorhabditis elegans*. *J Neurosci* **5**, 956–964 (1985).

165. S. J. Cook, *et al.*, Whole-animal connectomes of both *Caenorhabditis elegans* sexes. *Nature* **571**, 63–71 (2019).

166. G. P. Sarma, *et al.*, OpenWorm: overview and recent advances in integrative biological simulation of *Caenorhabditis elegans*. *Philosophical Transactions of the Royal Society B: Biological Sciences* **373**, 20170382 (2018).

167. J. Kim, W. Leahy, E. Shlizerman, Neural Interactome: Interactive Simulation of a Neuronal System. *Front Comput Neurosci* **13** (2019).

168. Q. Wen, S. Gao, M. Zhen, *Caenorhabditis elegans* excitatory ventral cord motor neurons derive rhythm for body undulation. *Philosophical Transactions of the Royal Society B: Biological Sciences* **373**, 20170370 (2018).

169. M. A. Hilliard, C. I. Bargmann, P. Bazzicalupo, *C. elegans* Responds to Chemical Repellents by Integrating Sensory Inputs from the Head and the Tail. *Current Biology* **12**, 730–734 (2002).

170. C. I. Bargmann, E. Hartwieg, H. R. Horvitz, Odorant-selective genes and neurons mediate olfaction in *C. elegans*. *Cell* **74**, 515–527 (1993).

171. E. Z. Macosko, *et al.*, A Hub-and-Spoke Circuit Drives Pheromone Attraction and Social Behavior in *C. elegans*. *Nature* **458**, 1171–1175 (2009).

172. H. Jang, *et al.*, Dissection of neuronal gap junction circuits that regulate social behavior in *Caenorhabditis elegans*. *Proc Natl Acad Sci U S A* **114**, E1263–E1272 (2017).

173. Z. F. Altun, B. Chen, Z.-W. Wang, D. H. Hall, High resolution map of *Caenorhabditis elegans* gap junction proteins. *Developmental Dynamics* **238**, 1936–1950 (2009).

174. E. Yemini, *et al.*, NeuroPAL: A Multicolor Atlas for Whole-Brain Neuronal Identification in *C. elegans*. *Cell* **184**, 272-288.e11 (2021).

175. A. Rosenberg, *Reduction and Mechanism*, 1st Ed. (Cambridge University Press, 2020) https:/doi.org/10.1017/9781108592949 (February 22, 2022).

176. K. Marx 1818-1883, *Das Kapital, a critique of political economy* (Chicago: H. Regnery, 1959., 1959).

177. B. Latour, *Laboratory life: the construction of scientific facts* (Princeton, N.J.: Princeton University Press, [1986] ©1986, 1986).

178. J. W. Krakauer, A. A. Ghazanfar, A. Gomez-Marin, M. A. MacIver, D. Poeppel, Neuroscience Needs Behavior: Correcting a Reductionist Bias. *Neuron* **93**, 480–490 (2017).

179. T. S. Kuhn author, *The structure of scientific revolutions* (Second edition, enlarged. Chicago: University of Chicago Press, © 1970. ©1962., 1970).

180. P. Feyerabend, *Against method*, 3rd ed (Verso, 1993).

181. S. Shapin, S. Schaffer, T. Hobbes, *Leviathan and the air-pump: Hobbes, Boyle, and the experimental life: including a translation of Thomas Hobbes, Dialogus physicus de natura aeris by Simon Schaffer* (Princeton University Press, 1985).

182. D. Hume, *An Enquiry Concerning Human Understanding* (London: Electric Book, 2019. ©2019., 2019).

183. M. Yoshihara, M. Yoshihara, "Necessary and sufficient" in biology is not necessarily necessary. Confusions and erroneous conclusions resulting from Misapplied logic in the field of biology, especially neuroscience. *J Neurogenet* **32**, 53–64 (2018).

184. S. H. Siddiqi, K. P. Kording, J. Parvizi, M. D. Fox, Causal mapping of human brain function. *Nat Rev Neurosci*, 1–15 (2022).

185. L. N. Ross, Causal Concepts in Biology: How Pathways Differ from Mechanisms and Why It Matters. *The British Journal for the Philosophy of Science* **72**, 131–158 (2021).

186. C. D. Stern, The 'Omics Revolution: How an Obsession with Compiling Lists Is Threatening the Ancient Art of Experimental Design. *BioEssays* **41**, 1900168 (2019).

187. L. E. Kay, *The molecular vision of life: Caltech, the Rockefeller Foundation, and the rise of the new biology* (Oxford University Press, 1993).

188. N. Cermak, *et al.*, Whole-organism behavioral profiling reveals a role for dopamine in state-dependent motor program coupling in *C. elegans*. *eLife* **9**, e57093 (2020).

189. J. Likitlersuang, G. Stephens, K. Palanski, W. S. Ryu, *C. elegans* Tracking and Behavioral Measurement. *J Vis Exp*, 4094 (2012).

190. M. Scholz, D. J. Lynch, K. S. Lee, E. Levine, D. Biron, A scalable method for automatically measuring pharyngeal pumping in *C. elegans*. *J Neurosci Methods* **274**, 172–178 (2016).

191. A. Guisnet, M. Maitra, S. Pradhan, M. Hendricks, A three-dimensional habitat for *C. elegans* environmental enrichment. *PLOS ONE* **16**, e0245139 (2021).

192. D. S. Chelur, M. Chalfie, Targeted cell killing by reconstituted caspases. *Proceedings of the National Academy of Sciences* **104**, 2283–2288 (2007).

193. A. G. Fraser, *et al.*, Functional genomic analysis of *C. elegans* chromosome I by systematic RNA interference. *Nature* **408**, 325–330 (2000).

194. L. Timmons, A. Fire, Specific interference by ingested dsRNA. *Nature* **395**, 854–854 (1998).

195. J. Singh, A. Aballay, Endoplasmic Reticulum Stress Caused by Lipoprotein Accumulation Suppresses Immunity against Bacterial Pathogens and Contributes to Immunosenescence. *mBio* **8** (2017).

APPENDIX

Supplementary Figures

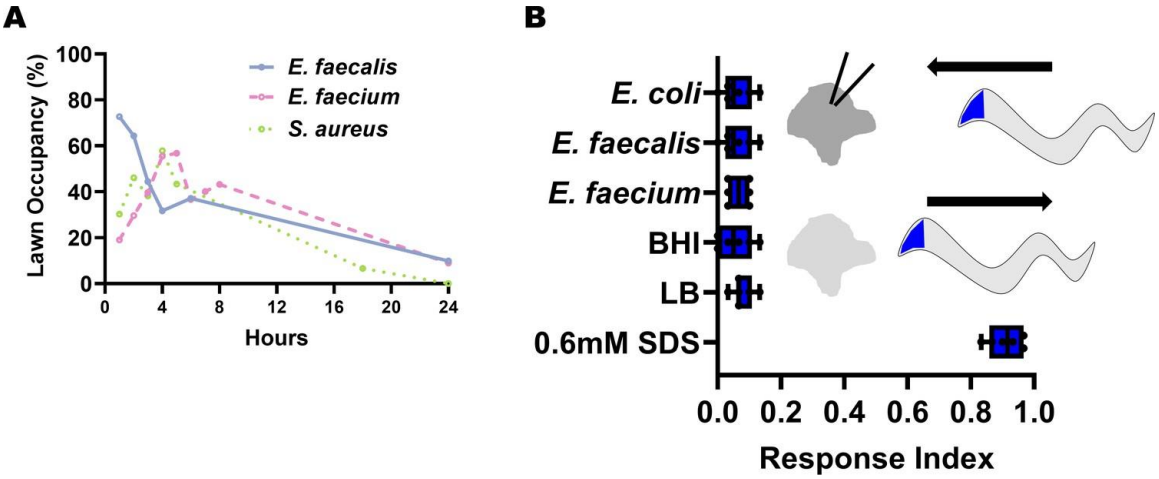

Fig. S1. Avoidance of Gram-positive pathogens. (**A**) Occupancy index time course of N2 animals on either *E. faecalis*, *E. faecium*, or *S. aureus.* N = 3 for each point. Points represent the mean. (**B**) Response index of N2 animals to dry drops of *E. coli*, *E. faecalis*, *E. faecium*, BHI, LB, or 0.6 mM SDS buffer. Response Index = number of responses/total number of drops.

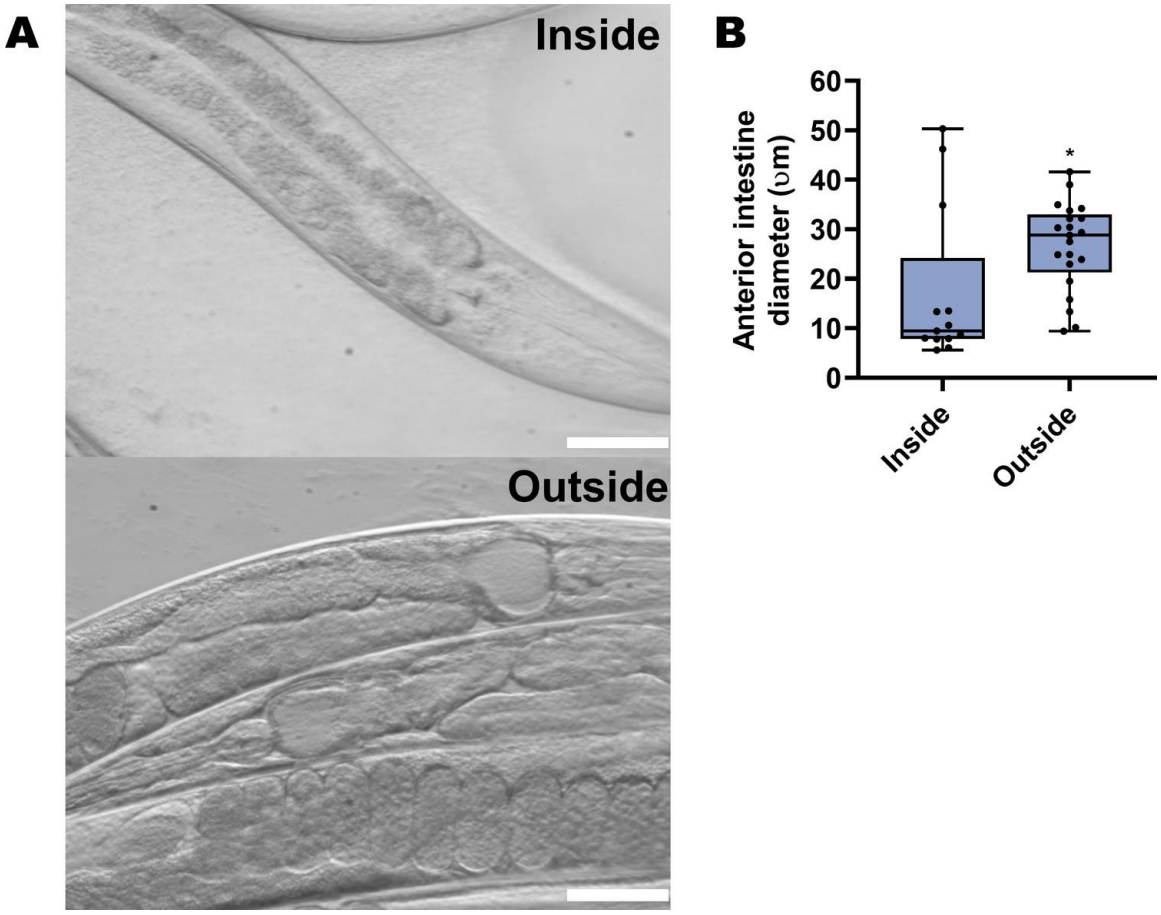

Fig. S2. Animals evacuating *E. faecalis* lawns show significant anterior intestinal distention. (**A**) Representative photomicrographs of wild-type animals taken from inside (top) or outside (bottom) a lawn of *E. faecalis*. Outside animals were picked immediately after they left the lawn, with animals inside the lawn picked at the same time. Scale bar, 50 μm. (**B**) Quantification of anterior intestinal diameter of animals as represented in **A**. An unpaired t-test was performed.

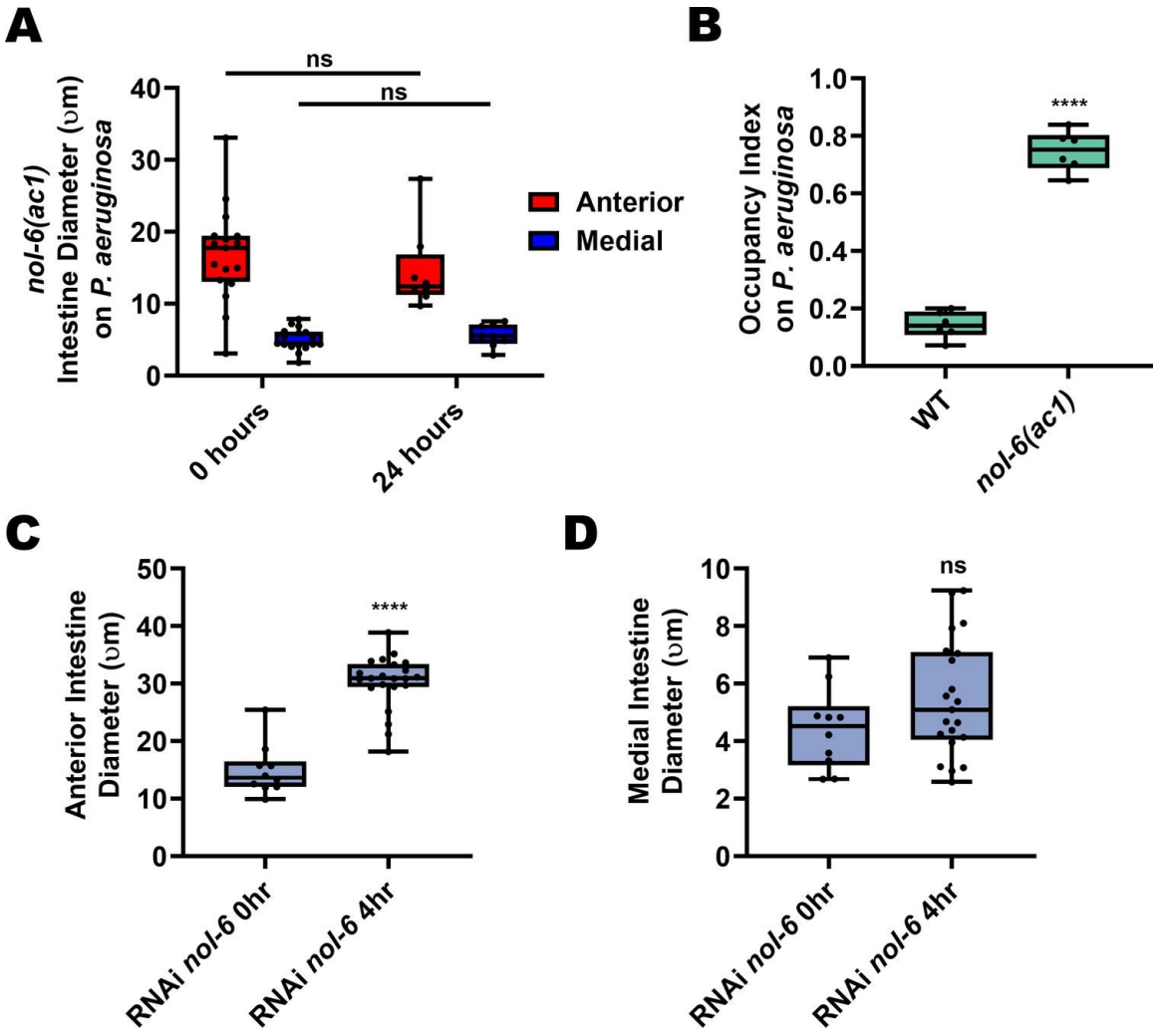

Fig. S3. *E. faecalis* but not *P. aeruginosa* causes anterior intestinal distention in *nol-6* animals. (**A**) Quantification of anterior and medial intestinal lumen diameter of *nol-6(ac1)* animals after 0 and 24 hr on *P. aeruginosa*. (**B**) Occupancy index of WT and *nol-6(ac1)* animals on *P. aeruginosa* at 24 hr. An unpaired t-test was performed. (**C**) Quantification of anterior intestinal lumen diameter of *nol-6* RNAi animals at 0 and 4 hr on *E. faecalis.* An unpaired t-test was performed. (**D**) Quantification of medial intestinal lumen diameter of *nol-6* RNAi animals at 0 and 4 hr on *E. faecalis*. An unpaired t-test was performed.

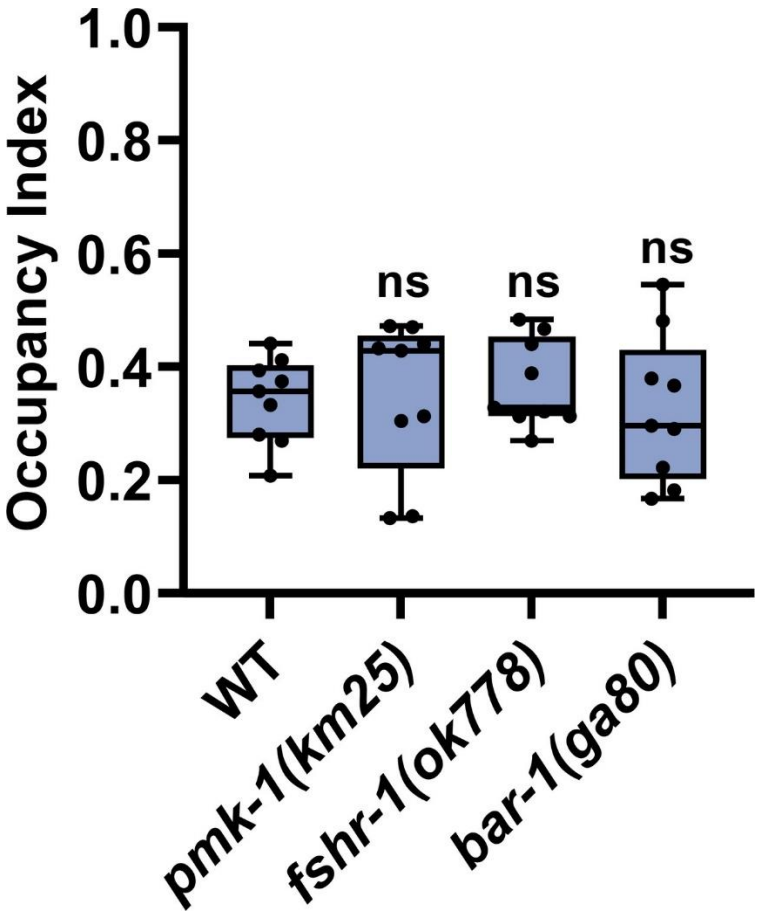

Fig. S4. Loss of key immune genes does not affect avoidance of *E. faecalis*. Occupancy index for wild-type, *pmk-1(km25)*, *fshr-1(ok778)*, and *bar-1(ga80)* on *E. faecalis* at 4 hr. One-way ANOVA with comparison to the WT group was performed.

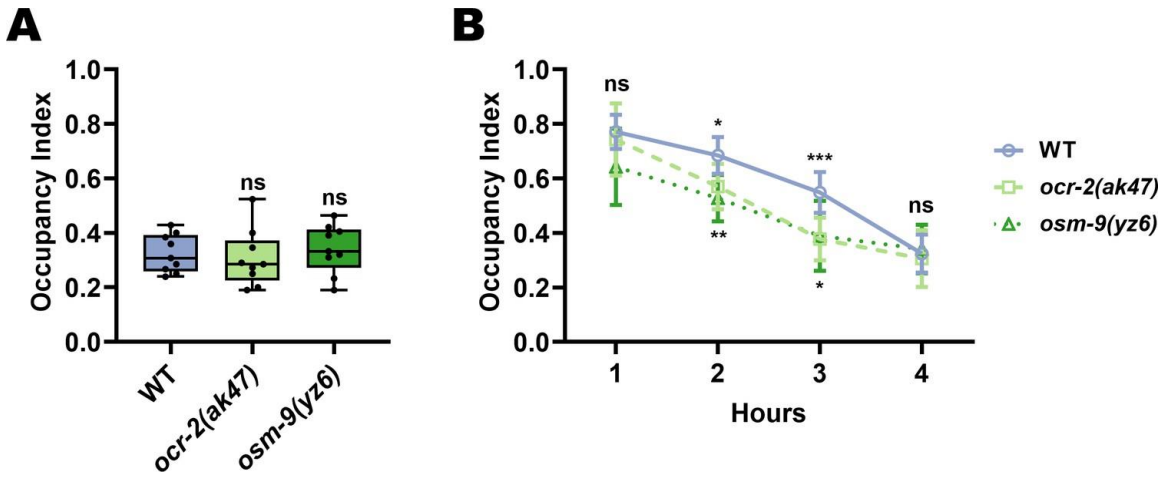

Fig. S5. The TRPV subunits OCR-2 and OSM-9 slightly speed up avoidance of *E. faecalis*. (**A**) Occupancy index of WT animals compared to *ocr-2(ak47)* and *osm-9(yz6)* animals on *E. faecalis* at 4 hr. One-way ANOVA with subsequent comparison to WT animals was performed. (**B**) Occupancy index time course for WT animals compared to *ocr-2(ak47)* and *osm-9(yz6)* on *E. faecalis*. Two-way ANOVA with comparison to WT animals at each time point was performed. N = 9 for each point. Points represent the mean and error bars are the standard deviation.

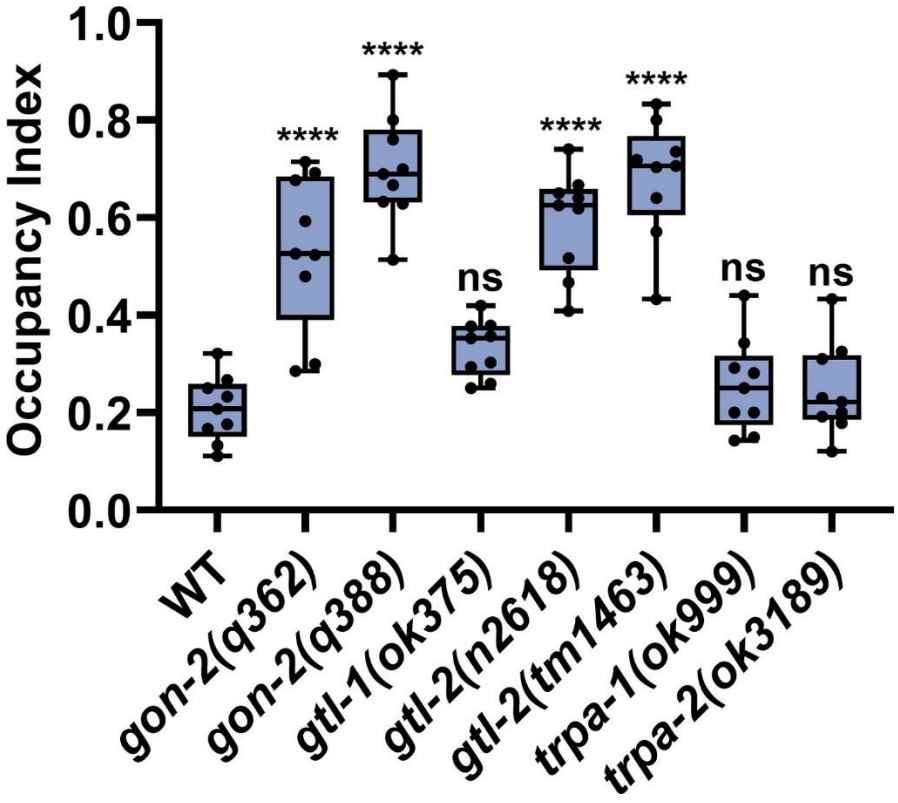

Fig. S6. Screening TRP channels for effect on avoidance of *E. faecalis*. Occupancy index of WT animals on *E. faecalis* at 4 hr compared to five different TRP channel mutants: *gon-2(q362)*, *gon-2(q388)*, *gtl-2(n2618)*, and *gtl-2(tm1643)*. One-way ANOVA with subsequent comparison to WT animals was performed.

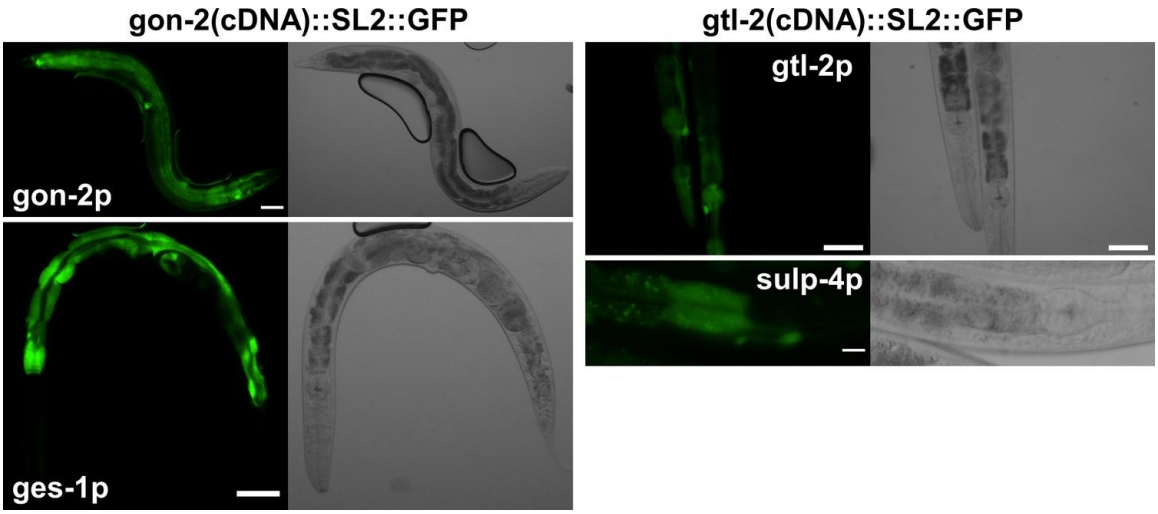

Fig. S7. Rescue of *gon-2* and *gtl-2* expression in mutant backgrounds. Representative micrographs of each rescue strain are shown. Top left: *gon-2(q388); gon-2p::gon-2(cDNA)::SL2::GFP*. Bottom left: *gon-2(388);ges-1p::gon-2(cDNA)::SL2::GFP*. Top right: *gtl-2(tm1463);gtl-2p::gtl-2(cDNA)::SL2::GFP*. Bottom right: *gtl-2(tm1463);sulp-4p::gtl-2(cDNA)::SL2::GFP*. Scale bars in order: 50 μm, 50 μm, 50 μm, and 10 μm.

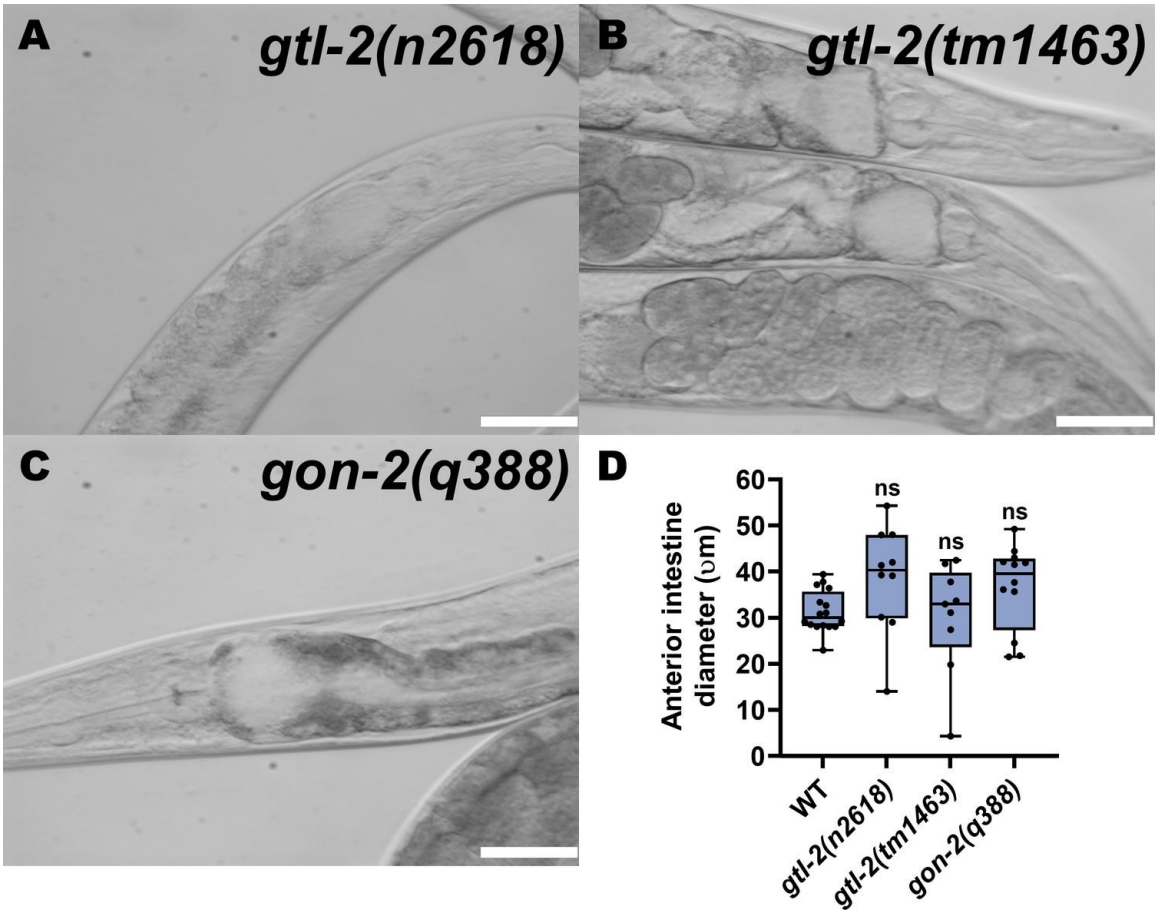

Fig. S8. Loss of GON-2 or GTL-2 function does not affect anterior intestinal distention on *E. faecalis*. (**A–C**) Representative photomicrographs of the anterior intestines of *gtl-2(n2618)*, *gtl-2(tm1463)*, and *gon-2(q388)* animals after 4 hr on *E. faecalis*. Scale bar, 50 μm. (**D**) Quantification of the anterior intestinal diameters of animals represented in (**A–C**). One-way ANOVA with subsequent comparison to WT animals was performed.

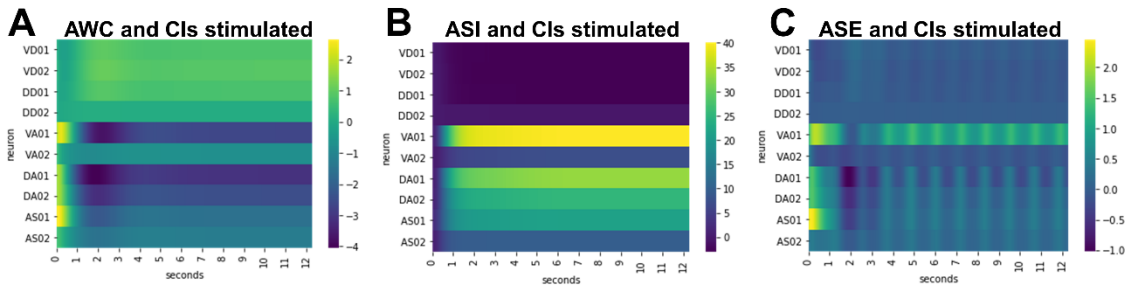

Fig. S9. AWC, ASI, and ASE neurons do not lead to oscillations in motor neurons important for backward locomotion. Activity of VD, DD, VA, DA, and AS motor neurons in the Neural Interactome upon 0.9 nA stimulation of the CIs and 5.0 nA stimulation of AWC (**A**), ASI (**B**), and ASE (**C**).

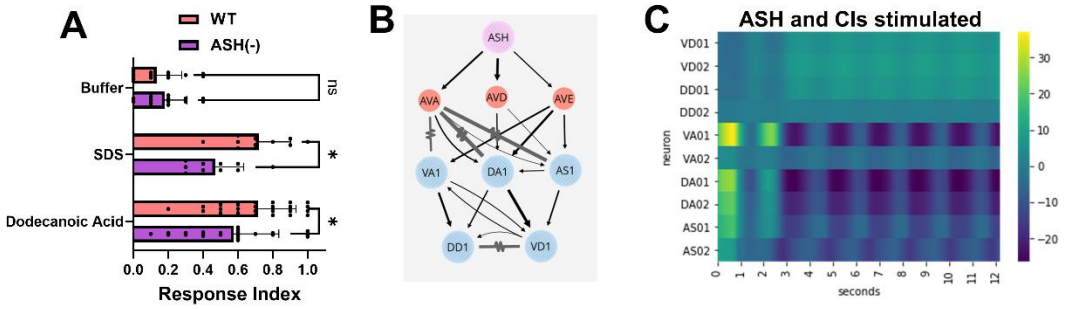

Fig. S10. The response to SDS and dodecanoic acid are ASH mediated and can be modeled in the Neural Interactome. (**A**) Response index to buffer, 0.6 mM SDS, or 1mM dodecanoic acid for animals with no neurons ablated (WT, red) or ASH neurons ablated (ASH(-), purple). Two-way ANOVA with subsequent comparison to the WT groups was performed. Error bars depict standard deviation. N = 15 for buffer, 10 for SDS, and 25 for dodecanoic acid (individual dots). (**B**) Diagram of the circuit for reflexive aversion to SDS and dodecanoic acid. Arrows represent chemical synapses, while jagged lines represent electrical synapses. (**C**) Activity for the motor neurons VD, DD, VA, DA, and AS (rows) upon 5.0 nA stimulation of ASH neurons and 0.9 nA stimulation of the CIs in the Neural Interactome.

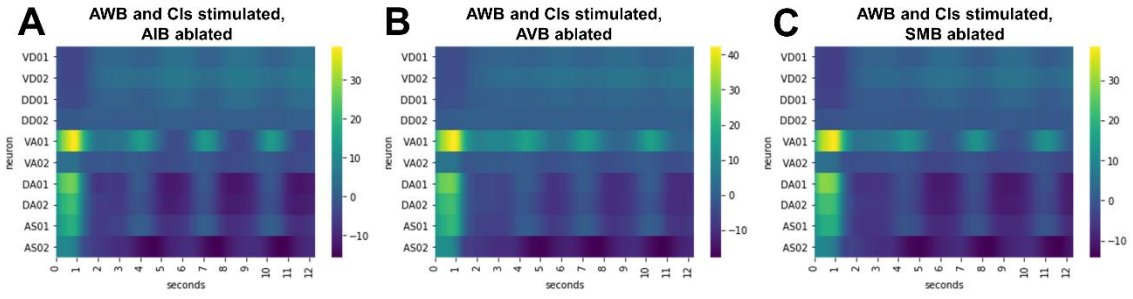

Fig. S11. AIB, AVB, or SMB neuron ablation does not diminish oscillations in backward locomotion-associated motor neurons. Activity of motor neurons (rows) upon 5.0 nA stimulation of AWB neurons and 0.9 nA stimulation of the CIs with AIB (**A**), AVB (**B**), or SMB (**C**) neurons ablated in the Neural Interactome.

Fig. S12. Genetic ablation of AUA and RMG neurons. (**A**) Representative fluorescent micrographs of NY2078 ynIs78 [*flp-8p::GFP*] (left) and AY178 ynIs78 [*flp-8p::GFP*]; *flp-8p::ced-3 (p15)::nz + flp-32::cz::ced-3 (p17) + unc-122p::rfp* (right) animals. (**B**) Representative fluorescent micrographs of NY2087 ynIs87 [*flp-21p::GFP* (left) and AY179 ynIs87 [*flp-21p::GFP*]; *flp-21p::ced-3 (p15)::nz + ncs-1p::cz::ced-3 (p17) + unc-122p::rfp* (right) animals. Greyscale and green fluorescent channels have been merged for all micrographs. White, filled arrows point to intact AUA or RMG neurons, while white, unfilled arrows point to the lack of AUA or RMG neurons. Scale bars are 50 µm.

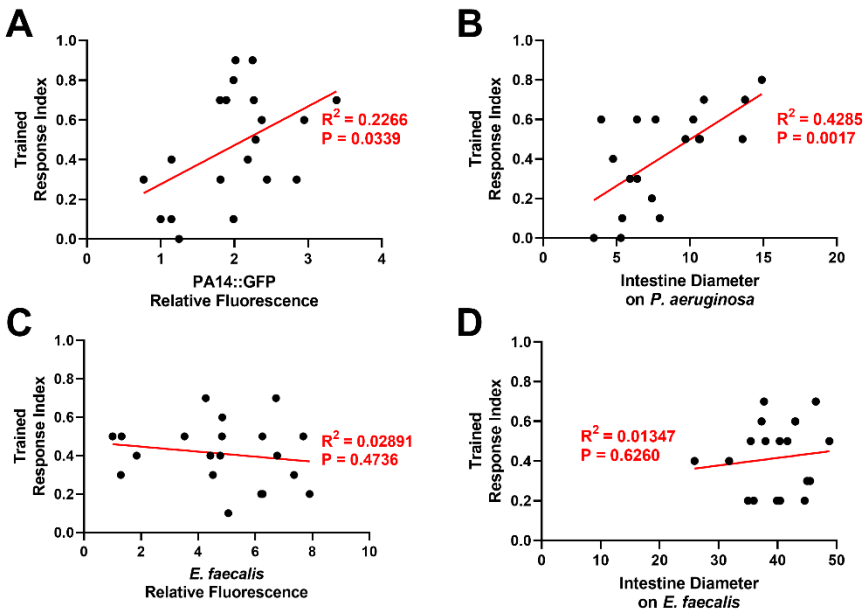

Fig. S13. Correlation of intestinal distention and learned reflexive aversion for *P. aeruginosa* but not *E. faecalis* exposure. (**A**) PA14::GFP relative fluorescence in the intestine (x-axis) and the trained response index to *P. aeruginosa* (y-axis) were measured in individual animals (dots), and linear regression was performed (red line). (**B**) Same as **A** but with intestinal diameter on *P. aeruginosa* (x-axis). (**C**) Same as **A** but with *E. faecalis*. (**D**) Same as **B** but with *E. faecalis*. R^2 and P-values are shown next to linear regression lines in red.

Code for Neural Interactome Analysis

The original code for the Neural Interactome was developed by Jimin Kim in the Shlizerman lab at the University of Washington, and can be found at https://github.com/shlizee/C-elegans-Neural-Interactome. To run this code, Python was installed on Windows using Anaconda, and the additional packages necessary for the Neural Interactome were installed using the instructions on the Interactome Github page. One line in the initialize.py code had to be changed to get the Interactome to run:

```
357   socketio = SocketIO(app) -> socketio = SocketIO(app,
cors_allowed_origins='*')
```

See the Materials and Methods section for more details on how the simulation was run. The following python code was executed in a Jupyter notebook and used to generate the simulated data figures found in Chapter 3.

In [1]:

```
import numpy as np
import pandas as pd
import seaborn as sns
import matplotlib.pyplot as plt
```

In [2]:

```
dynamics = np.load('AWB Backward.npy')
```

In [3]:

```
neurons = pd.read_csv('neuron_names.txt',header=None)
neurons = neurons.transpose()
neurons = neurons.drop(1,axis=0)
neurons = neurons.replace(to_replace=("u'","'",),value="",regex=True)
df = pd.DataFrame(dynamics,columns=neurons.iloc[0])
df.insert(0,'seconds',df.index/100)
df.set_index('seconds', inplace=True)
```

In [4]:

```
neurons_display = df[[' VD01',' VD02',' DD01',' DD02',' VA01',' VA02','
DA01',' DA02',' AS01',' AS02']]
```

In [5]:

```
ax = sns.heatmap(neurons_display.transpose(), cmap='viridis')
ax.set(ylabel='neuron')
ax.set_xticks(np.arange(0, 1300, step=100))
ax.set_xticklabels(['0', '1', '2', '3',
'4','5','6','7','8','9','10','11','12'])
plt.show()
```

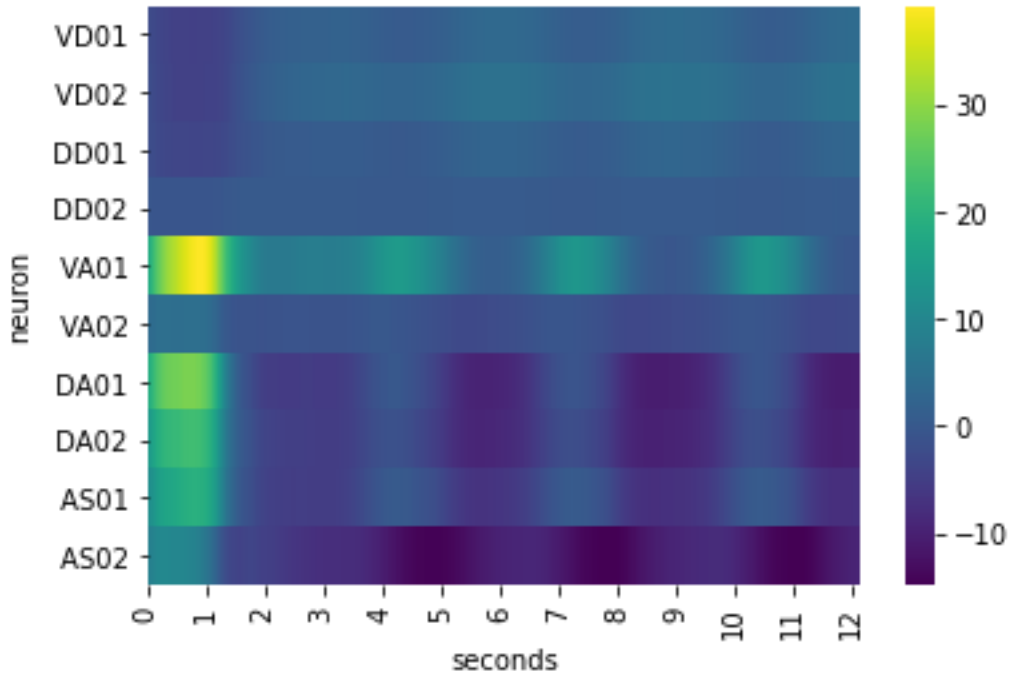

In [6]:

```
AUA = df[[' AUAL',' AUAR']]
```

In [7]:

```
ax = sns.heatmap(AUA.transpose(),cmap='viridis')
ax.set(ylabel='neuron')
ax.set_xticks(np.arange(0, 1300, step=100))
ax.set_xticklabels(['0', '1', '2', '3',
'4','5','6','7','8','9','10','11','12'])
plt.show()
```

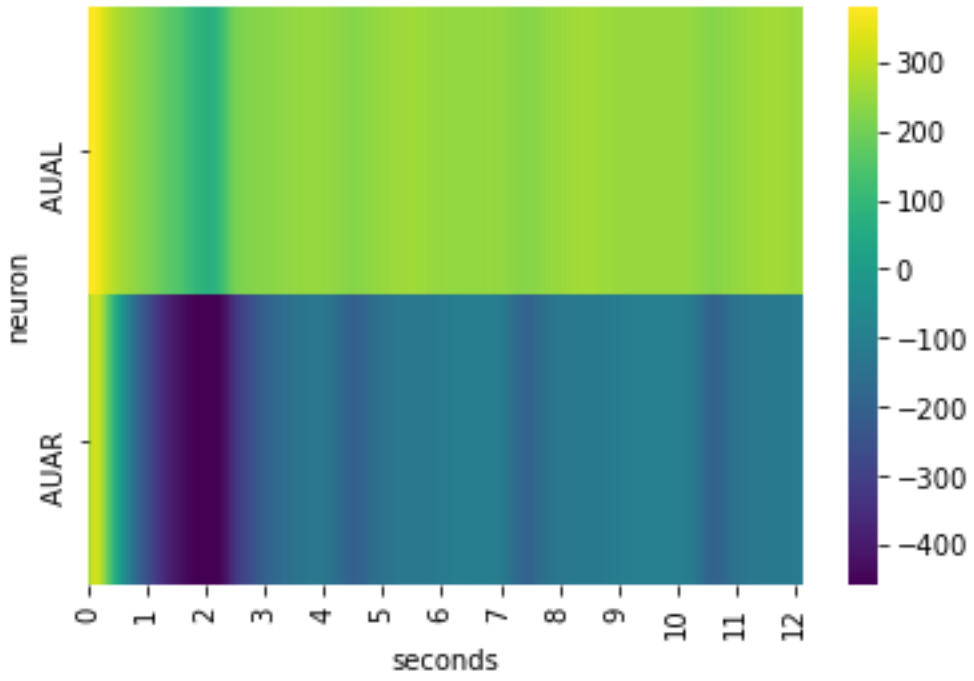

In [8]:

```
RMG = df[[' RMGL', ' RMGR']]
```

In [9]:

```
ax = sns.heatmap(RMG.transpose(), cmap='viridis')
ax.set(ylabel='neuron')
ax.set_xticks(np.arange(0, 1300, step=100))
ax.set_xticklabels(['0', '1', '2', '3',
'4','5','6','7','8','9','10','11','12'])
plt.show()
```

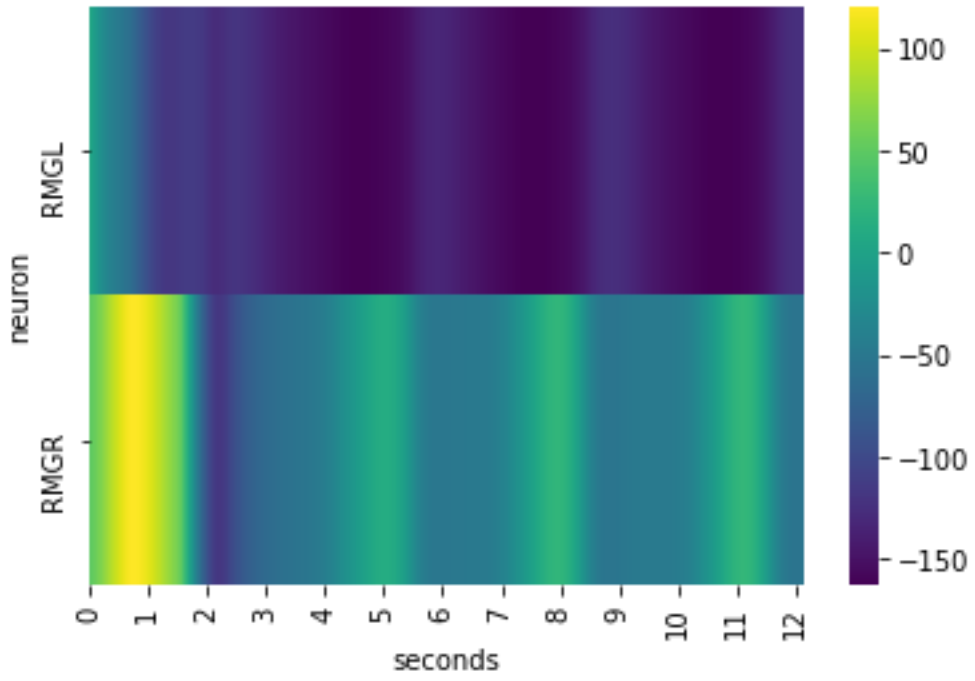

In [10]:

```
dynamics = np.load('AWB RMGabl Backward.npy')
```

In [11]:

```
neurons = pd.read_csv('neuron_names.txt',header=None)
neurons = neurons.transpose()
neurons = neurons.drop(1,axis=0)
neurons = neurons.replace(to_replace=("u'","'",),value="",regex=True)
df = pd.DataFrame(dynamics,columns=neurons.iloc[0])
df.insert(0,'seconds',df.index/100)
df.set_index('seconds', inplace=True)
```

In [12]:

```
neurons_display = df[[' VD01',' VD02',' DD01',' DD02',' VA01',' VA02','
DA01',' DA02',' AS01',' AS02']]
```

In [13]:

```
ax = sns.heatmap(neurons_display.transpose(), cmap='viridis')
ax.set(ylabel='neuron')
ax.set_xticks(np.arange(0, 1300, step=100))
ax.set_xticklabels(['0', '1', '2', '3',
'4','5','6','7','8','9','10','11','12'])
plt.show()
```

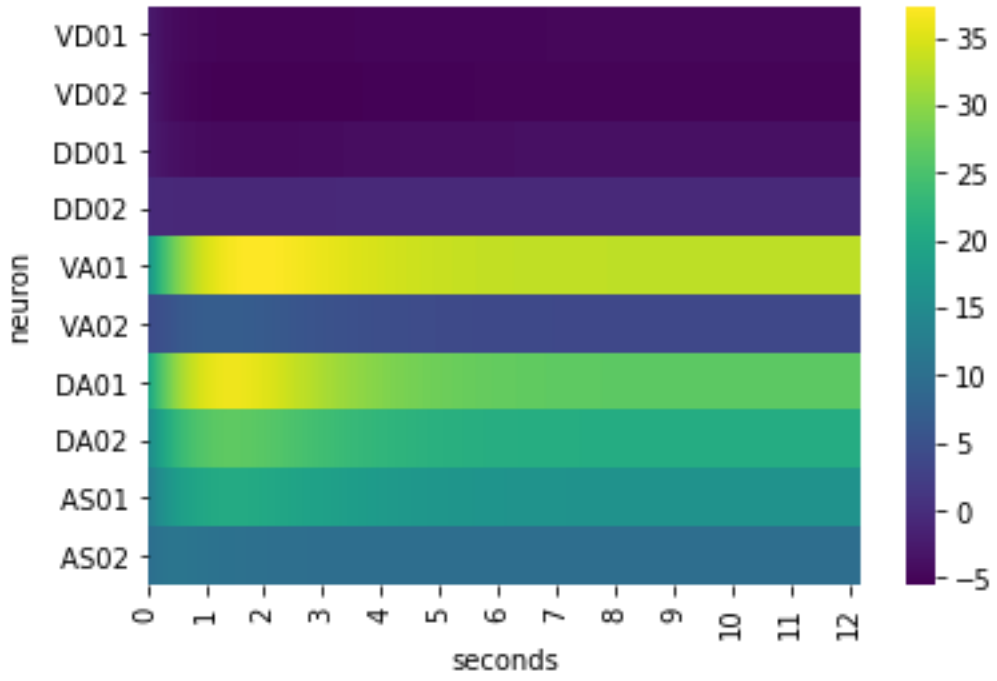

In [14]:

```
dynamics = np.load('AWB AUAabl Backward.npy')
```

In [15]:

```
neurons = pd.read_csv('neuron_names.txt',header=None)
neurons = neurons.transpose()
neurons = neurons.drop(1,axis=0)
neurons = neurons.replace(to_replace=("u'","'",),value="",regex=True)
df = pd.DataFrame(dynamics,columns=neurons.iloc[0])
df.insert(0,'seconds',df.index/100)
df.set_index('seconds', inplace=True)
```

In [16]:

```
neurons_display = df[[' VD01',' VD02',' DD01',' DD02',' VA01',' VA02','
DA01',' DA02',' AS01',' AS02']]
```

In [17]:

```
ax = sns.heatmap(neurons_display.transpose(), cmap='viridis')
ax.set(ylabel='neuron')
ax.set_xticks(np.arange(0, 1300, step=100))
ax.set_xticklabels(['0', '1', '2', '3',
'4','5','6','7','8','9','10','11','12'])
plt.show()
```

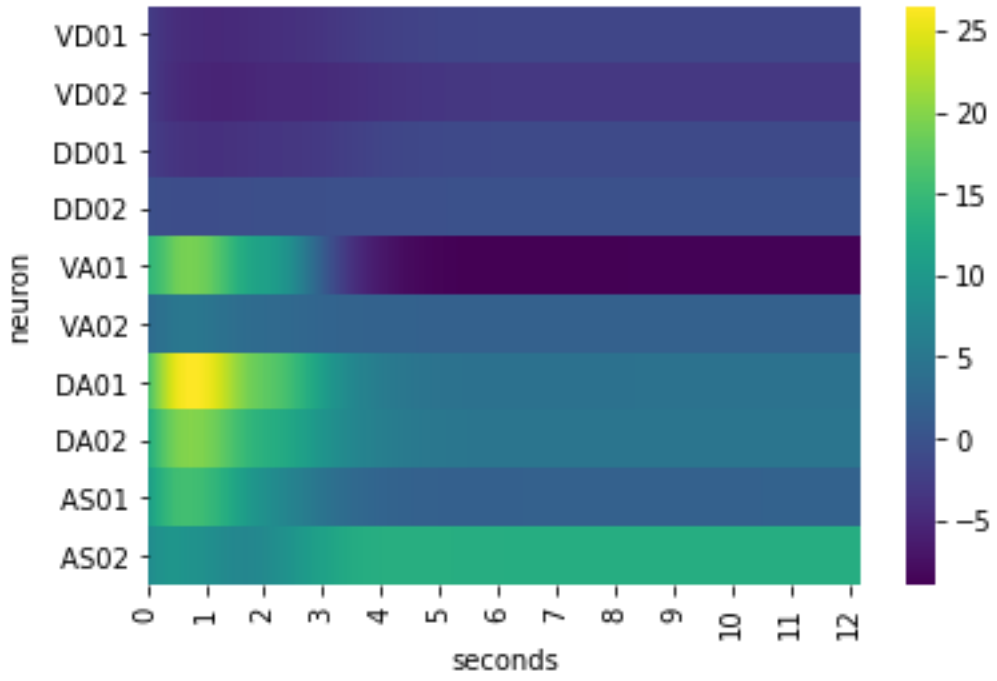

In [18]:

```
dynamics = np.load('AWB AIBabl.npy')
```

In [19]:

```
neurons = pd.read_csv('neuron_names.txt',header=None)
neurons = neurons.transpose()
neurons = neurons.drop(1,axis=0)
neurons = neurons.replace(to_replace=("u'","'",),value="",regex=True)
df = pd.DataFrame(dynamics,columns=neurons.iloc[0])
df.insert(0,'seconds',df.index/100)
df.set_index('seconds', inplace=True)
```

In [20]:

```
neurons_display = df[[' VD01',' VD02',' DD01',' DD02',' VA01',' VA02','
DA01',' DA02',' AS01',' AS02']]
```

In [21]:

```
ax = sns.heatmap(neurons_display.transpose(), cmap='viridis')
ax.set(ylabel='neuron')
ax.set_xticks(np.arange(0, 1300, step=100))
ax.set_xticklabels(['0', '1', '2', '3',
'4','5','6','7','8','9','10','11','12'])
plt.show()
```

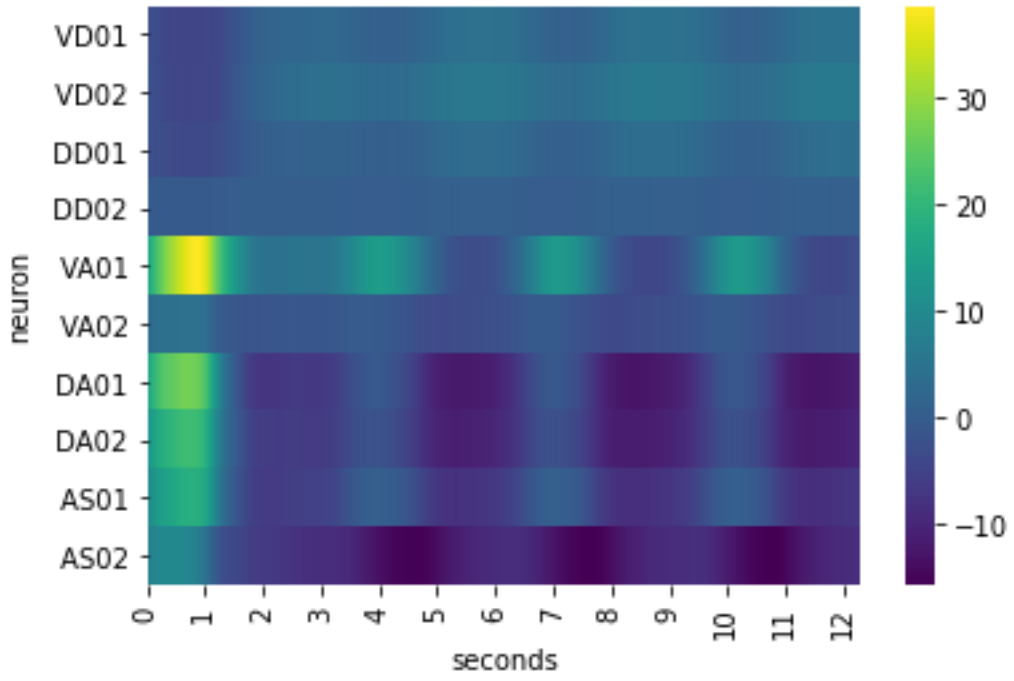

In [22]:

```
dynamics = np.load('AWB AVBabl.npy')
```

In [23]:

```
neurons = pd.read_csv('neuron_names.txt',header=None)
neurons = neurons.transpose()
neurons = neurons.drop(1,axis=0)
neurons = neurons.replace(to_replace=("u'","'",),value="",regex=True)
df = pd.DataFrame(dynamics,columns=neurons.iloc[0])
df.insert(0,'seconds',df.index/100)
df.set_index('seconds', inplace=True)
```

In [24]:

```
neurons_display = df[[' VD01',' VD02',' DD01',' DD02',' VA01',' VA02','
DA01',' DA02',' AS01',' AS02']]
```

In [25]:

```
ax = sns.heatmap(neurons_display.transpose(), cmap='viridis')
ax.set(ylabel='neuron')
ax.set_xticks(np.arange(0, 1300, step=100))
ax.set_xticklabels(['0', '1', '2', '3',
'4','5','6','7','8','9','10','11','12'])
plt.show()
```

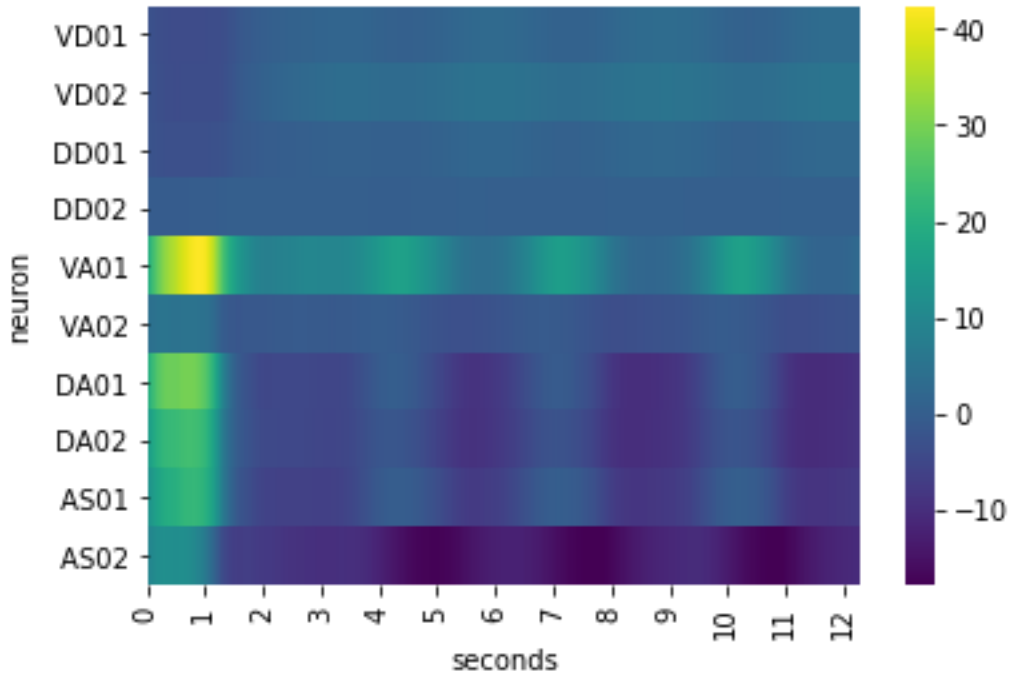

In [26]:

```
dynamics = np.load('AWB SMBabl.npy')
```

In [27]:

```
neurons = pd.read_csv('neuron_names.txt',header=None)
neurons = neurons.transpose()
neurons = neurons.drop(1,axis=0)
neurons = neurons.replace(to_replace=("u'","'",),value="",regex=True)
df = pd.DataFrame(dynamics,columns=neurons.iloc[0])
df.insert(0,'seconds',df.index/100)
df.set_index('seconds', inplace=True)
```

In [28]:

```
neurons_display = df[[' VD01',' VD02',' DD01',' DD02',' VA01',' VA02','
DA01',' DA02',' AS01',' AS02']]
```

In [29]:

```
ax = sns.heatmap(neurons_display.transpose(), cmap='viridis')
ax.set(ylabel='neuron')
ax.set_xticks(np.arange(0, 1300, step=100))
ax.set_xticklabels(['0', '1', '2', '3',
'4','5','6','7','8','9','10','11','12'])
plt.show()
```

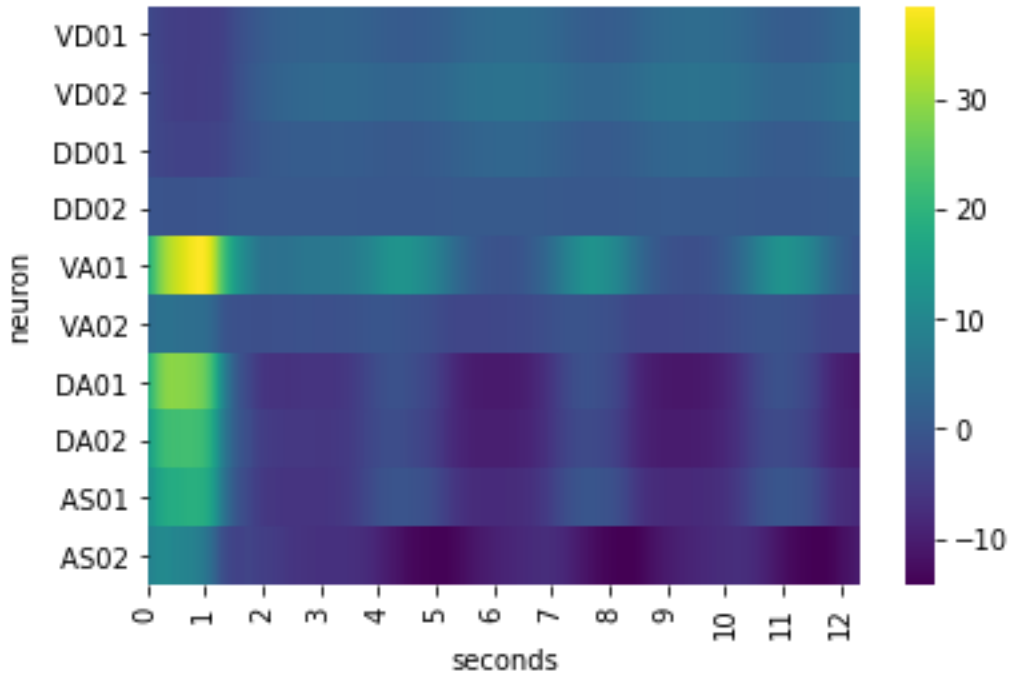

In [30]:

```
dynamics = np.load('AWB no interneuron stim.npy')
```

In [31]:

```
neurons = pd.read_csv('neuron_names.txt',header=None)
neurons = neurons.transpose()
neurons = neurons.drop(1,axis=0)
neurons = neurons.replace(to_replace=("u'","'",),value="",regex=True)
df = pd.DataFrame(dynamics,columns=neurons.iloc[0])
df.insert(0,'seconds',df.index/100)
df.set_index('seconds', inplace=True)
```

In [32]:

```
neurons_display = df[[' VD01',' VD02',' DD01',' DD02',' VA01',' VA02','
DA01',' DA02',' AS01',' AS02']]
```

In [33]:

```
ax = sns.heatmap(neurons_display.transpose(), cmap='viridis')
ax.set(ylabel='neuron')
ax.set_xticks(np.arange(0, 1300, step=100))
ax.set_xticklabels(['0', '1', '2', '3',
'4','5','6','7','8','9','10','11','12'])
plt.show()
```

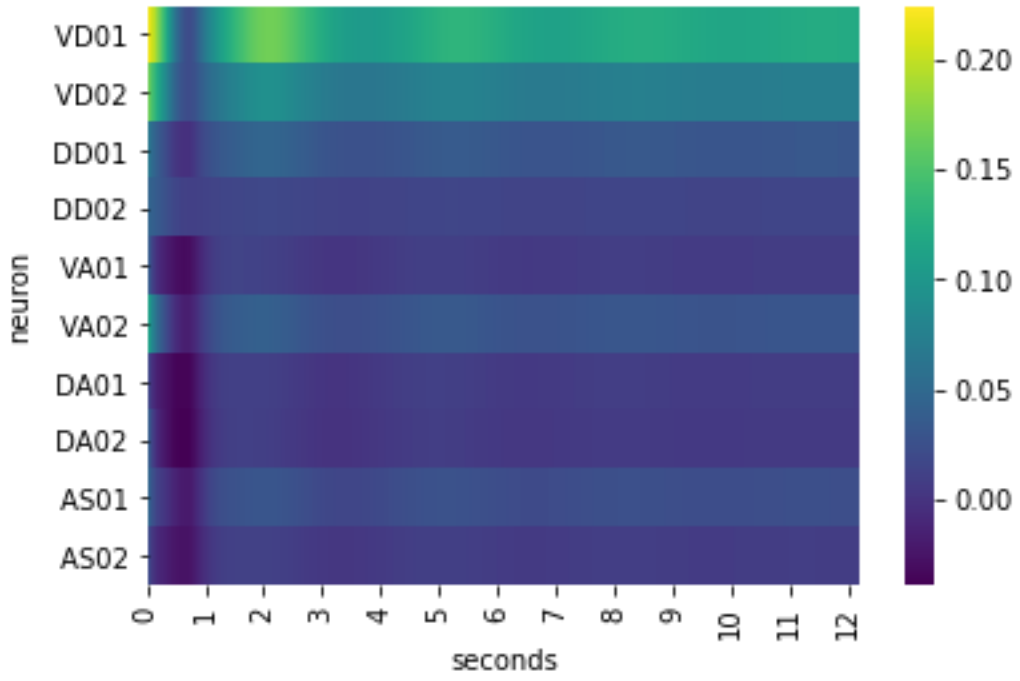

In [34]:

```
dynamics = np.load('AWC Backward.npy')
```

In [35]:

```
neurons = pd.read_csv('neuron_names.txt',header=None)
neurons = neurons.transpose()
neurons = neurons.drop(1,axis=0)
neurons = neurons.replace(to_replace=("u'","'",),value="",regex=True)
df = pd.DataFrame(dynamics,columns=neurons.iloc[0])
df.insert(0,'seconds',df.index/100)
df.set_index('seconds', inplace=True)
```

In [36]:

```
neurons_display = df[[' VD01',' VD02',' DD01',' DD02',' VA01',' VA02','
DA01',' DA02',' AS01',' AS02']]
```

In [37]:

```
ax = sns.heatmap(neurons_display.transpose(), cmap='viridis')
ax.set(ylabel='neuron')
ax.set_xticks(np.arange(0, 1300, step=100))
ax.set_xticklabels(['0', '1', '2', '3',
'4','5','6','7','8','9','10','11','12'])
plt.show()
```

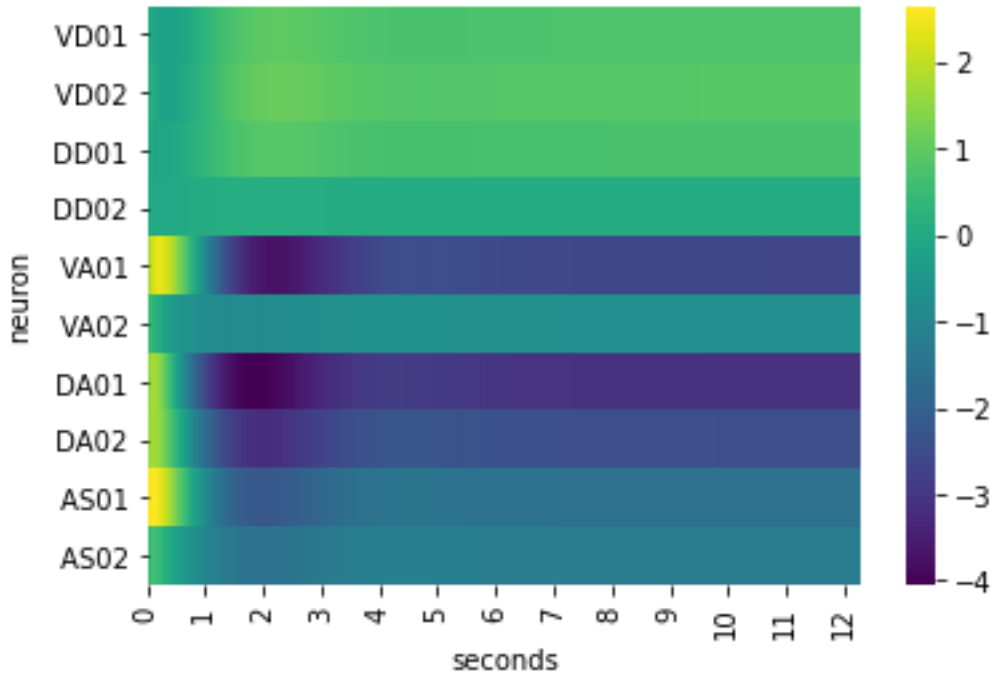

In [38]:

```
dynamics = np.load('ASI Backward.npy')
```

In [39]:

```
neurons = pd.read_csv('neuron_names.txt',header=None)
neurons = neurons.transpose()
neurons = neurons.drop(1,axis=0)
neurons = neurons.replace(to_replace=("u'","'",),value="",regex=True)
df = pd.DataFrame(dynamics,columns=neurons.iloc[0])
df.insert(0,'seconds',df.index/100)
df.set_index('seconds', inplace=True)
```

In [40]:

```
neurons_display = df[[' VD01',' VD02',' DD01',' DD02',' VA01',' VA02','
DA01',' DA02',' AS01',' AS02']]
```

In [41]:

```
ax = sns.heatmap(neurons_display.transpose(), cmap='viridis')
ax.set(ylabel='neuron')
ax.set_xticks(np.arange(0, 1300, step=100))
ax.set_xticklabels(['0', '1', '2', '3',
'4','5','6','7','8','9','10','11','12'])
plt.show()
```

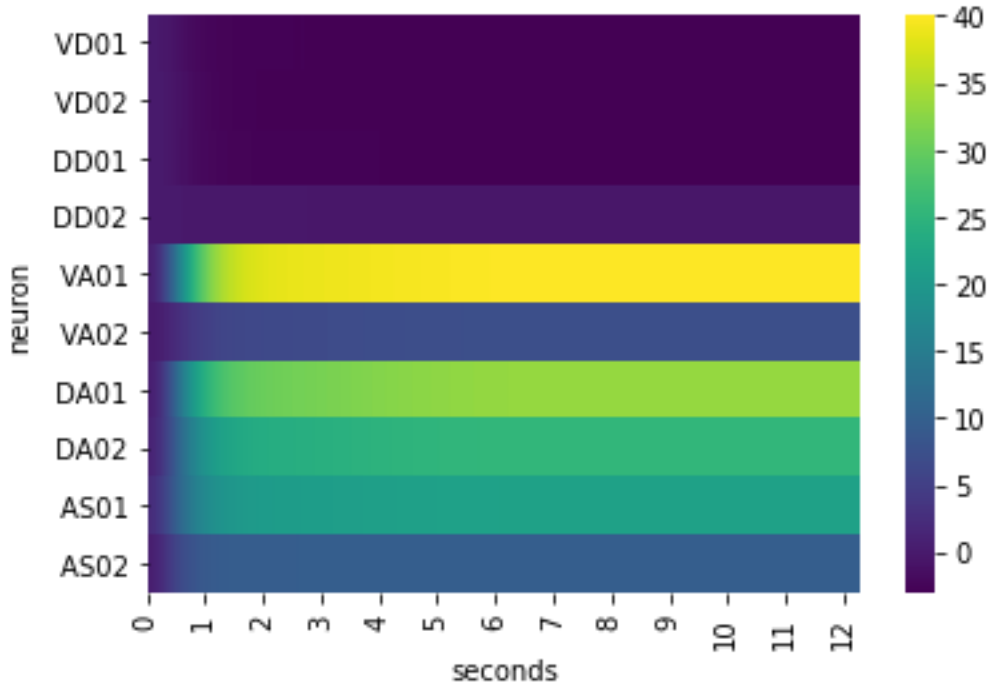

In [42]:

```
dynamics = np.load('ASE Backward.npy')
```

In [43]:

```
neurons = pd.read_csv('neuron_names.txt',header=None)
neurons = neurons.transpose()
neurons = neurons.drop(1,axis=0)
neurons = neurons.replace(to_replace=("u'","'",),value="",regex=True)
df = pd.DataFrame(dynamics,columns=neurons.iloc[0])
df.insert(0,'seconds',df.index/100)
df.set_index('seconds', inplace=True)
```

In [44]:

```
neurons_display = df[[' VD01',' VD02',' DD01',' DD02',' VA01',' VA02','
DA01',' DA02',' AS01',' AS02']]
```

In [45]:

```
ax = sns.heatmap(neurons_display.transpose(), cmap='viridis')
ax.set(ylabel='neuron')
ax.set_xticks(np.arange(0, 1300, step=100))
ax.set_xticklabels(['0', '1', '2', '3',
'4','5','6','7','8','9','10','11','12'])
plt.show()
```

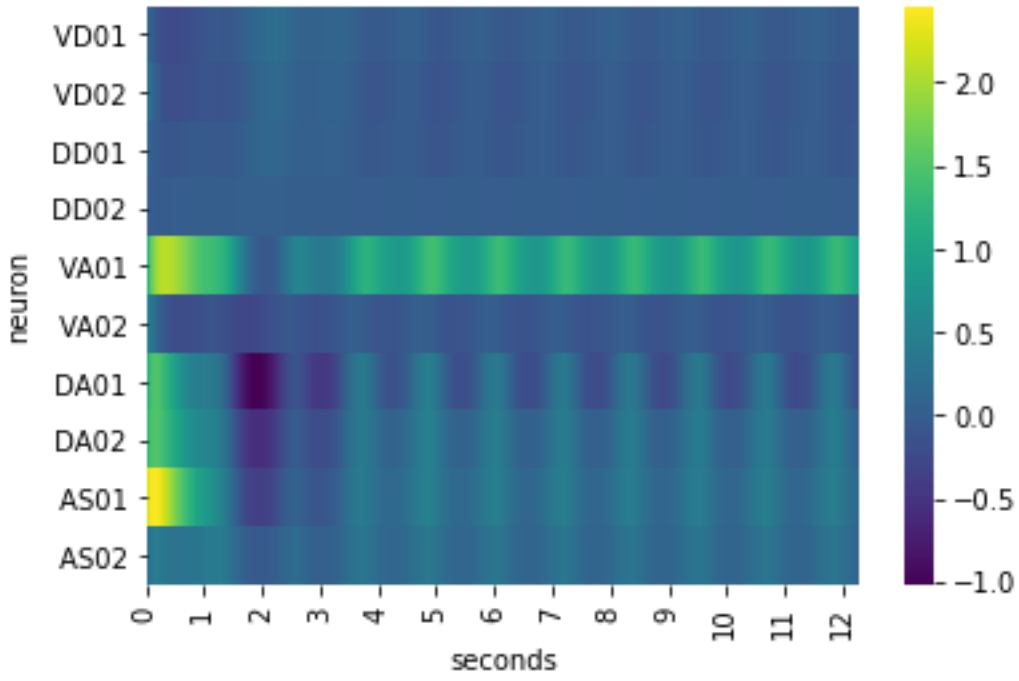

In [46]:

```
dynamics = np.load('Tran et al onlyASHstim.npy')
```

In [47]:

```
neurons = pd.read_csv('neuron_names.txt',header=None)
neurons = neurons.transpose()
neurons = neurons.drop(1,axis=0)
neurons = neurons.replace(to_replace=("u'","'",),value="",regex=True)
df = pd.DataFrame(dynamics,columns=neurons.iloc[0])
df.insert(0,'seconds',df.index/100)
df.set_index('seconds', inplace=True)
```

In [48]:

```
neurons_display = df[[' VD01',' VD02',' DD01',' DD02',' VA01',' VA02','
DA01',' DA02',' AS01',' AS02']]
```

In [49]:

```
ax = sns.heatmap(neurons_display.transpose(), cmap='viridis')
ax.set(ylabel='neuron')
ax.set_xticks(np.arange(0, 1300, step=100))
ax.set_xticklabels(['0', '1', '2', '3',
'4','5','6','7','8','9','10','11','12'])
plt.show()
```

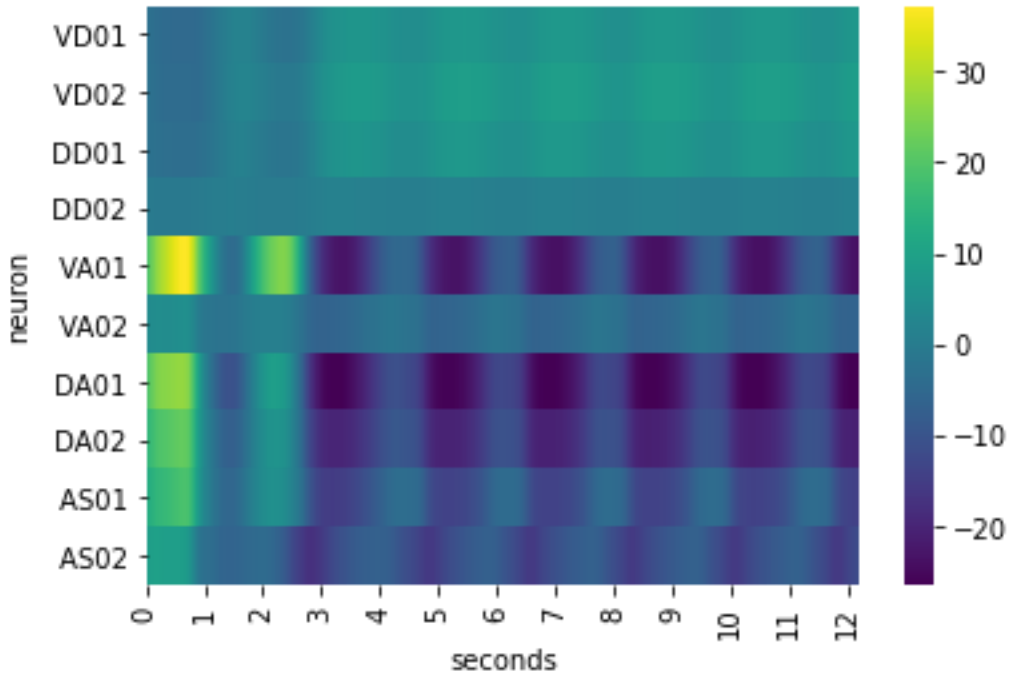
VD01
VD02
DD01
DD02
VA01
VA02
DA01
DA02
AS01
AS02
neuron
0
1
2
3
4
5
6
7
8
9
10
11
12
seconds
30
20
10
0
−10
−20